

# Integrated Production Planning and Control System for Prefabrication of Panelized Construction for Residential Building

by

Mohammed Sadiq Altaf

A thesis submitted in partial fulfillment of the requirements for the degree of

Doctor of Philosophy

In

Construction Engineering and Management

Department of Civil and Environmental Engineering  
University of Alberta

© Mohammed Sadiq Altaf, 2016

# ABSTRACT

---

Panelized construction has been recognized as a promising approach to residential construction. However, its full potential in terms of productivity improvement has not yet been realized due to the absence of an automated production planning and control system. This research thus conceives an integrated production planning and control system for a prefabricated panelized home production facility. The proposed system consists of four primary modules: (1) a real-time data acquisition module, which is employed in this study to collect time and location information of building panels from the production floor in real time; (2) a scheduling module, which generates an optimized building panel production schedule with the objective of minimizing the production lead time and material waste on the basis of detailed job information from a 3D BIM model; (3) a discrete-event simulation (DES) module, which is developed based on the historical data from the data acquisition module in order to provide a performance benchmark; and (4) a financial module, which provides total labour cost for every job as well as unit labour cost for each workstation. These four modules are seamlessly integrated through a central database in order to generate the production schedule, real-time location tracking, simulation-based performance evaluation, and cost control. The proposed system is implemented and validated in a panelized wall production facility at ACQBUILT, Inc., a prefabricated home builder in Edmonton, Canada.

# ACKNOWLEDGEMENTS

---

First I would like to express my gratitude to my co-supervisors, Dr. Mohamed Al-Hussein and Dr. Ahmed Bouferguene, for their continuous encouragement and inspiration. With their support, I have learned valuable lessons about how to be professional and how to conduct myself as a qualified researcher. The projects I participated in ignited my passion for engineering design, innovation, and development.

Dr. Haitao Yu and Francisco Villaroel from Landmark Group of Companies and ACQBUILT, Inc. and all other ACQBUILT colleagues (Michael Loowell, Suat Demirer, Christina Law, Efren Garza Plata...) are very much appreciated for their support and sharing of their many years of knowledge and experience. This unique experience not only laid a solid foundation for me as an engineer, but also contributed to my maturation as a thinker and innovator.

At the University of Alberta, I have also been surrounded by many exceptional colleagues: Ronald, Hexu, Ahmad, Sang, Lei, Hamid, Sherry, Rita, Jonathan, and Claire. I had the opportunity to work with them to produce interesting and high quality research outputs.

Finally, my deepest gratitude is given to my parents, who have been a great support behind me over the years. They have always encouraged me during this journey and provided valuable guidance. My wife, Samia, is also very much appreciated for her kind and continuous company through this phase of my life.

## TABLE OF CONTENTS

1	Introduction.....	1
1.1	Background and Motivation.....	1
1.2	Research Objectives.....	5
1.3	Thesis Organization.....	6
2	Literature Review.....	8
2.1	Prefabricated Home Building.....	8
2.2	Application of Simulation in Construction.....	10
2.3	Production Planning and Control.....	11
2.4	Flow Shop Scheduling Problem.....	14
2.5	Application of RFID Technology.....	16
2.6	Simulation Model Verification and Validation.....	18
3	Methodology.....	20
3.1	Scheduling Module.....	21
3.2	Data Collection Module.....	22
3.3	Simulation Module.....	30
3.4	Simulation based production scheduling.....	33
3.5	Financial Module.....	36
4	Implementation and Results.....	39
4.1	Overview of the Wall Production Line.....	39
4.1.1	Framing station.....	40
4.1.2	Sheathing station.....	42
4.1.3	Multi-function bridge.....	42
4.1.4	Butterfly table station.....	44
4.1.5	Exterior insulation booth.....	45
4.1.6	Window/door installation line.....	46
4.1.7	Window bypass line.....	47
4.1.8	Wall magazine line.....	48
4.1.9	Loading.....	48
4.2	Multipanel Optimization.....	49

4.2.1	Mathematical model.....	49
4.2.2	Results.....	53
4.3	RFID System.....	54
4.3.1	Real-time location tracking.....	59
4.3.2	Production data analysis.....	60
4.4	Simulation Model Development.....	65
4.4.1	Input modelling - Task time formula.....	66
4.4.2	Input modelling - Panel information.....	69
4.4.3	Simphony.NET.....	71
4.4.4	Model Validation.....	76
4.4.5	Results.....	77
4.5	Simulation-based Production Schedule Optimization.....	82
4.5.1	Particle swarm optimization.....	83
4.5.2	Simulated annealing.....	88
4.5.3	Comparison between PSO and SA optimization result.....	91
4.5.4	Optimizing in the presence of noise.....	95
4.6	Financial Module.....	98
5	Conclusion.....	103
5.1	Summary.....	103
5.2	Research Contributions.....	105
5.2.1	Academic contributions.....	105
5.2.2	Industrial contributions.....	106
5.3	Limitations and Future Research.....	107
	References.....	111

## LIST OF FIGURES

Figure 1.1: Different types of house models.....	2
Figure 1.2: Multipanel generation from single-wall panels.....	3
Figure 1.3: Work load for different wall types .....	4
Figure 3.1: Overview of the proposed method .....	20
Figure 3.2: Timestamps collection for wall panels at consecutive stations .....	22
Figure 3.3: Processing time for a set of similar exterior wall panels at workstation no. 1.....	23
Figure 3.4: Application of the Kalman filter to noisy processing time data.....	26
Figure 3.5: Entity-relationship (ER) diagram .....	32
Figure 4.1: Process map of wall production line .....	40
Figure 4.2: Framing station (courtesy of ACQBUILT, Inc.).....	41
Figure 4.3: Sheathing station (courtesy of ACQBUILT, Inc.) .....	43
Figure 4.4: Multi-function bridge (courtesy of ACQBUILT, Inc.) .....	44
Figure 4.5: Butterfly table station (courtesy of ACQBUILT, Inc.) .....	45
Figure 4.6: Exterior insulation booth (courtesy of ACQBUILT, Inc.).....	46
Figure 4.7: Window/door installation line (courtesy of ACQBUILT, Inc.).....	47
Figure 4.8: Window bypass line (courtesy of ACQBUILT, Inc.) .....	48
Figure 4.9: Wall magazine line (courtesy of ACQBUILT, Inc.).....	49
Figure 4.10: Loading trailer (courtesy of ACQBUILT, Inc.).....	49
Figure 4.11: Data collection module flowchart .....	55
Figure 4.12: RFID System at ACQBUILT, Inc.....	56
Figure 4.13: RFID antenna and reader location at the wall production line.....	57
Figure 4.14: Transfer cart antenna arrangement detail .....	57
Figure 4.15: Screenshot of query table containing timestamps values.....	58
Figure 4.16: Real-time wall panel tracking system .....	59
Figure 4.17: Wall magazine capacity detail.....	60
Figure 4.18: Actual versus filtered processing time at framing station for exterior multipanel from 20-30 ft.....	61
Figure 4.19: Framing station throughput time breakdown .....	63
Figure 4.20: Actual and filtered utilization comparison .....	63

Figure 4.21: Probability distribution function of exterior wall waiting time at framing station .....	65
Figure 4.22: Simulation module information flow .....	66
Figure 4.23: Probabilistic density chart for window and spray-booth area processing time .....	69
Figure 4.24: Screenshot of multipanel data table.....	70
Figure 4.25: Screenshot of single-wall panel data table .....	70
Figure 4.26: Simulation model developed in Simphony.NET using general purpose template .....	72
Figure 4.27: Cut-panel composite element detail .....	74
Figure 4.28: Cumulative density function of total production time.....	78
Figure 4.29: Framing station throughput time comparison .....	80
Figure 4.30: Sheathing station throughput time comparison .....	80
Figure 4.31: Multi-function bridge station throughput time comparison .....	81
Figure 4.32: Delay identification .....	82
Figure 4.33: PSO algorithm for multipanel sequencing .....	87
Figure 4.34: SA algorithm for multipanel sequencing.....	90
Figure 4.35: Distribution of makespan for original sequence, PSO and SA .....	93
Figure 4.36: Convergence charts of PSO and SA optimization.....	94
Figure 4.37: Effect of noise in the estimated solution .....	96
Figure 4.38: Mean, 90 <sup>th</sup> percentile, and runtime for different number of replications .....	97
Figure 4.39: Optimal solution for different run-length.....	97
Figure 4.40: Financial module information flow .....	100

## LIST OF TABLES

Table 4.1: Multipanel optimization result for different house model.....	53
Table 4.2: Filtered value and upper limit of different sub-group of multipanel for framing station .....	62
Table 4.3: Framing station productivity detail.....	63
Table 4.4: Probabilistic model of workstation takt time.....	64
Table 4.5: Example of task time formula for different tasks of wall prefabrication process.....	67
Table 4.6: Comparison of actual and simulated workstation throughput time .....	76
Table 4.7: Comparison of simulated and actual total production time .....	77
Table 4.8: Waiting time and utilization of workstation .....	79
Table 4.9: Optimization result for PSO and SA algorithm.....	92
Table 4.10: Target cost and actual cost of each work area over one week period .....	100
Table 4.11: Daily labour cost for some work area of house model A .....	101

# 1 Introduction

---

## 1.1 Background and Motivation

Prefabricated home building has become a popular construction method among homebuilders due to the associated improved productivity, reduced waste, and increased quality. The prefabricated construction process known as panelized construction reduces waste and construction time compared to traditional stick-built construction (National Association of Home Builders 2009). This system breaks down a building into wall, floor, and roof elements, which are manufactured in a plant and are then shipped to site to be installed. As the majority of activities in the panelized approach are performed in a factory setting, the controlled environment makes it possible to greatly improve productivity. This system provides a high level of flexibility, and wall, floor, and roof panels can be custom manufactured based on the project requirements.

The Canadian prefabricated housing market is currently in a state of steady growth. According to the Canadian Manufactured Housing Institute, the total production of manufactured single-family housing in 2013 was approximately 16,020 units, accounting for 14% of all single-family housing starts in Canada in 2013 (Canadian Manufactured Housing Institute 2013). In the residential housing industry, the most commonly built houses include the single-family home (with attached or detached garage), the condo, the townhome, the duplex, and the bungalow (as shown in Figure 1.1). These homes vary in size and shape, and

involve different processes in the production line. Furthermore, each type of house has a different base model with various customization options for clients, making each house model unique. Since various house models are produced on the same production line, the building production line is deemed a mixed model assembly line (Liker 2004).

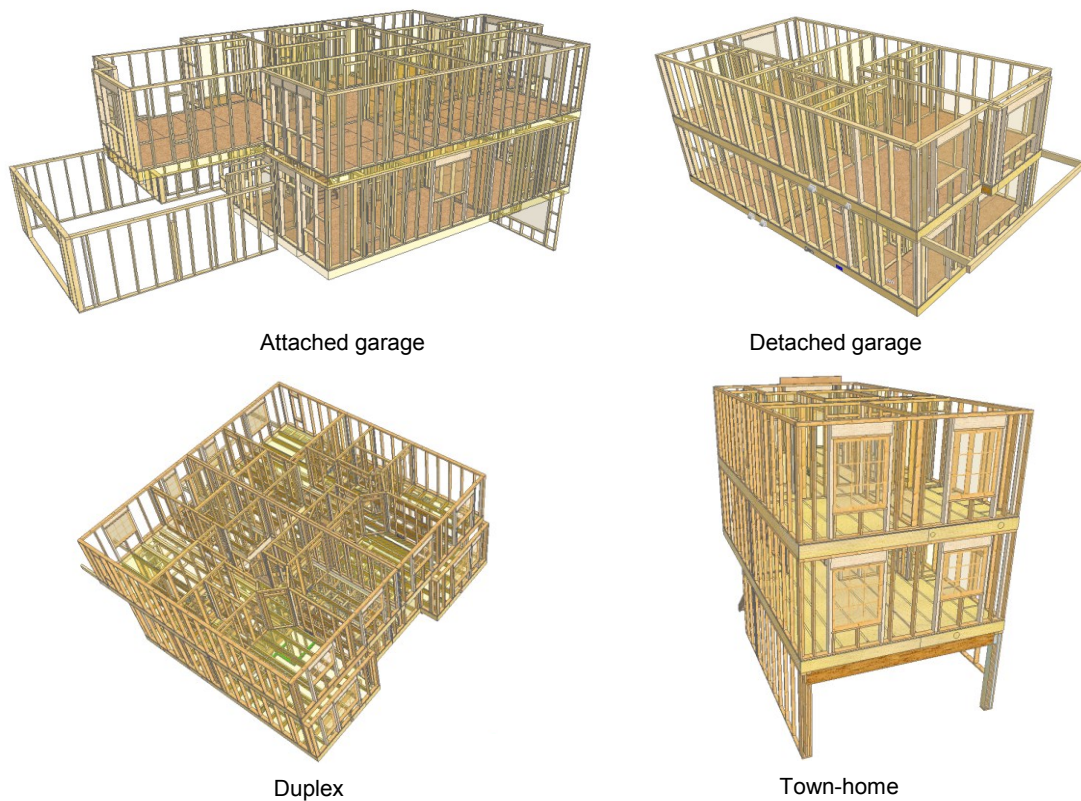


**Figure 1.1: Different types of house models**

In the wall production line, wall panels travel through various workstations, spending different amounts of time at each station based on the parameters of the given panel. Despite the fact that single-wall panels can be merged into multipanels in order to reduce material waste and increase machine utilization (as shown in Figure 1.2), the majority of multipanels are still unique due to the variation in stud size and location, window/door opening, as well as wall height

and thickness. As such, the cycle times spent at each workstation vary. These variations in cycle time may increase the amount of time a panel remains idle between stations. Furthermore, the prefabrication process involves work at manual workstations, which poses a challenge to production managers seeking to obtain accurate production data without an automated data collection system. The lack of sufficient production data forces production controllers to base their decision making upon their experience, which leads to human error, lack of communication between production floor and controller, and production delays. Furthermore, the managers have to rely on a manual reporting system for daily progress, thereby rendering their planning efforts time-consuming and error-prone.

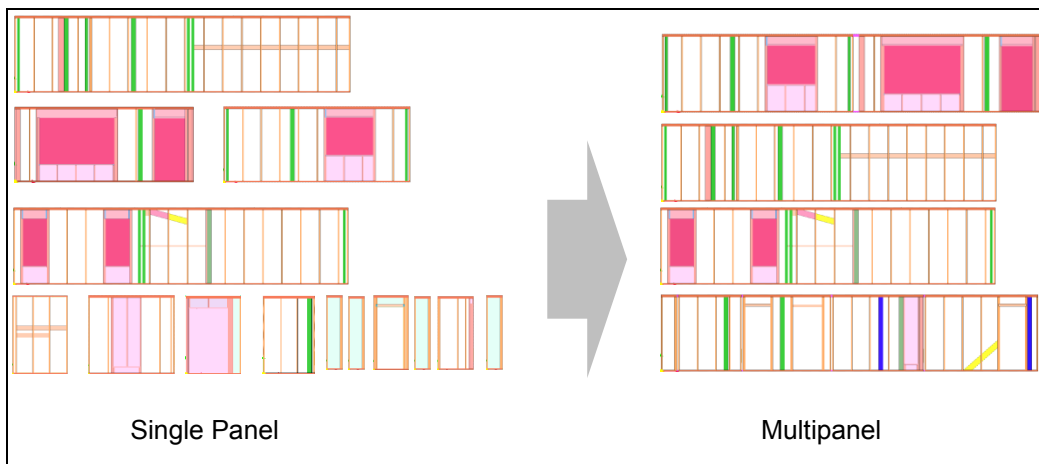


**Figure 1.2: Multipanel generation from single-wall panels**

As shown in Figure 1.3, the volume of work needed to produce a wall panel can vary significantly depending on the wall type. Interior walls require only framing and loading, while exterior walls require framing, sheathing, insulation, siding, window/door installation (if needed), and loading. This variation can cause line imbalance, resulting in waiting time in the production line. Proper sequencing of

wall panels can minimize this effect and can reduce waiting times and delays. However, due to the complex nature of wall panel production, where multipanel and single-wall panels are produced on the same production line, it is challenging to optimize panel sequencing and balance the production line with reasonable model runtime. This panel sequencing is a classical combinatorial optimization problem, which is proven to be non-deterministic polynomial-time hard (NP-hard), and is also known as a flow shop scheduling problem. Furthermore, each station cycle time has stochastic elements such as delay and waiting time, and this randomness makes this a probabilistic flow shop scheduling problem.

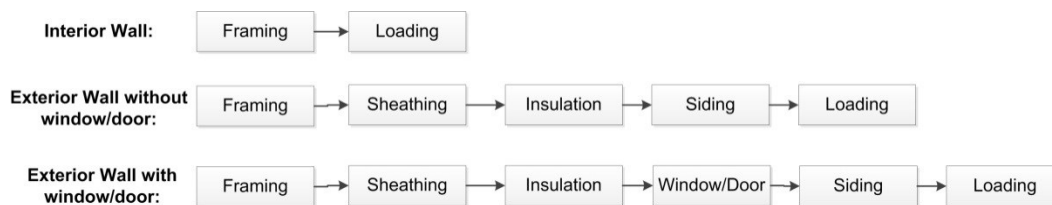


**Figure 1.3: Work load for different wall types**

Currently, production performance for panelized construction is not standardized. The regular performance indicators are  $\text{ft}^2/\text{day}$ , linear  $\text{ft}/\text{day}$  and  $\text{cost}/\text{ft}^2$ . However, given that production time largely depends on the type of wall panel and other attributes, such as the number of windows and the area to be insulated with spray foam, these indicators do not reflect the actual performance. For example, a wall panel with three windows takes more time than a wall panel with no windows, even if the total square footage is similar. As a result, a simulation model that takes into account the appropriate factors that have an impact on productivity and/or cost can be a useful tool for managers, since they will be able

to accurately predict the performance of production lines in consideration of the complexity of the manufactured elements.

Moreover, in conventional home building production, jobs are quoted based on labour hours for framing, finishing, and so on. However, in a manufacturing facility, different parts of the house are being built separately in different locations. For example, the framing of a house is divided into wall framing, stair building, floor framing, and roof framing. The costs associated with these areas also vary. And as different jobs are mixed during production to increase efficiency, it is a challenge to quote the customer accurate labour costs associated with individual jobs as well as to have an effective cost control tool for the plant.

In order to address these issues, an integrated production planning and control system, based on discrete-event simulation (DES) and a radio frequency identification (RFID) system, is proposed. Specifically, the RFID system is utilized for the purpose of real-time production data collection. A DES model is integrated with the RFID system and optimization model for automated production scheduling and real-time performance evaluation. The cost control module is developed for the prefabricated home building facility using the RFID system.

## **1.2 Research Objectives**

The proposed research is built upon the following hypothesis:

*“An integrated production planning and control system with an RFID and simulation will level the process and improve the productivity of the prefabrication of panelized homes.”*

In order to test this hypothesis, the following research objectives are pursued:

- (i) Design a data collection system using RFID technology for a prefabricated wall production facility.
- (ii) Develop a method to utilize production data collected from the RFID system for the purpose of performance monitoring and simulation modelling.
- (iii) Develop a framework to simulate the panel production process.
- (iv) Develop a simulation-based optimization model for the purpose of production scheduling.
- (v) Develop a cost control module for prefabricated home building facilities.

### **1.3 Thesis Organization**

This thesis consists of five chapters. **Chapter 1** provides the background and motivation of the work and outlines the research scope. **Chapter 2** presents an overview of the literature describing prefabricated home building, applications of DES in construction industry, production planning and control, flow shop scheduling methods, application of RFID technology and simulation model verification and validation. **Chapter 3** reviews the methodology of the four modules—formulation of the scheduling model, data collection module design using RFID system, DES model development and simulation-based optimization

model for scheduling, and cost control module. **Chapter 4** presents the implementation results of the proposed methodology at ACQBUILT's prefabrication plant, and **Chapter 5** outlines the summary of the thesis and the academic and industrial contributions of the work.

# 2 Literature Review

---

The literature review focuses on the following research areas: (1) prefabricated home building; (2) application of discrete-event simulation (DES) in construction; (3) production planning and control; (4) the flow shop scheduling problem; (5) application of RFID technology; and (6) simulation model verification and validation. An in-depth literature review is conducted in order to support understanding of the current practice, existing studies, and research opportunities.

## **2.1 Prefabricated Home Building**

Prefabrication is emerging as a popular method of housing construction. Garza-Reyes et al. (2012) have compared manufactured home construction with the traditional stick-built method and have summarized several advantages of manufacturing-based construction over traditional construction, such as better inventory control, higher utilization of workers, easier implementation of new technology, and controlled working environment. The researchers have conducted time studies to evaluate the manufactured home production line, and have used simulation to find the optimum balance for every stage in the home production process. Hammad et al. (2002) have developed a simulation model for the manufactured housing process to improve both productivity and the quality of the product. Jeong et al. (2011) have proposed a product mix and sequence optimization model for the manufactured housing industry; they have created a new supply chain management framework, including market demand planning,

facility location, layout planning, inventory planning, and production planning. They have developed an optimized product mix model based on linear programming to maximize the profit, as well as the optimal product sequence model using the just-in-time (JIT) goal chasing approach. The optimization model has provided better space utilization, labour utilization, and has maximized the profit per day. Senghore et al. (2004) have developed a simulation model for manufactured housing in order to improve the production process. Two manufactured housing plants in northern Indiana were used as case studies to develop the simulation model. The authors combined process mapping, time and motion studies, and simulation modelling to develop the model. Four different “what-if” scenarios were performed to demonstrate the possible improvement in the production process. Shewchuk and Guo (2012) have utilized the concept of lean manufacturing to optimize prefabricated wall panel stacking and sequencing in residential construction. Their approach reduces the number of panel stacks as well as walking distances for workers carrying the panels. Several studies have been carried out focusing on improving the production process at a panel prefabrication facility in Edmonton, Canada. Yu (2010) has developed a lean production approach for the home building industry; Xie et al. (2011) have developed a simulation model of the panelized production line; and Shafai (2012) has described a methodology to improve the panelized home production process through lean principles and simulation tools. Although some researchers have in separate studies focused on panel sequencing, product mix design, and simulation modelling, this study proposes integrating production sequencing, RFID based

real-time location system, simulation based performance analysis, and cost control by developing a simulation-based planning and control system for panelized home production.

## **2.2 Application of Simulation in Construction**

The simulation model has been utilized as a planning tool in various sectors of the construction and manufacturing industry. Its application can improve the understanding of a complex system and can be a useful decision support tool. Many researchers have used simulation models in construction and production planning in order to schedule activities, perform “what-if” analysis, allocate resource, and implement layout optimization. Halpin (1977) has introduced CYCLONE, a simulation environment that created the foundation for the progress of construction simulation. AbouRizk and Hajjar (1998) have proposed a framework for the application of simulation in construction, specifically focusing on construction practitioners. They have presented the concept of special-purpose simulation (SPS), which is a computer-based environment specially built for experts in the area, the advantage of this environment being that the user does not need to have knowledge of simulation. AbouRizk and Mohamed (2000) have introduced Symphony.NET, an integrated environment to model construction activities. This simulation software supports both DES and continuous simulation. It can provide different model outputs, such as standard statistical averages, resource utilization, standard deviation, minima and maxima, and charts such as histograms, cumulative density functions (CDFs), and time graphs. Al-bataineh et al. (2013) have presented a case study in which a simulation model for a tunneling

project in Edmonton, Canada was developed in Symphony.NET as a decision support system for the project management team. Alvanchi et al. (2012) have developed a DES model of the steel girder bridge fabrication process for the purpose of providing a solution for the complex process of planning off-site girder bridge construction. Lui et al. (2015) have introduced a SPS template for the panelized construction process and linked the simulation model with building information modelling (BIM). Lu et al. (2008) have developed an automated resource-constrained critical path analysis using DES and particle swarm optimization (PSO). Based on their study, simulation modelling enables engineers to precisely examine different approaches in order to complete the project. Performing this type of analysis in advance yields reduced costs, improved quality, and improved productivity (AbouRizk 2010). In this study, the simulation model is developed in the Symphony.NET platform, and is integrated with an optimization algorithm for the purpose of providing an optimal production schedule that is also integrated with a real-time data collection system to develop a simulation-based production monitoring system.

### **2.3 Production Planning and Control**

As the construction industry moves toward factory-based construction, it is important to apply the knowledge of operations and production research for the purpose of production planning and control. There has been ample research on production planning and control focusing on different types of manufacturing. Researchers have used DES, radio frequency identification (RFID) data, lean principles, and optimization algorithms to develop planning and control as a

decision support system. Peters and Smith (1998) have presented a simulation control system developed at the Texas A&M Computer Aided Manufacturing Laboratory (TAMCAM). The authors used this control system to evaluate on-line simulation for process control. Online simulation links the information system with the simulation model to provide actual production performance. The authors have concluded that an online simulation-based real-time control system can be very useful for flexible manufacturing systems. Mirdamadi et al. (2007) have also presented a DES-based real-time shop floor control system using on-line simulation. Azimi et al. (2011) have presented an integrated project control and monitoring framework, implemented in a steel fabrication project. Their study applied RFID technology to collect real-time data and integrate it to the control system framework, along with DES and visualization, as a decision support system. This system helps the project manager to detect deviations in the production line and to help mitigate the problem. AlDurgham and Barghash (2008) have summarized the literature on simulation applications in manufacturing and have presented a framework for the application of simulation in different decision areas—manufacturing strategies, material handling, layout, sequencing and scheduling policies, and manufacturing processes and resources. Meyer et al. (2011) have presented an intelligent product-based control and monitoring system; the researchers have proposed a decentralized control system to deal with all types of disturbances, including small delays that had been ignored in previous studies. In a decentralized system, a lower level component operates on local information to achieve global goals. The system detects every

disturbance from the intelligent products labelled with auto-ID technologies (RFID/barcode), and also proposes solutions to the appropriate person. They validated the framework using simulation experiments, concluding that a centralized system serves better for planning purposes while a decentralized monitoring and control system provides more robustness. Mönch (2007) has described simulation-based benchmarking approaches for complex manufacturing systems. The author used the DES technique to emulate the complex manufacturing system and its stochastic nature. The characteristics of a complex manufacturing system include a large number of products with changing product mix, sequence-dependent set-up times, unrelated parallel machines, and a mix of different process types, including batch processing, internal and external disturbances, and so on. The paper identified advantages over static benchmarking process such as real world scenarios, and that stochastic behaviour can be treated accordingly and can consider dynamic situations. Long simulation model runtime is identified as the main disadvantages of the system. Son et al. (2003) have formulated a simulation-based shop floor control system by developing a resource model, a coordination execution model, and a simulation model. Altinkilinc (2004) has used simulation to generate a layout plan for a manufacturing plant in order to improve production performance. Serrano et al. (2008) have developed a methodology, based on multiple case studies, which uses value stream mapping—a lean production tool—as a graphical tool for the purpose of redesigning a manufacturing system. Dengiz and Alabas (2000) have used a simulation model together with a tabu search to find the optimum number of *kanbans* in a just-in-

time (JIT) system. Rezg et al. (2004) have proposed a methodology of combining simulation and GA to optimize maintenance and inventory control policies. However, there has not been any research focusing on the development of a planning and control system for the prefabricated home building industry that is unique in its nature due to the product variability and the prefabrication process. This study thus utilizes the RFID system as the data collection module and uses simulation and optimization models to generate the cost control module, and a real-time production tracking system.

#### **2.4 Flow Shop Scheduling Problem**

The flow shop scheduling problem has been a key area in the field of operations and production research. In a flow shop situation, all the jobs go through a set of machines sequentially. The sequencing of all jobs through a set of machines in the manufacturing line is a combinatorial optimization problem which is proven to be a non-deterministic polynomial-time hard (NP-hard) problem (Baker and Trietsch, 2009). To keep computational time to what is practically reasonable (especially when dealing with large problems), researchers have developed different heuristic rules to address this problem (Burns and Daganzo, 1987; Emory, 1983; Johnson, 1954). Several studies have been conducted which have sought to optimize job sequences in a flow shop configuration using simulation, genetic algorithm (GA), particle swarm optimization (PSO), tabu search, simulating annealing, and ant colony (Cagnina and Esquivel 2004; Leu and Hwang 2002; Li et al. 2004; Liu et al. 2010; Lu et al. 2008; Tasgetiren et al. 2004). Taha et al. (2011) have optimized job sequences and factory layout using a

GA for a job shop manufacturing plant. The optimization models were integrated with simulation to generate a virtual production line. Völker and Gmilkowsky (2003) have presented a method of creating a reduced simulation model to perform simulation-based optimization for medium term production scheduling. Liker (2004) has presented the concept of production levelling which is known as *Heijunka* in lean theory. According to *Heijunka*, the products are not produced based on actual customer order, but it takes all the orders for a period and generates a product mix in order to level the production.

However, these studies have focused on solving the flow shop scheduling problem with fixed activity time. In reality, uncertainty is an inherent part of the production process and few previous studies have tried to solve the scheduling problem with variable station cycle time. Beck and Wilson (2007) have developed a framework to solve the probabilistic job shop scheduling problem with branch-and-bound search and Monte Carlo simulation. They also used constraint programming and tabu search to solve deterministic scheduling and evaluated the solution candidates with Monte Carlo simulation. Wu et al. (2009) have represented the single-machine scheduling problem with variable processing time as a constraint model, and have developed three different models to minimize the risk of exceeding the mean flow time. Ranjbar et al. (2012) have used two branch-and-bound algorithms to optimize parallel machine scheduling in a stochastic environment. The current literature on this subject has not addressed the probabilistic flow shop scheduling problem for a large scale manufacturing project consisting of several machines in a series configuration. This thesis

investigates different optimization techniques in conjunction with discrete-event simulation (DES) to provide practical solutions to the flow shop scheduling problem in a stochastic environment for prefabricated home building industries.

## **2.5 Application of RFID Technology**

The RFID system has been used for the purpose of real-time data collection in the construction industry and manufacturing operations. RFID technology is a wireless sensor technology that can detect an electromagnetic signal for the purpose of proximity identification and data transaction. A typical RFID system includes an antenna, a reader, and a tag which is electronically programmed with unique identifier (Domdouzis et al. 2007). RFID has a similar concept to bar coding; however, it is superior in terms of non-optical proximity communication, information density, and two-way communication ability (Roberts 2006). RFID technology, and in particular its components (i.e., tags, reader, antenna) has been a prime focus of academic research in recent years, and more academic literature is expected on the industrial application of the RFID system (Ngai et al. 2008). Ferrer et al. (2011) have evaluated the use of RFID technology in a large remanufacturing job shop. The authors provided a framework for adopting the RFID system for the identification of components in the manufacturing process. Jaselskis et al. (1995) have presented the potential construction application of RFID technology, including concrete processing and handling, cost coding for labour and equipment, and material control. The authors have developed a conceptual design system for these applications and have concluded that RFID can save time, money, and effort in operational procedures and it is important to

learn about the technology prior to its implementation and also to involve the end users into the development process. Montasir and Moselhi (2012) have presented a method to automatically track the earthmoving operation using RFID technology. The method provided a practical and easy approach to estimate the productivity of the earthmoving operation. Guo et al. (2015) have proposed an RFID-based decision support system for production control and monitoring in a distributed manufacturing environment. RFID technology was used for real-time data acquisition and an optimization model was used to generate the production schedule. Huo et al. (2010) have proposed an RFID-based just-in-time (JIT) production system. This system can improve the Kanban system by increasing accuracy. Ngai et al. (2012) have described an RFID-based manufacturing process management system and implemented it in a garment manufacturing company. This type of system can help improve production line visibility, efficiency, and effectiveness. Arkan and Landeghem (2013) have presented an RFID-based RLTS (real-time location system) solution for multi-item work-in-process manufacturing facilities. The paper identified that the RFID-based RLTS system can provide up to date, automatically collected, rich and detailed shop floor data compared to traditional measurement tools. Ghanem and AbdelRazig (2006) have proposed an RFID-based model to track the progress of completed work on a construction site. Goodrum et al. (2006) have used RFID technology to develop a tool tracking and inventory system for construction job sites. Zhong et al. (2013) have presented an RFID-enabled real-time manufacturing execution system where RFID devices are installed on the shop floor to track the products and collect real-

time production data. In another work, Zhong et al. (2015) have used RFID technology to collect production shop floor data to obtain precise and reasonable estimates of advanced production planning and scheduling (APPS) model parameters such as arrival of customer orders, and standard operation times. In this thesis, RFID technology has been used to develop a real-time location system (RTLS) for a panelized wall production line, and to obtain production data in real time. The shop-floor data is used for simulation input modelling as well as model validation.

## **2.6 Simulation Model Verification and Validation**

Verification and validation are essential parts of the simulation modelling process. Simulation models are used as a decision support tool by replicating the real world scenario. Without verification and validation, though, the simulation model result cannot be reliable for decision-making purposes. According to Whitner and Balci (1989), errors in a simulation model can arise from a number of areas in the process, including input data, conceptual model, simulation model (implementation phase), and simulation model development environment. These errors can be identified and eliminated by the process of verification and validation. Carson (2002) has defined verification as the process of finding and fixing model errors—creating a properly functioning model based on the agreed upon assumptions and specifications. The validation process involves the model developer and others with knowledge of the real system working together to make sure the model represents the real system. Sargent (2010) has proposed the definition of model verification as “ensuring that the computer program of the

computerized model and its implementation are correct”, and model validation as “substantiation that a computerized model within its domain of applicability possesses a satisfactory range of accuracy consistent with the intended application of the model” (Sargent 2010, page 166). The primary goal of the verification process is to identify the errors that can occur in the model building process, such as logical errors, syntax errors, data errors, experimental errors, and bugs within the simulation environment (AbouRizk et al. 2015). Several verification techniques can be used, such as animation/visualization of the model, trace logs, entity counter, integrity check, investigation of input-output relations, and sensitivity analysis (AbouRizk et al. 2015; Sargent 2010). AbouRizk et al. (2015) have also outlined several validation approaches such as face validity, comparison to other models, degenerate tests, event validity, and historical data validation. The simulation model validation process is similar to the hypothesis testing in traditional research studies. This process attempts to demonstrate that the model is valid in its application domain. Sargent (2010) has also referred to this process as operational validity. In order to obtain a high degree of confidence in a simulation model and its results, it is important to perform both the verification and validation of the model. In this research, the simulation model is verified using input output analysis, static and dynamic testing to ensure an error free simulation model. Then the simulation model has been validated using actual data collected from the RFID.

# 3 Methodology

Figure 3.1 shows the overview of the proposed planning and control system for a prefabricated home building facility, including input parameters, main process, criteria, and model outputs. The main process consists of four modules: (1) a scheduling module (SCH); (2) a data collection module (RFID); (3) a simulation module (SIM); and (4) a financial module (FINC). These four modules are integrated in a central database to provide production scheduling, performance benchmarking, panel processing time, job cost, and other outputs based on the model inputs and criteria.

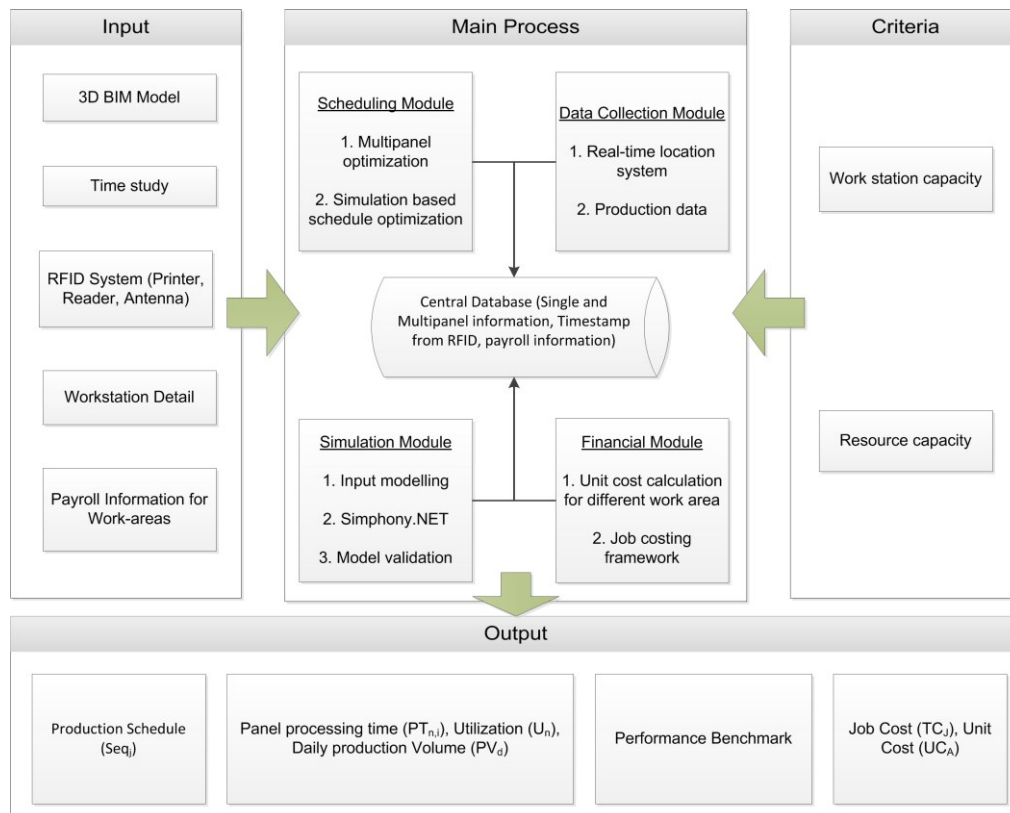


**Figure 3.1: Overview of the proposed method**

### 3.1 Scheduling Module

Formally, each of the four modules can be viewed as a vector-valued function which outputs a vector containing the information relevant to the module of interest. For instance, the scheduling module may be formalized as,

$$SCH: \left( \left\{ MP_{i,J} \right\}_{i=1,2,\dots,M_J}, \left\{ Seq_{i,J} \right\}_{i=1,2,\dots,M_J}, Q_J \right) = f \left( \left\{ SP_{i,J} \right\}_{i=1,2,\dots,N_J} \right) \quad (1)$$

Where  $\left\{ SP_{i,J} \right\}_{i=1,2,\dots,N_J}$  is the set of single-wall panels corresponding to job  $J$  whose characteristics, (e.g., length, width, number of studs, etc.), are extracted from the 3D BIM model;  $\left\{ MP_{i,J} \right\}_{i=1,2,\dots,M_J}$  is the set of multipanels obtained by concatenating selected single-wall panels;  $\left\{ Seq_{i,J} \right\}_{i=1,2,\dots,M_J}$  is the (optimal) sequence for assembling the multipanels; and  $Q_J$  is the quantity of material required for project  $J$ . To ensure utilization of the assembly stations, subsets of  $\left\{ SP_{i,J} \right\}_{i=1,2,\dots,N_J}$  are selected and combined (or concatenated) to form a multipanel object to be constructed as it moves along the assembly line. Multipanel objects are defined as,

$$MP_{k,J} = SP_{k_1,J} \parallel SP_{k_2,J} \parallel \dots \parallel SP_{k_n,J} \text{ and such that } L(MP_{k,J}) \leq L_{\max} \quad (2)$$

In which the operator  $\parallel$  represents the operation of concatenation of selected single-wall panels,  $SP_{k_1,J}, SP_{k_2,J}, \dots, SP_{k_n,J}$ , subject, however, to a maximum length  $L(MP_{k,J})$  not exceeding  $L_{\max}$  (representing the length of the assembly table). In addition to the set of multipanels, the scheduling function also outputs the optimal

multipanel assembly sequence  $\{Seq_{i,J}\}_{i=1,2,\dots,M,J}$  allowing bottlenecks to be avoided. This aspect is of particular importance since the stations of the assembly line do not have buffers that could prevent the propagation of a bottleneck. As in panelized home construction, the objects being processed are too voluminous; it is not practical to add a buffer line due to space constraints. The simulation-based production schedule optimization is presented in detail in later sections of this chapter.

### 3.2 Data Collection Module

The data collection/RFID module is dedicated to collecting data, i.e., time stamps, allowing the productivity of the assembly stations to be monitored. For this purpose, each wall panel is equipped with an RFID tag used to record the timestamps as it enters a station, cf. Figure 3.2.

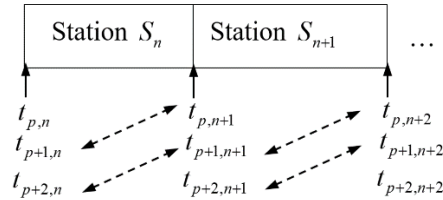


**Figure 3.2: Timestamps collection for wall panels at consecutive stations**

From the timestamps collected for each panel as it moves along the assembly line, idle time, i.e., the time during which a given station is in a starvation mode, can be calculated satisfying Equation (3),

$$IT_{p,n} = t_{p+1,n} - t_{p,n+1}, \quad p = 1, 2, \dots \quad (3)$$

where  $IT_{p,n}$  is the idle time associated with panel  $P$  at station  $n$ ;  $t_{p+1,n}$  and  $t_{p,n+1}$  are the timestamps corresponding to panel  $P+1$  entering the station and the previous panel (i.e.,  $P$ ) leaving it for station  $n+1$ , cf. Figure 3.2. At this juncture, it is important to note while idle time (i.e., starvation mode) can easily be calculated from the times indicating when each panel enters the workstations, the waiting time  $WT_{p,n}$  (i.e., the time a panel needs to wait because of a delay at the next station) cannot be directly calculated from the timestamps. To circumvent this difficulty, a filtering procedure is applied to the data collected at each station. However, because processing time varies based on the structural complexity of the wall panels, these are first clustered into categories based on the following attributes: (1) type (i.e., exterior, interior, or mechanical), (2) length, (3) width, (4) number of studs, (5) number of windows, and (6) number of doors. For instance, the processing time at station #1 for a set of  $10976\text{mm} \times 2476\text{mm}$  exterior walls with similar attributes led to the data shown in Figure 3.3.

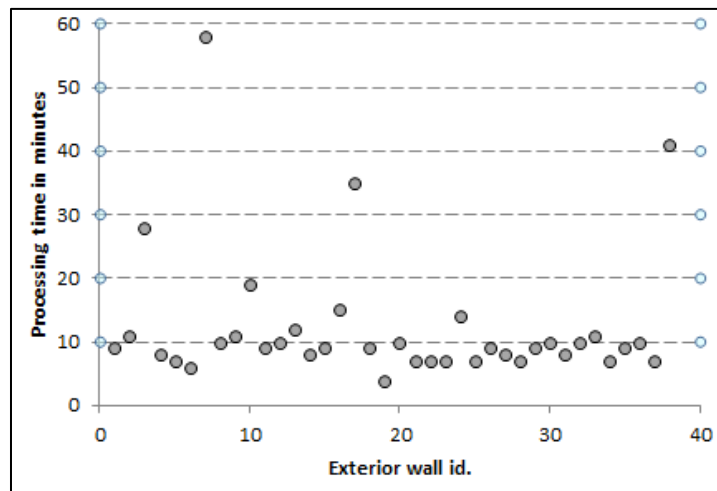


Figure 3.3: Processing time for a set of similar exterior wall panels at workstation no. 1

According to Figure 3.3, it is clear that the processing times fluctuate around some constant value similar to a (constant) signal which contains a noise component. This can be written as,

$$PT_{p,n}^{Real} = t_{p,n+1} - t_{p,n} = PT_{p,n}^{Productive} + N_{p,n}, \quad p = 1, 2, \dots \quad (4)$$

where  $PT_{p,n}^{Real}$ ,  $PT_{p,n}^{Productive}$  and  $N_{p,n}$  are, respectively, the measured processing time, the part of this time used to create value and the noise component (i.e., non-productive time) for panel  $P$  at station  $n$ . Given the similarity between the data in Figure 3.3 and the measurements of a noisy signal, filtering techniques from the field of digital signal analysis may help extract from the stations' data, the productive processing time. Furthermore, since data acquisition for this research was made in a real production setup, it was impossible to build a schedule which would indicate when data for a given panel type would be available, since the demand for panels is driven by homebuyers' orders. In this context, the most appropriate filtering method is probably the Kalman filter because it proceeds iteratively as measurements are collected. Rather than going into the general equations of Kalman filtering, it is more instructive to limit ourselves to the case at hand and provide the formulas associated with filtering a constant signal (the processing time at a given workstation in the context of this work) which satisfies Equation (4),

$$\begin{cases} PT_{k,n}^{Productive} = PT_{k-1,n}^{Productive} + W_{k,n} \\ Z_{k,n} = PT_{k,n}^{Productive} + V_{k,n} \end{cases} \quad (4)$$

The first equation, known as the evolution equation, describes the (productive) processing times (i.e., the signal)  $PT_{k,n}^{Productive}$  over time, which are essentially expressed as a difference equation contaminated by Gaussian noise  $W_{k,n}$ . As for  $z_{k,n}$ , it represents the measurement of  $PT_{k,n}^{Productive}$  contaminated by a Gaussian noise  $v_{k,n}$  (i.e., the timestamps varying because of waiting times). In essence, the Kalman filter tries to extract the productive processing times  $PT_{k,n}^{Productive}$  by correlating the (noisy) predictions of the signal with the (noisy) measurements  $z_{k,n}$  in such a way as to minimize the error (or equivalently, the root mean square). From a computer implementation perspective, Kalman's approach is built upon two sets of equations (i.e., prediction and correction) satisfying Equation 5,

$$\begin{cases} PT_{k,n}^- = PT_{k-1,n}^+ \\ P_{k,n}^- = P_{k-1,n} + Q \end{cases} \quad (5)$$

$$\begin{cases} K_{k,n} = P_{k,n}^- (P_{k,n}^- + R)^{-1} \\ PT_{k,n}^+ = PT_{k,n}^- + K_{k,n} (z_{k,n} - PT_{k,n}^-) \\ P_{k,n} = (1 - K_{k,n}) P_{k,n}^- \end{cases}$$

where  $PT_{k,n}^-$  is an estimate of  $PT_{k,n}^+$  which represents the filtered (or corrected) evaluation of  $PT_{k,n}^{Productive}$ . Similarly,  $P_{k,n}^-$  is the estimation of the corrected value  $P_{k,n}$ , which is used to define the Kalman gain  $K_{k,n}$  chosen in such a way as to minimize the error between the measurements  $z_{k,n}$  and the predictions. As for  $Q$  and  $R$ , they represent the variances of the Gaussian noises contaminating the

predictions and the measurements. These values are often selected empirically and adjusted to fine tune the filter. For instance, in the case where  $R = (0.1)^2$  and  $Q = 0.0$ , the data shown in Figure 3.3 is transformed into that of Figure 3.4,

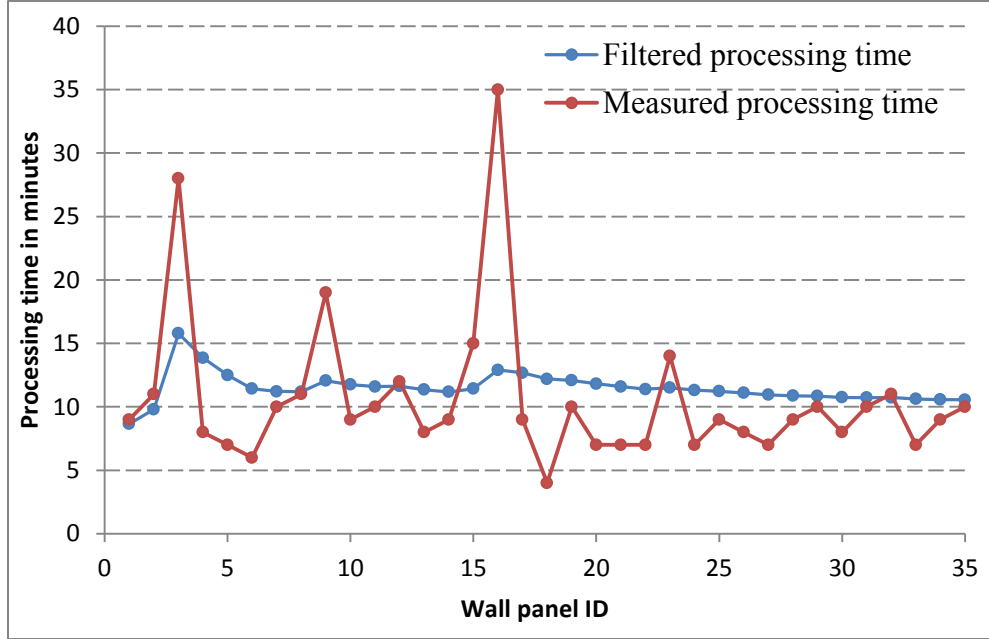


Figure 3.4: Application of the Kalman filter to noisy processing time data

According to Figure 3.4, after 35 iterations, the corrected (true) processing time obtained from the Kalman filtered data is approximately 10.45 minutes. Note that, even though a few of the data points in Figure 3.4 may appear as (extreme) outliers, their presence could be indicative of potential (lengthy) waiting times and their presence did not notably deteriorate the convergence of the Kalman filter. At this juncture it is important to note that relying on a single value to describe the productive processing time would implicitly ignore the natural variability that is inherent to manual work. As a result, it is necessary to analyze the differences  $(PT_{p,n}^{real} - PT_n^{Filtered})$  in order to avoid over estimating the waiting

time. In the context of this work, an empirical upper limit of the productive processing is defined to satisfy Equation (6),

$$PT_{p,n}^{Productive} \leq PT_n^{Filtered} + \min(Q_\pi, \bar{e} + t_{\alpha/2, N-1} \times SE) \quad (6)$$

where  $Q_\pi$  is the  $\pi^{th}$  percentile of the dataset  $\{PT_{p,n}^{real} - PT_n^{Filtered}\}_{p=1,2,\dots}$ ;  $\bar{e}$  is its average and SE the corresponding standard error. As for  $t_{\alpha/2, N-1}$ , it represents the t-distribution score associated with a two-sided  $100(1-\alpha)\%$  confidence interval. Even though it is practically impossible (in the current setup of data collection) to obtain the values of  $\pi$  and  $\alpha$  from first principles, the values  $\pi = 0.80$  and  $\alpha = 0.9$  are found to lead to acceptable limits for the productive processing times. At this juncture, combining the (filtered) productive processing times with the cumulated timestamp differences allows us to define a utilization metric satisfying Equation (7),

$$U_n = \frac{\sum_{p=1}^{p_{max}} PT_{p,n}^{Productive}}{\sum_{p=1}^{p_{max}} (PT_{p,n}^{real} + IT_{n,j})} \approx \frac{\sum_{p=1}^{p_{max}} PT_{p,n}^{real}}{ESL^*} \quad (7)$$

In which  $U_n$  is the utilization of workstation  $n$ ;  $PT_{p,n}^{real}$  and  $IT_{n,j}$  are, respectively, the (measured) processing time and idle time for panel  $P$  at the workstation  $n$ . As for  $ESL^*$ , it represents the effective shift length, which essentially is the regular shift from which lunch and break times are subtracted. It is important to note that in Equation (7), while the formulation using processing

and idle time is more accurate, it requires the knowledge of the productive processing times, which, in the current monitoring setup, are only accessible through filtering. In contrast, the second form uses the actual processing times  $PT_{p,n}^{real}$  (which may include waiting time) and the effective shift length to obtain an approximate value of the utilization, assuming waiting time is a rare event and is short compared to the productive processing time. In the context of this work, both formulations in Equation (7) will be compared in order to gain insight into the frequency and the length of waiting times.

While understanding the utilization of workstations is an important aspect for measuring the efficiency of the assembly stations, it is equally important (for scheduling purposes) to develop a mechanism for estimating the *takt* time associated with each panel category. In this respect, as the volume of panel- and station-specific data increases, it is possible to build probability models describing the processing times that include uncertainties due to the variability in manual work and waiting times. For the sake of simplicity, even though waiting times are correlated to the panel types downstream, since processing times can vary from one panel to another which may lead to an upstream delay, a waiting time, with an appropriate volume of data, will probably be captured in the probability model. As a result, a probability distribution describing the real processing times (i.e., timestamp differences) for each station and each panel category is built according to the general form in Equation (8),

$$PT_{n,P}^{real} \sim f_n(t; \{\lambda_k\}_{k=1,2,\dots}) \quad n = 1, 2, \dots \quad (8)$$

where  $\{\lambda_k\}_{k=1,2,\dots}$  is the set of parameters controlling the probability distribution  $f$ . The daily takt time for each workstation  $Tk_n$  can be calculated from real processing time and number of panels produced satisfying Equation (9),

$$Tk_n = \frac{\sum_{p=1}^{p_{\max}} PT_{p,n}^{real}}{\sum p}; \quad (9)$$

The productive processing times  $PT_{k,n}^{Productive}$  are subtracted from the actual processing time  $PT_{p,n}^{real}$  to estimate the waiting time  $\{PT_{p,n}^{real} - PT_n^{Productive}\}_{p=1,2,\dots}$  for different types of panel,  $P$ . A probability distribution model is developed for waiting time in the general form in Equation (10),

$$WT_{n,P} \sim f_n(t; \{\lambda_k\}_{k=1,2,\dots}) \quad n = 1, 2, \dots \quad (10)$$

The frequency of the waiting time  $F_n^{noise}$  at different workstations  $n$  is also calculated from the instances of noise observed  $n_s$  and the total number of observations  $N$  satisfying Equation (11). The waiting time percentage,  $WT_n^{percent}$ , and the idle time percentage,  $IT_n^{percent}$ , are calculated satisfying Equation (12) and Equation (13).

$$F_n^{noise} = \frac{n_s}{N} \quad n = 1, 2, \dots \quad (11)$$

$$WT_n^{percent} = \frac{\sum_{p=1}^{p_{max}} WT_{p,n}}{\sum_{p=1}^{p_{max}} (PT_{p,n}^{real} + IT_{n,J})} \quad (12)$$

$$IT_n^{percent} = \frac{\sum_{p=1}^{p_{max}} IT_{p,n}}{\sum_{p=1}^{p_{max}} (PT_{p,n}^{real} + IT_{n,J})} \quad (13)$$

A database has been designed to integrate RFID data  $PT_{p,n}^{real}$  and single-wall panel  $\{SP_{i,J}\}_{i=1,2,\dots,N_J}$ , multipanel  $\{MP_{i,J}\}_{i=1,2,\dots,M_J}$ , and sequence  $\{Seq_i\}_{i=1,2,\dots,M_J}$  information. The entity-relationship (ER) diagram is shown in Figure 3.5. Single-wall panel, multipanel, and PrintLog data tables are linked with the primary and foreign key relationship. The TagDetail table contains an RFID tag ID and time stamp  $t_{p,n}$  for panel  $P$  at workstation  $n$ . The TagDetail table is linked to the single-wall panel table via the PrintLog table. The sequence table contains the multipanel sequence for job  $J$ . The location tag table contains different workstation information to identify the panel location from the RFID system. The database is connected to the simulation model to provide multipanel, single-wall panel, sequence of multipanel, panel processing time distribution, and waiting time distribution into the simulation model.

### 3.3 Simulation Module

In the simulation model, workstation processing time is estimated based on task time study. In the task time study, a task time formula is developed based on the

time needed to perform each task for a given panel and station. The process time at each workstation is considered deterministic by splitting the entire task into sub-task groups. By modelling in this way, the probabilistic variation can be ignored and may be considered as almost deterministic (Halpin and Riggs, 1992). Equation (14) shows the developed task time formula for the workstation  $n$ .

$$T_{n,P}^{time} = t_{plate} + (n_{stud} \times t_{stud}) + (n_{Mstud} \times t_{Mstud}) + (n_{window} \times t_{window}) + (n_{door} \times t_{door}) + (n_{drill} \times t_{drill}) + (n_{cut} \times t_{cut}) + t_{refill} \quad (14)$$

where  $T_{n,P}^{time}$  is the total processing time for panel  $P$ ;  $t_{plate}$  is the time needed to place the top and bottom plates;  $t_{stud}$  and  $t_{Mstud}$  are the time needed to place single and multi-studs;  $n_{stud}$  and  $n_{Mstud}$  are the number of single-studs and multi-studs in panel  $P$ ;  $t_{window}$  and  $t_{door}$  are the time needed to place the window and door frame;  $n_{window}$  and  $n_{door}$  are the number of windows and doors in panel  $P$ ;  $n_{drill}$  and  $n_{cut}$  are the number of drill holes and cuts in panel  $P$ ;  $t_{drill}$  and  $t_{cut}$  are the time needed to drill holes and make a cut mark; and  $t_{refill}$  is the time needed to refill the nails.

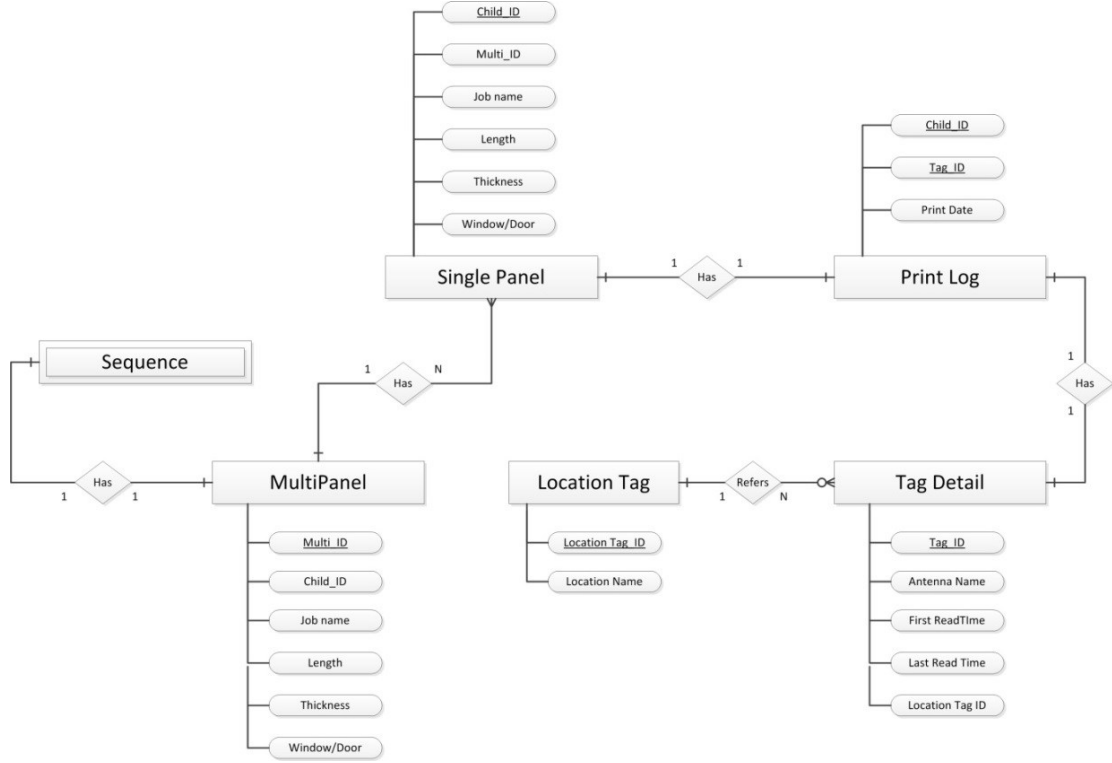


**Figure 3.5: Entity-relationship (ER) diagram**

The actual processing time collected from the RFID system is also used in some workstations where the amount of time a panel stays in the workstation is not dependant on the panel attributes as workers work on multiple panels simultaneously. A probabilistic model is developed based on the real processing time  $PT_n^{Real}$  to estimate the throughput time of these stations. The simulation module can be formalized as,

$$SIM : \left( U_n^{simulation}, TH_n^{simulation}, WT_n^{expected} \right) = f \left( \left\{ SP_{i,J} \right\}_{i=1,2,\dots,N_J}, \left\{ MP_{i,J} \right\}_{i=1,2,\dots,M_J}, \left\{ Seq_{i,J} \right\}_{i=1,2,\dots,M_J}, T_{n,P}^{time}, PT_{n,P}^{real} \sim f_n(t; \{ \lambda_k \}_{k=1,2,\dots}) \right) \quad (15)$$

The simulation model utilizes multipanel, single-wall panel, RFID data, task time formula, and production sequence to provide standard workstation utilization

$U_n^{simulation}$ , standard workstation throughput  $TH_n^{simulation}$ , and expected waiting time  $WT_n^{expected}$  for each workstation. The output from the simulation model is used for

performance benchmarking. Actual throughput  $\frac{\sum_{p=1}^{p_{max}} PT_{p,n}^{real}}{p}$  and standard throughput from simulation model as well as workstation utilization can be compared to measure the efficiency level as shown in Equations (16) and (17).

$$\frac{\sum_{p=1}^{p_{max}} PT_{p,n}^{real}}{p} > TH_n^{simulation} \quad \text{and} \quad U_n^{real} < U_n^{simulation} \rightarrow \text{low efficiency} \quad (16)$$

$$\frac{\sum_{p=1}^{p_{max}} PT_{p,n}^{real}}{p} \leq TH_n^{simulation} \quad \text{and} \quad U_n^{real} \geq U_n^{simulation} \rightarrow \text{high efficiency} \quad (17)$$

### 3.4 Simulation based production scheduling

The simulation model is integrated with an optimization algorithm for the purpose of production scheduling (sequencing of multipanel). Both simulation and optimization are used as decision-making tools in the construction and manufacturing industry. In simulation, the effects of changing different decision variables on a complex system are analyzed; where in the optimization model, a mathematical formula and/or heuristic rules are used to determine the optimal value of the decision variables to achieve the best output from the system. In a complex model, simulation models are used in the optimization algorithm as the fitness function to see the effect of different decision variables as the optimization

algorithm narrows toward the optimal solution. A simulation-based optimization problem can be written in a general form as,

$$\min_{x \in \Theta} f(x) \quad (18)$$

where  $f$  and  $x$  represent the objective function and decision variables subject to constraints  $x \in \Theta$ . In the multipanel scheduling problem, the objective function is to minimize the total production time and the changing variables are the different order of multipanels into the initial machine (framing station). The model constraints are captured within the simulation model, which include station capacity, resource availability, and required task time and production flow for panels. In a deterministic optimization problem, the objective function and model constraints are linear or non-linear; however, in a simulation optimization problem, objective function and/or model constraints involve randomness and exact evaluation is not possible. In the multipanel scheduling problem, the panel task time involves noise due to machine breakdown, manual task involvement, and other delays. This makes the constraint function in the optimization model random. The objective function of the simulation optimization problem with variable constraint function can be written as,

$$\begin{aligned} f(x) &= Ef(x, \xi), \text{ and} \\ \Theta &= \{x : Eg(x, \xi) \geq 0\} \end{aligned} \quad (19)$$

where  $\xi$  represents the randomness in the system,  $x$  is the set of decision variables,  $f(x, \xi)$  is the output of the simulation model for one replication,

$g(x, \xi)$  is the output of the model constraints for one replication. The expected value of the constraint function  $Eg(x, \xi)$  as well as the objective function  $Ef(x, \xi)$  can be estimated by running multiple replications of the simulation model. In the simulation-based optimization model, it is not possible to find the exact optimal solution of the problem; one can only obtain a good estimate of  $f(x)$ . Researchers have developed different techniques and tools to solve this problem such as sample average approximation, metamodeling, stochastic approximation and gradient estimation, ranking and selection, and random search methods (Jian and Henderson 2015). In the multipanel scheduling problem, two meta-heuristic algorithms, i.e., particle swarm optimization (PSO) and simulated annealing (SA), have been used as a searching method to obtain an optimal multipanel schedule that will minimize the overall production time. The optimization model follows the following rules. For each iteration,  $n = 1, 2, \dots$  :

1. Sample: choose a sampling strategy  $L_n$  based on the PSO and/or SA.

Sample a set of problem solutions  $x_n^1, x_n^2, \dots, x_n^{r(n)}$  in  $\Theta$  using  $L_n$  for multipanel,  $1, 2, \dots, r$ .

2. Evaluate: use the simulation model to estimate the total production time

$f(x_n^s), s = 1, 2, \dots, r(n)$  for a set of multipanels,  $s$ . From multiple simulation runs for the current solution (multipanel sequence), calculate an approximation of  $f'(x_n^s)$ .

From all possible solutions, the optimal set of multipanel sequence  $\hat{x}_n^1, \hat{x}_n^2, \dots, \hat{x}_n^{r(n)}$  is selected that gives the best estimate for the objective function  $f'(\hat{x}_n^s)$ , i.e., the minimum production time. In the implementation chapter, the proposed method is applied using PSO and SA; and, the effect of the number of replications in the simulation model to the optimization model runtime, and the result, is discussed.

### 3.5 Financial Module

To facilitate effective cost tracking for a prefabricated home building facility, the entire production process is divided into several work-areas  $A$  such as wall framing, exterior insulation, exterior wall finishing, stairs, decks and verandas, floors, roofs, roof shingling, material handling, and logistics. The financial module can be formalized as,

$$FINC: (UC_{A,p}, TC_J) = f(Q_J, PV_{A,d}^J, C_{A,p}^e) \quad (20)$$

where  $UC_{A,p}$  is the unit cost per work-area  $A$  for a pay-period  $p$ ,  $TC_J$  is the total cost of a job  $J$ . Each worker  $e$  in the production line is assigned to a specific work-area, and the labour cost  $C_{A,p}^e$  is tracked within the corresponding work-area for every pay-period. The RFID system provides daily production volume  $PV_{A,d}^J$  for every job  $J$  in work-area  $A$ , and total production volume per pay-period  $PV_{A,p}$  is calculated. Based on this information, the financial module

provides the unit cost for each work area satisfying Equation (21) where the total cost for a work-area per pay-period  $TC_{A,p}$  is calculated from Equation (22).

$$UC_{A,p} = \frac{TC_{A,p}}{PV_{A,p}} \quad (21)$$

$$TC_{A,p} = \sum_{e=1}^{e_{\max}} C_{A,p}^e \quad (22)$$

Daily percentage volume  $\tilde{P}V_{A,d}^i, i=1,2,\dots,J$  is calculated for every job based on Equation (23). The total cost of one job is calculated based on Equation (24), where total cost of material is calculated from quantity take-off,  $Q_J$ , and material unit price,  $UP_M$ ; labour cost is calculated from daily total cost per area,  $TC_{A,d}$ , and daily percentage volume for job,  $J$ .

$$\tilde{P}V_{A,d}^i = \frac{PV_{A,d}^i}{\sum_{J=1}^{J_{\max}} PV_{A,d}^i} \quad (23)$$

$$TC_J = \left\{ \sum_{d=1}^{d_{\max}} \tilde{P}V_{A,d}^J \times TC_{A,d} \right\} + \{Q_J \times UP_M\}, \quad d = day_1, day_2, \dots, d_{\max} \quad (24)$$

The integrated production planning and control system utilizes the BIM model to get panel information to optimize single-wall panels into multipanels, then production schedule is generated using simulation based optimization model. In production, RFID system provides real time location system and actual production data, finally after the completion of production, simulation model

provides performance evaluation and financial module provides labour cost associated to the job and unit cost for each work area.

# 4 Implementation and Results

---

The proposed methodology is implemented at ACQBUILT, Inc., a major production homebuilder based in Edmonton, Alberta. ACQBUILT has established a wood-frame panelized construction plant where open-wall panels (not including electrical and plumbing items), floor panels, and roof panels are produced, which are then transported on-site for assembly. This manufacturing facility is equipped with state-of-the-art computer numerical control (CNC) production lines capable of producing building framing components (walls, floors, roof, and stairs) for three homes in an 8-hour shift. As a part of ACQBUILT's continuing efforts to improve their construction process, both in the plant and on site, a research program has been initiated in conjunction with the University of Alberta which seeks to utilize advanced simulation techniques and optimization in order to improve the productivity of the panelized construction process. In this chapter, the overview of ACQBUILT's wall production process is presented, followed by the multipanel builder optimization model, RFID system implementation, simulation model development for wall panel production, simulation-based optimization, and cost control system.

## 4.1 Overview of the Wall Production Line

The wall prefabrication process at ACQBUILT, Inc. involves framing, sheathing, insulation, window and door installation, and loading operation. The wall production process is shown in Figure 4.1 and the detail tasks associated with each workstation are outlined in the following sections.

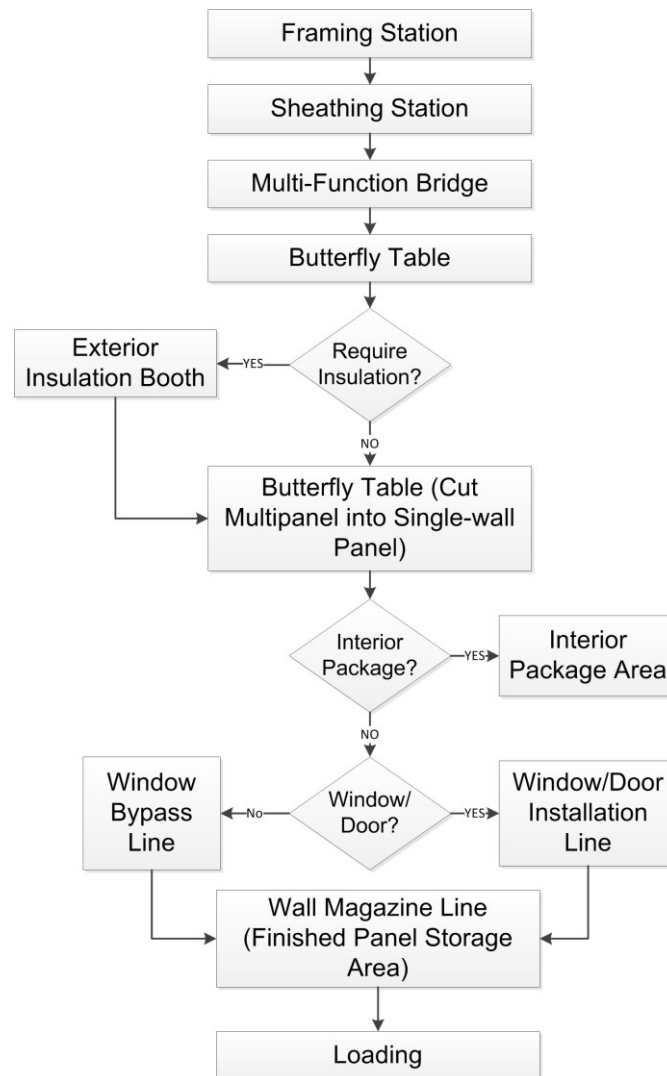


**Figure 4.1: Process map of wall production line**

#### **4.1.1 Framing station**

The wall panel production begins at the framing station (Figure 4.2), where exterior and interior walls are assembled using CNC machinery. Components

such as windows and doors are built in the component table station and fed to the framing station for the assembly. To maximize the utilization of the CNC table, the fabricated multipanels will be equal in length to the maximum length of the CNC table (40 ft). Most of the multipanels are generated by merging several single-wall panels together and can be up to 40 ft in length.

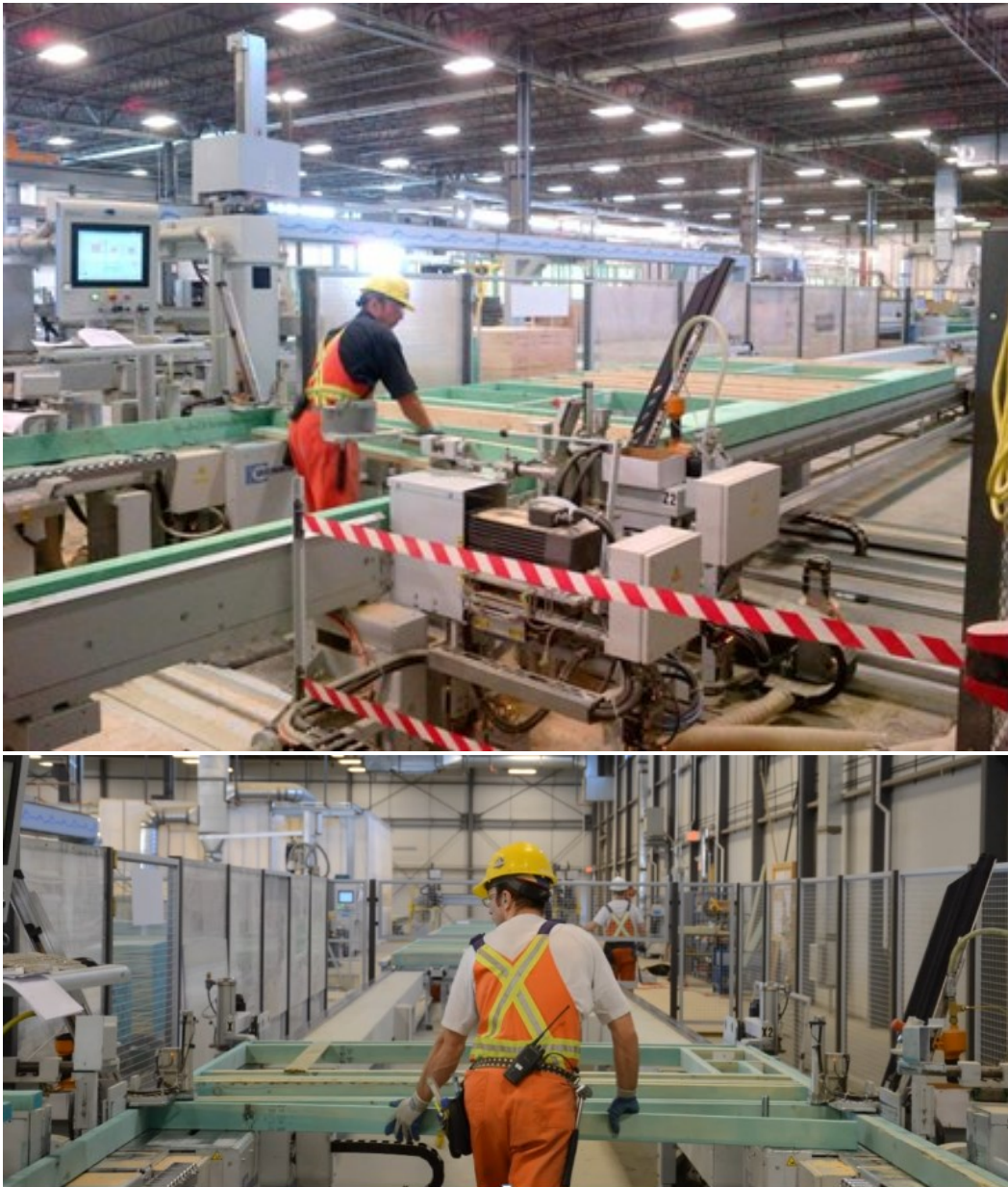


**Figure 4.2: Framing station (courtesy of ACQBUILT, Inc.)**

#### **4.1.2 Sheathing station**

From the framing station, the multipanels move to the sheathing station (Figure 4.3), which is divided into two 40 ft tables. At table-1, any error from the framing station is corrected and the wall panel name is marked. Then, a hook is placed for crane lifting, and building wrap is placed for a 2<sup>nd</sup> level wall panel. At table-2, sheets of sheathings are placed for exterior wall panels, and then the wall panel is moved to the multi-function bridge for machine nailing. Generally, four workers work in this area.

#### **4.1.3 Multi-function bridge**

At the multi-function bridge (Figure 4.4), exterior sheathings are nailed thoroughly by a CNC machine. This station is completely automated, and only requires one worker from the sheathing station to (i) bring the panel in, (ii) initiate the nailing process, and (iii) move the multipanel out.

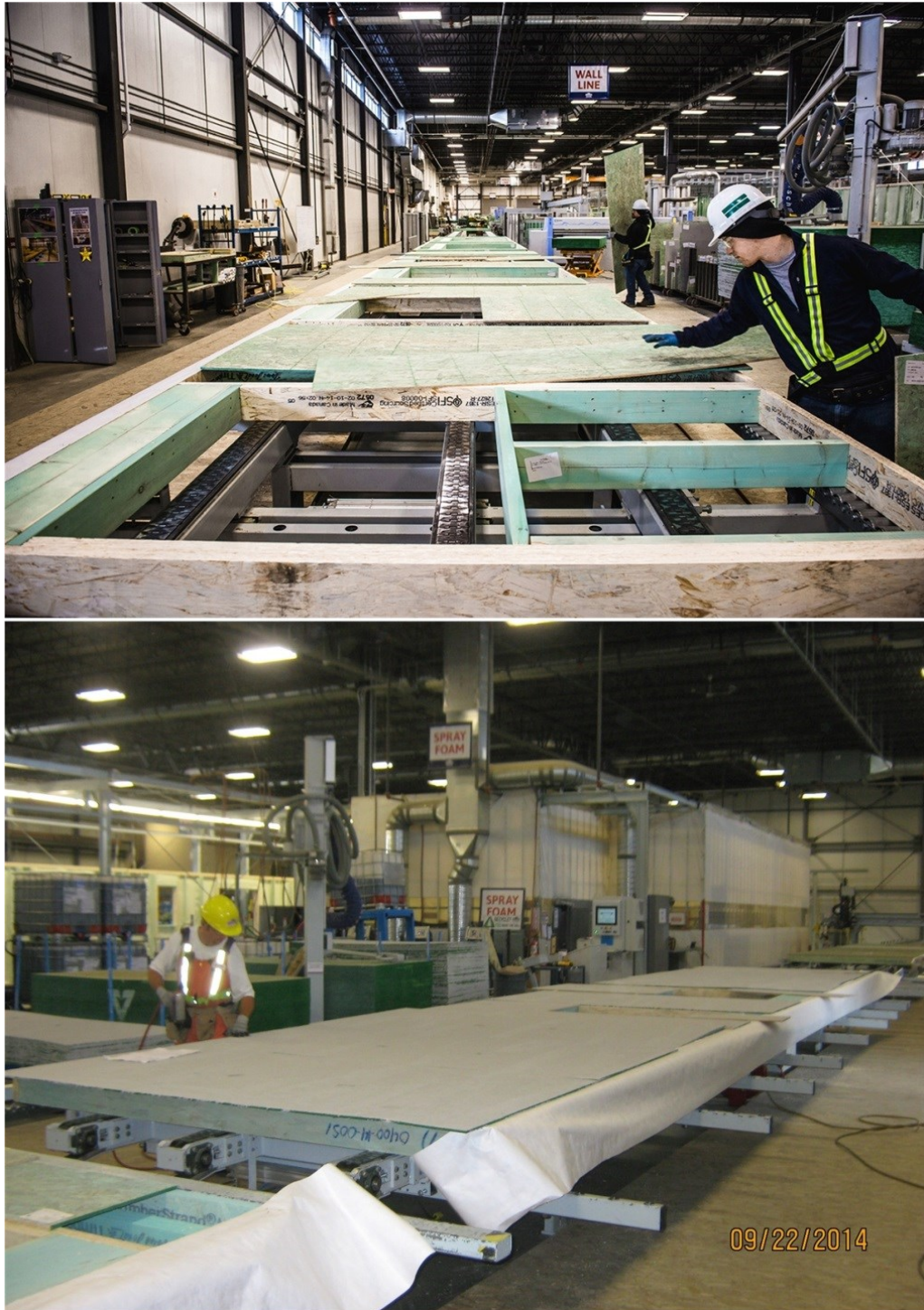


Figure 4.3: Sheathing station (courtesy of ACQBUILT, Inc.)



**Figure 4.4: Multi-function bridge (courtesy of ACQBUILT, Inc.)**

#### **4.1.4 Butterfly table station**

From the multi-function bridge, the multipanel moves to the butterfly table station (Figure 4.5). There are two tables in this area. The first table can rotate from horizontal to vertical position, and can transfer the wall panel to a second butterfly table that can also rotate. This table can move along the line to transfer the wall to different vertical lines based on the type of wall panel. Interior multipanels are cut into single-wall panels and short walls (less than 12 ft) are moved from the wall line as a package. Exterior wall panels are transferred to the exterior insulation booth. After the application of insulation, the butterfly table receives the multipanel from the insulation booth, and the process of cutting the multipanel into single-wall panels occurs. Exterior walls with no window/door opening as well as long interior and garage walls are transferred to the window bypass line

while exterior wall panels with window and door openings are moved to the window/door installation line.



**Figure 4.5: Butterfly table station (courtesy of ACQBUILT, Inc.)**

#### **4.1.5 Exterior insulation booth**

At the exterior insulation booth (also known as spray-booth), insulation is applied (by spraying) to the exterior multipanels (Figure 4.6). There are three spray lines that can hold up to three 40 ft multipanels. Three workers can simultaneously spray the multipanels. After spraying, multipanels are transferred to the butterfly table, in order to be routed for other activities.



**Figure 4.6: Exterior insulation booth (courtesy of ACQBUILT, Inc.)**

#### **4.1.6 Window/door installation line**

The window/door installation line (Figure 4.7) is 150 ft in length. In general, five workers work in this area. They install building wrap around the window opening, place and nail the window/door, apply insulation around the window, and secure the window by nailing a protection bar around it. After installing the window/door, the wall is transferred to the storage area known as the wall magazine line using a transfer cart.



Figure 4.7: Window/door installation line (courtesy of ACQBUILT, Inc.)

#### 4.1.7 Window bypass line

Long interior walls, garage walls, and exterior walls without window/door opening are placed in the window bypass line (Figure 4.8); this line is also 150 ft in length. Backings for kitchen cabinets, stairs, and toilet paper hangers are installed at this line. After processing, the walls are transferred to the wall magazine line using the transfer cart.



**Figure 4.8: Window bypass line (courtesy of ACQBUILT, Inc.)**

#### **4.1.8 Wall magazine line**

The wall magazine line is the work-in-process temporary storage area at the end of the wall prefabrication line. There are 13 storage lines (136 ft in length) that can hold wall panels vertically (Figure 4.9). This area helps to maintain production flow if on-site panel installation is delayed due to bad weather.

#### **4.1.9 Loading**

From the magazine line, wall panels are moved to a loading cart and are then attached to an overhead crane to be transferred into the trailer for transportation (Figure 4.10). Wall panels are loaded into the trailer bases on the site installation sequence: main floor panels are loaded first, followed by 2<sup>nd</sup> floor panels.



Figure 4.9: Wall magazine line (courtesy of ACQBUILT, Inc.)



Figure 4.10: Loading trailer (courtesy of ACQBUILT, Inc.)

## 4.2 Multipanel Optimization

### 4.2.1 Mathematical model

In order to combine single-wall panels into a multipanel,  $m$ , the single-wall panels,  $n$ , must all have identical heights,  $H_{n,m}$ , and thicknesses,  $T_{n,m}$ . There are also optional criteria which include the independent combination of exterior

walls, interior walls, and floors. Based on these criteria, single-wall panels are categorized into different batches; all single-wall panels within each batch are then optimized to build multipanels. The maximum length of a multipanel,  $L_{\max}$ , is defined by the user and is dependent on the length of the framing station and the maximum available length of the top and bottom plate of a wall. In the case where a multipanel length,  $L_{multi}$ , is less than a minimum length,  $L_{\min}$ , defined by the user, the wall is marked as a manually-built wall panel since the framing machine cannot build walls of this length. The objective function of the optimization model is to minimize the number of multipanels,  $N_{Multi}$ , and manual panels,  $N_{Manual}$ , in order to increase machine efficiency and maximize the average length of multipanels,  $L_{avg}$ , to reduce material waste. The decision variables,  $X_{ij}$ , are the different combinations of single wall panels,  $i$ . The optimization model is formulated as follows:

$$\text{Objective Function : } \min(N_{Multi}, N_{Manual}) \quad \max(L_{avg}) \quad (25)$$

$$\text{Decision Variables : } X_{i,j}, \quad i = \text{single wall}, j = \text{multipanel} \quad (26)$$

Subject to:

$$L_{multi} \leq L_{\max} \quad \text{and} \quad L_{multi} > L_{\min}; \quad H_{n_1, m} = H_{n_2, m} = \dots = H_{n_{\max}, m};$$

$$\text{and} \quad T_{n_1, m} = T_{n_2, m} = \dots = T_{n_{\max}, m}$$

The multipanel optimization process is based on a simulated annealing algorithm. To begin, wall panels are sorted based on their length (largest to smallest), and a multipanel is created with the first wall panel; here, the length is set as the current length. For the subsequent wall panel, if the sum of the current length and the next single-wall panel length is less than or equal to the maximum multipanel length, the two walls are combined together and the current length is set as the sum of the two lengths. If the sum of the two lengths is more than the maximum length, then a new multipanel is created with that single-wall panel and the length is set as the current length. Upon the completion of this process for all single-wall panels, the current fitness function is checked with the best fitness function; fitness check is described in the following pseudo code.

```
private void Check_Fitness()
{
    if (multipanel_count < best_multipanelcount)
        {update_best_fitness()
         no_improvement = 0;}
    else if (multipanel_count = best_multipanelcount & manualcount <
best_manualcount)
        {update_best_fitness()
         no_improvement = 0}
    else if (multipanel_count = best_multipanelcount & manualcount =
best_manualcount & avglength > best_avglength)
        {update_best_fitness()
         no_improvement = 0;}
    else
        no_improvement++
}
}
```

After the initial iteration, two randomly chosen wall positions are swapped to generate a neighbouring solution, and the same procedure is followed to generate the multipanel combination. However, if the fitness value of the neighbouring solution  $f_n$  is not better than the best fitness function  $f_b$  (i.e.,  $f_n - f_b \leq 0$ ),

rather than discarding the solution, an acceptance probability value is calculated based on Equation (27).

$$a = e^{-\frac{f_n - f_b}{T}} \quad (27)$$

where  $a$  is acceptance probability and  $T$  is temperature. The initial value of  $T$  is set as 1 and, after every iteration,  $T$  is decremented by a factor of 0.9 (i.e.,  $T^{k+1} = T^k \times 0.9$ ). After calculating the acceptance probability, it is compared to a randomly generated number between 0 and 1. If the acceptance probability,  $a$ , is greater than the random value, then the best fitness,  $f_b$ , is updated by the neighbouring solution,  $f_n$ .

$$\text{if } \{a > \text{Rand}(0,1)\} \rightarrow f_b = f_n \quad (28)$$

This process is repeated until there is no improvement made for 20 consecutive iterations. The initial values for *best\_multipanelcount* and *best\_manualcount* are set as very high numbers and *best\_avglength* is set as zero. The *no\_improvement* variable counts the consecutive iterations without any improvement. After each improvement, this variable is reset to zero. If there is a multipanel which is smaller than the user-defined minimum value, that multipanel is added to the next batch as a pseudo wall panel if the height and thickness match. After completing all batches, multipanels are created that are tailored to the parameters of the CNC machines, and panel information is stored in the database.

## 4.2.2 Results

The optimization results for different house models are summarized in Table 4.1, which shows the number of single-wall, multipanel, and manually-built wall panels, as well as the average length of the multipanels. The maximum length of a multipanel is set as the length of the framing station, which is 40 ft. The minimum length of a multipanel is set as 4 ft; all walls that are less than 4 ft in length must be built manually. Exterior and interior walls are optimized separately, and main floor walls are optimized first, followed by second floor walls.

**Table 4.1: Multipanel optimization result for different house types**

House Type	Single-Panel	Multipanel	Manually-built Wall	Avg. Length (ft)
Single-Family with Garage	52	18	0	31.59
Single-Family without Garage	43	12	0	35.28
Duplex	99	26	0	34.44
Town-home	71	21	0	34.68

The multipanel optimization result shows that the number of wall panels required to achieve a given level of production output at the framing station can be reduced by 65-73%, making the process more efficient. For example, the number of panel to be produced for single family house with attached garage is reduced from 52 to 18 panels, reducing the production quantity by  $[(52-18)/18]$  or 65%. If each panel requires 0.5 minutes set up time, the multipanel system can reduce framing station processing time by 15 to 36 minutes per job. Also, top and bottom plates are fed to the framing station in only one size (40 ft in length). In a single-wall panel

production system, plates are required in multiple sizes as the variability of panel length is high. The need to only supply one size of plate makes the material handling easier and also reduces material waste.

### **4.3 RFID System**

The data collection module is developed based on the RFID system as shown in Figure 4.11. The RFID system collects real-time production data to enable automated production monitoring and reporting, financial reporting, historical data collection, and simulation modelling. The RFID print file generated from the scheduling module feeds the RFID printer with single-wall panel names and job numbers, and a unique ID tag is assigned by the printer to each single-wall panel; this information is stored into the database. At the framing station, the framer attaches the associated RFID tag to each wall, and the antenna picks up the tag signal as the given wall passes through the read-zone. RFID antennas are installed at every workstation in order to capture the movement of each wall panel. The antennas are connected to an RFID reader through which timestamp data are captured into the database.

The RFID system at ACQBUILT's wall production line consists of five Motorola FX9500 RFID readers, 12 Motorola AN440 high performance dual antennas, and one Zebra ZD500R RFID label printer. Figure 4.12 shows four components of the RFID system at ACQBUILT's wall production line – RFID printer, tag, antenna and reader. Fig. 4.13 illustrates the RFID antenna and reader arrangement in the wall production line. There are five antennas installed at the entrance to the

framing table, buffer table, sheathing table, multi-function bridge, and tilt table. These five antennas are connected to one reader (R1) located near the sheathing table. In the first transfer cart, one main antenna (A6) and one location antenna (A7) are connected to a second reader (R2).

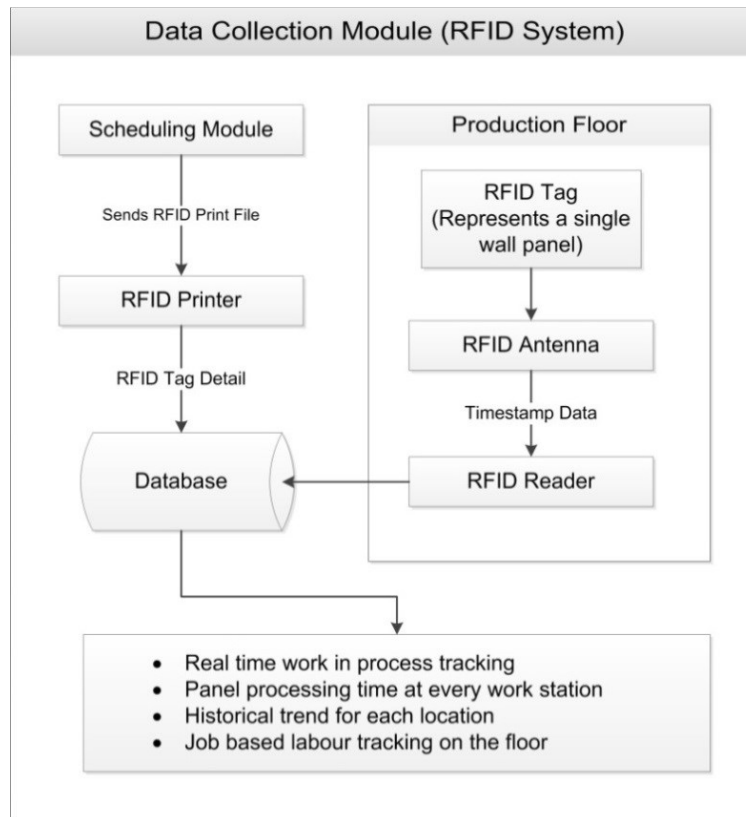


**Figure 4.11: Data collection module flowchart**

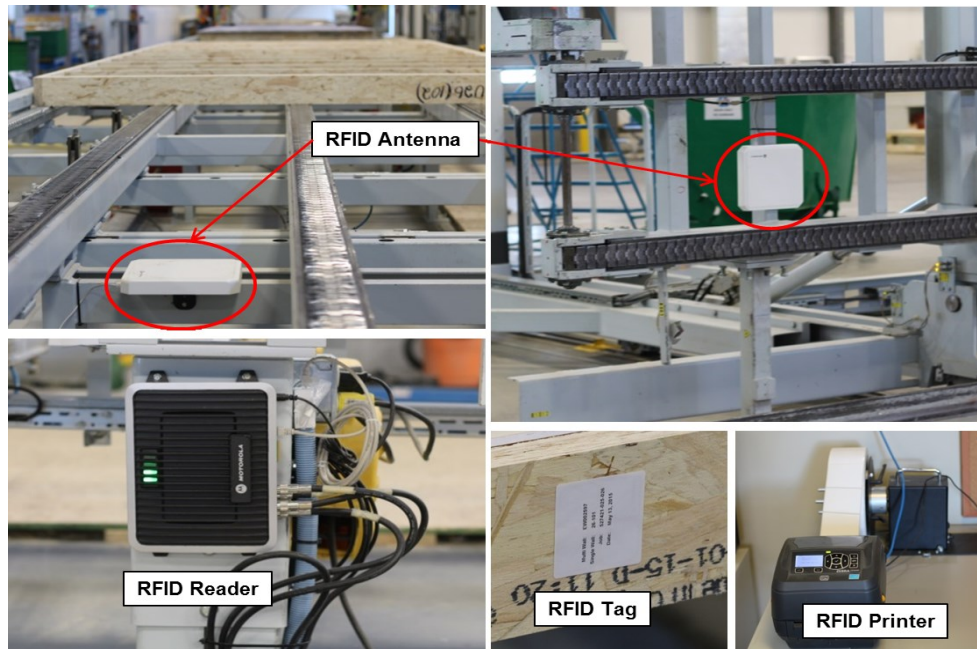


**Figure 4.12: RFID System at ACQBUILT, Inc.**

At the transfer cart, wall panels become vertical, and are then moved to one of five production lines. Three lines route to the spray-booth, one line is for window/door installation, and another line is for wall panels with no openings (referred to as the window bypass line). Each of these five lines has a permanent RFID tag installed at the front of the line floor; when the transfer cart is aligned with any of these lines, the location antenna picks up the location tag ID in order to identify the line, as shown in Figure. 4.14. This enables the RFID system to easily identify where the wall panel is being moved to from the transfer cart. The second transfer cart has a similar RFID instrumentation; however, there are two main antennas (A8 & A9) and one location antenna (A10) to record in and out times as a wall panel travels from right to left in the second transfer cart (as shown in Fig. 4.13). The location tags are used to identify the siding line and work-in-process storage lines. The loading cart has one antenna (A11) and one

reader (R4) to record the exit time from the work-in-process line. Another antenna (A12) and reader (R5) are installed at the end of the siding line to capture the exit time of the bump-out walls that are transferred to the trailer without the use of a loading cart.

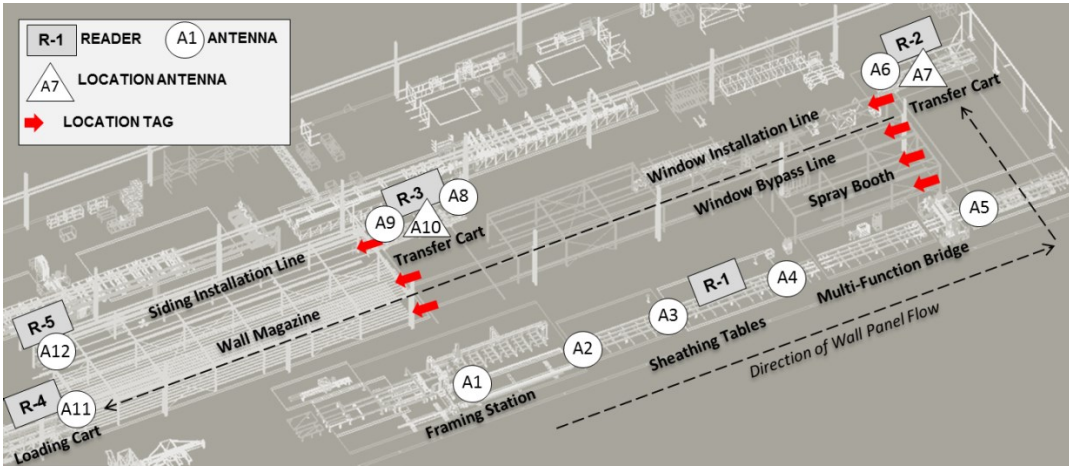


Figure 4.13: RFID antenna and reader location at the wall production line

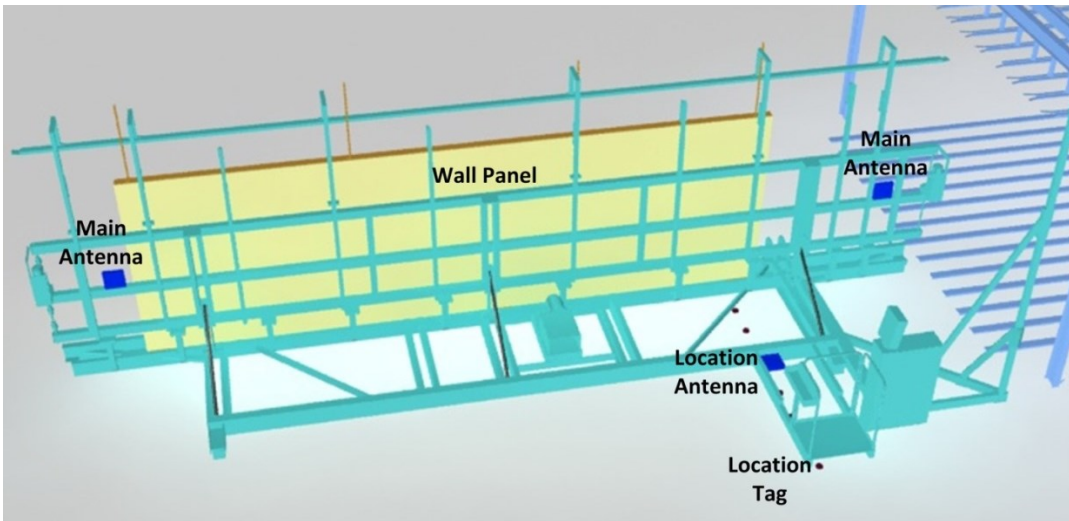


Figure 4.14: Transfer cart antenna arrangement detail

The RFID reader stores the timestamp data into the database in real time. The RFID database has four main data tables: (1) the PrintLog data table is populated at the time of RFID tag printing and stores the tag ID and associated panel name;

(2) the TagDetail data table contains the initial and last timestamp data for each tag ID for each antenna; (3) the ReaderAntenna is a static data table that holds the relationship between reader and antenna and the relationship between location antenna and main antenna; and (4) the LocationTag data table contains the permanent RFID location tag information for identifying the line number. Structured query language (SQL) is used to extract the necessary panel information from the database. Figure 4.15 shows an example query table of the database where timestamp values and location (if applicable) at different antennas (A1, A2, A6, A12...) are recorded in the TagDetail data table, and multipanel name and single-wall panel name are recorded in the PrintLog data table.

TagID	Multipanel	SinglePanel	InitialRead	LastRead	AntennaDescription	Location
3025015111012220000	EXT-14_1102-15-1821_00	00-104	11/10/15 4:48 PM	11/10/15 4:50 PM	A1	
59235115121011000000	MEC-42_10ATR-15-0033_00	00-114	12/10/15 2:15 PM	12/10/15 2:17 PM	A1	
101309115122112000000	EXT-24_10DES-15-0038_00	00-111	12/22/15 8:52 AM	12/22/15 8:53 AM	A1	
210897915110507000000	FW-INT-22_1003-15-4748_47	47-005	11/6/15 7:35 AM	11/6/15 7:35 AM	A1	
224753015122112000000	EXT-22_10DES-15-0038_00	00-201	12/22/15 9:23 AM	12/22/15 9:24 AM	A1	
240138515081112000000	EW-2_0100-14-1092_00	00-105	8/12/15 11:17 AM	8/12/15 11:18 AM	A1	
555064715102014000000	EXT-9_0400-15-0067_00	00-102	10/22/15 9:13 AM	10/22/15 9:14 AM	A1	
693768815111813000000	EXT-11_0400-15-0009_00	00-102	11/18/15 1:44 PM	11/18/15 1:45 PM	A1	
87921048641602000000000	EXT-12_0400-15-0069_00	00-204	2/8/16 2:04 PM	2/8/16 2:09 PM	A2	
26909550311602000000000	EXT-12_0400-15-0069_00	00-201	2/8/16 2:04 PM	2/8/16 2:04 PM	A2	
49948908631602000000000	INT-3_0400-15-0069_00	00-111	2/8/16 1:46 PM	2/8/16 1:46 PM	A2	
88936410311602000000000	INT-3_0400-15-0069_00	00-110	2/8/16 1:46 PM	2/8/16 1:46 PM	A2	
75080712261602000000000	INT-3_0400-15-0069_00	00-105	2/8/16 2:23 PM	2/8/16 2:23 PM	A6	SprayLine-1
69442315831602000000000	EXT-9_0400-15-0069_00	00-115	2/8/16 2:22 PM	2/8/16 2:22 PM	A6	SprayLine-2
50022600411602000000000	EXT-21_0400-15-0069_00	00-107	2/8/16 2:19 PM	2/8/16 2:19 PM	A6	SprayLine-3
72550304731602000000000	EXT-23_535413-003-004_003	00-105	2/8/16 12:43 PM	2/8/16 12:43 PM	A6	Bypass Line
61802413661602000000000	EXT-23_535413-003-004_003	00-113	2/8/16 12:42 PM	2/8/16 12:42 PM	A6	WindowLine
83826410321602000000000	EXT-23_535413-003-004_003	00-102	2/8/16 12:42 PM	2/8/16 12:42 PM	A6	WindowLine
89440117971602000000000	EXT-23_535413-003-004_003	004-116	2/8/16 12:42 PM	2/8/16 12:42 PM	A6	WindowLine
47066624881602000000000	EXT-10_1102-15-1818_00	00-103	2/8/16 8:38 AM	2/8/16 8:39 AM	A12	Line 1
47066624881602000000000	EXT-10_1102-15-1818_00	00-103	2/8/16 8:38 AM	2/8/16 8:38 AM	A12	Line 2
47066624881602000000000	EXT-10_1102-15-1818_00	00-103	2/8/16 8:37 AM	2/8/16 8:38 AM	A12	Line 3
15846163001602000000000	INT-27_535413-003-004_003	004-114	2/8/16 2:16 PM	2/8/16 2:17 PM	A12	Line 8
59963321211602000000000	INT-18_535413-003-004_003	004-136	2/8/16 2:14 PM	2/8/16 2:14 PM	A12	Line 9
54833664661602000000000	EXT-26_535413-003-004_003	003-109	2/8/16 2:10 PM	2/8/16 2:10 PM	A12	Line 9
98783590131602000000000	INT-42_535413-003-004_003	003-122	2/8/16 2:09 PM	2/8/16 2:10 PM	A12	Line 9
57290187781602000000000	INT-41_535413-003-004_003	004-123	2/8/16 2:06 PM	2/8/16 2:06 PM	A12	Line 9
79510240901602000000000	FW-INT-40_535413-003-004_003	004-026	2/8/16 2:02 PM	2/8/16 2:02 PM	A12	Siding Line 10
91235047011602000000000	EXT-38_535413-003-004_003	004-218	2/8/16 1:40 PM	2/8/16 1:40 PM	A12	Siding Line 13
79432726901602000000000	INT-18_535413-003-004_003	004-104	2/8/16 1:22 PM	2/8/16 1:22 PM	A12	Siding Line 11

Figure 4.15: Screenshot of query table containing timestamps values

### 4.3.1 Real-time location tracking

The RFID system is used to track the wall panel location in real time throughout the wall production line. Figure 4.16 shows the panel tracking interface which reads the database to obtain the latest wall panel location. This enables the production controller to track or search a wall panel within the production line. Also, the available capacity of each wall magazine line can be tracked separately as shown in Figure 4.17. For each line, current occupied length and available length are shown as well as the list of jobs that are currently located in that line. For any job, information such as the number of panels scheduled, in-process, and complete/loaded can be generated from the system.

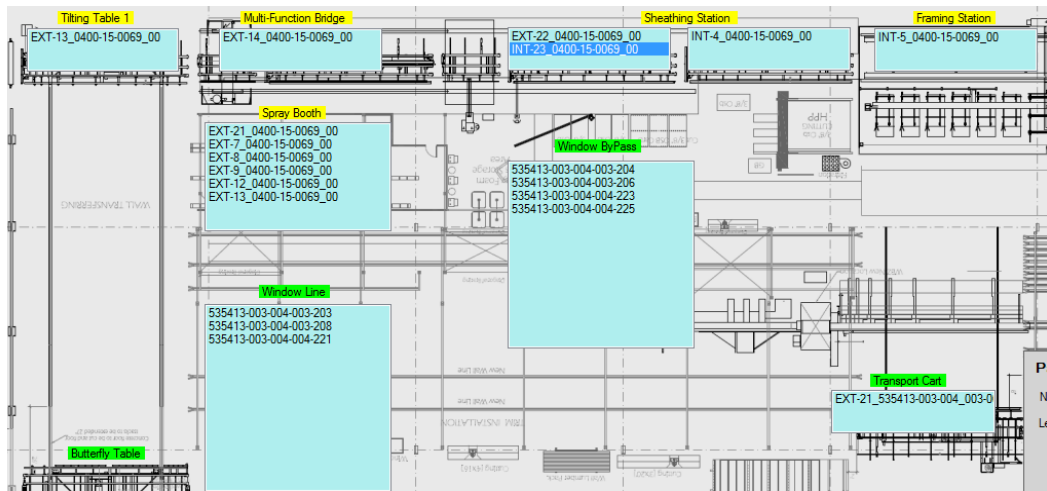


Figure 4.16: Real-time wall panel tracking system

Magazine	Current Length(ft)	Available Length (ft)	Job 1	Job 2
Line-1	0	136		
Line-2	119	17	30DES-15-0058-0071	
Line-3	129	7	1102-15-1818	535413-003-004
Line-4	120	16	30DES-15-0058-0071	
Line-5	102	34	30DES-15-0058-0071	
Line-6	101	35	30DES-15-0058-0071	
Line-7	136	0	30DES-15-0058-0071	
Line-8	95	41	535413-003-004	
Line-9	63	73	535413-003-004	
Line-10	114	22	1102-15-1818	535413-003-004
Line-11	130	6	10ATR-15-0034	535413-003-004
Line-12	73	63	535413-003-004	
Line-13	110	26	10ATR-15-0034	30DES-15-0058-0071

**Figure 4.17: Wall magazine capacity detail**

#### **4.3.2 Production data analysis**

The production data generated from the RFID system is used to calculate takt time, idle time, panel processing time, waiting time, utilization, daily production volume, daily volume per job and historical trend analysis. As mentioned in the methodology chapter, the RFID data is filtered using the Kalman filtering process in order to separate the noise component from the actual data. This process is only applicable to the first three workstations—framing, sheathing, and multi-function bridge—where one multipanel is processed per workstation. In the spray-booth, window installation line, and window bypass line, the workers have the ability to move from one panel to another in order to work on multiple panels simultaneously, as the capacity of these workstations in terms of panel length is up to 150 ft. The amount of time a wall panel stays in these workstations is not only dependent on its own attributes, but it also largely depends on those of the panel ahead of it in.

In order to apply Kalman filtering, the processing time data is clustered into different groups based on panel attributes. However, there are many different factors that can contribute to the processing time of a panel. To keep the filtering process simple, wall panels are divided into two main groups—exterior walls and interior walls. Each group is then divided into sub-groups based on their lengths.

Figure 4.18 show the actual processing time  $PT_{n,p}^{real}$  and filtered processing time  $PT_{n,p}^{Filtered}$  at the framing station for a sub-group—exterior multipanels from 20-30 ft.

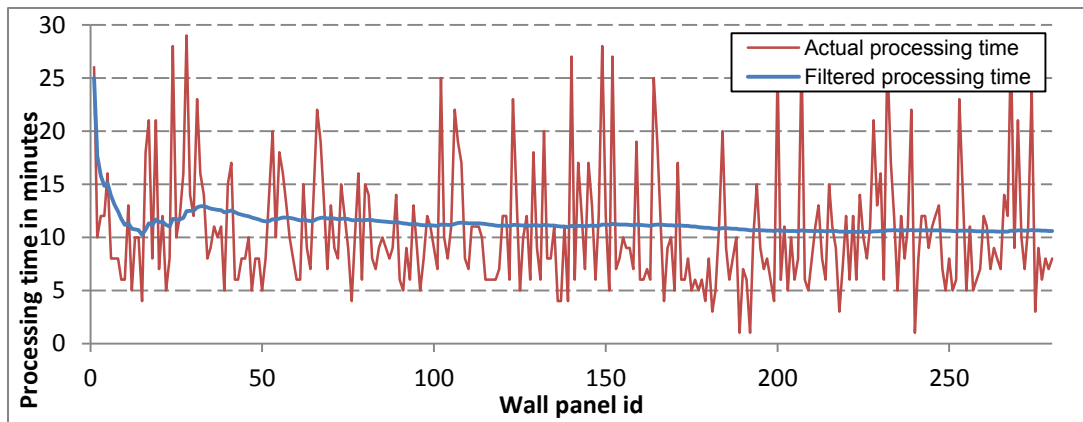


**Figure 4.18: Actual versus filtered processing time at framing station for exterior multipanel from 20 ft to 30 ft**

The filtered processing time is calculated based on Equation (5). Then an empirical upper limit for productive processing time is calculated based on Equation (6). Table 4.2 shows the Kalman filter and upper limit,  $UL_{n,g}$ , of different multipanel sub-groups for the framing station. This information is used to estimate productive processing time,  $PT_{n,p}^{productive}$ . Figure 4.19 shows the productive processing time, idle time, and waiting time of multipanels produced

in one day. If  $PT_{n,p}^{real} > UL_{n,g}$ , the difference is regarded as waiting time/delay; otherwise  $PT_{n,p}^{productive} = PT_{n,p}^{real}$ . The idle time is calculated based on Equation (3). Table 4.3 summarizes the takt time,  $Tk_n$ , utilization,  $U_n$ , waiting time percentage,  $WT_n^{percent}$ , and idle time percentage,  $IT_n^{percent}$ , at the framing station for different days satisfying Equations (9), (7), (12), and (13), respectively. Two utilization values are calculated;  $U_n^{real}$  is based on productive time,  $PT_{n,p}^{productive}$ , and  $U_n^{Productive}$  is based on  $PT_{n,p}^{real}$  and entire shift length (ESL), as shown in Equation (7). Actual utilization,  $U_n^{real}$ , and filtered utilization,  $U_n^{Productive}$ , values are compared in Figure 4.20. The result shows that the utilization of a workstation can be over calculated if real processing time is used without applying any filtering procedure.

**Table 4.2: Filtered value and upper limit of different sub-groups of multipanels for framing station**

Subgroup	Kalman Filter (minutes)	$\min(Q_\pi, \bar{e} + t_{\alpha/2, N-1} \times SE)$	Upper Limit (minutes)
EXT >35	12.50	0.50	13.01
EXT 30-35	10.59	0.66	11.25
EXT 20-30	9.57	0.71	10.29
EXT <20	7.84	0.68	8.52
INT >35	10.93	0.27	11.20
INT 30-35	10.55	0.64	11.19
INT 20-30	8.08	0.61	8.69
INT <20	5.85	0.38	6.23

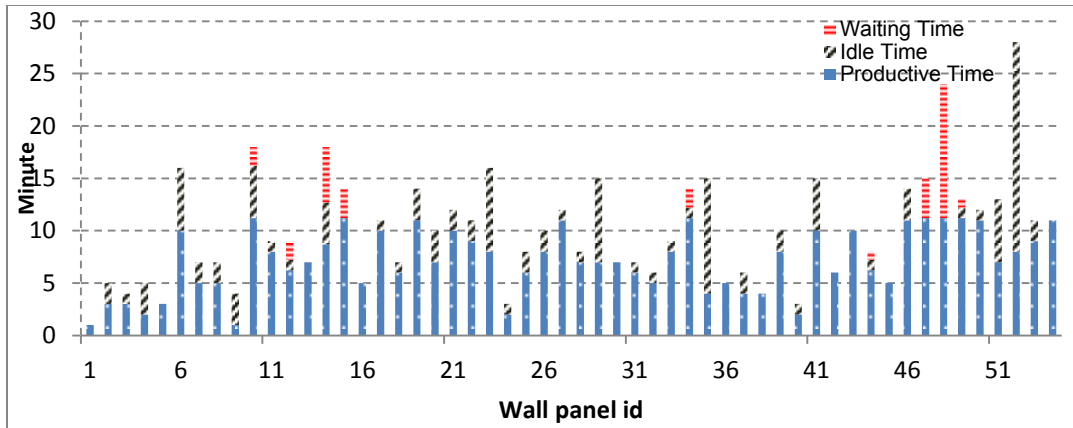


Figure 4.19: Framing station throughput time breakdown

Table 4.3: Framing station productivity detail

Obs.	$Tk_n$	$U_n^{real}$	$U_n^{Productive}$	$WT_n^{percent}$	$IT_n^{percent}$
1	7.44	78%	68%	13%	22%
2	7.70	77%	71%	8%	23%
3	7.19	79%	71%	8%	23%
4	8.96	81%	71%	13%	19%
5	7.83	78%	74%	5%	23%
6	8.65	68%	53%	21%	32%

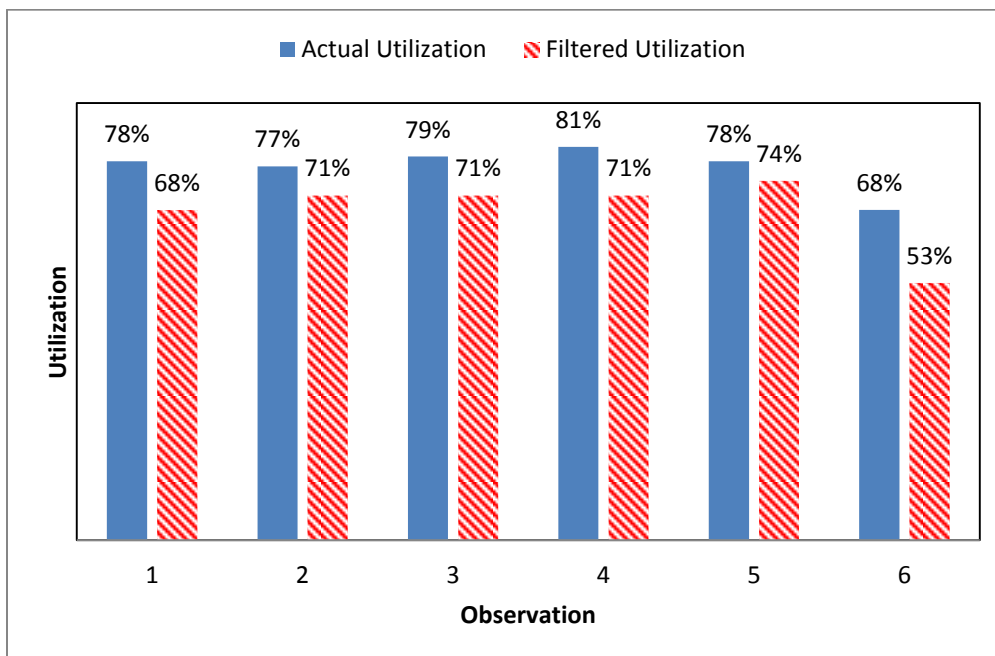


Figure 4.20: Actual and filtered utilization comparison

Table 4.2 shows that the productive processing time at framing station increases as the multipanel length increases, which validates the Kalman filtering process. However, one of the limitations of Kalman filtering is that, if the waiting time occurs frequently, it can overestimate the filtered value. The upper limit value for each type of panel can be adjusted based on simulation data in order to obtain better production data from the RFID system. As the proposed setup of the RFID system cannot distinguish the waiting time and productive processing time, the Kalman filter can provide an approximation of the processing time that can be used to calculate the workstation utilization.

From historical actual processing time data  $PT_{n,p}^{real}$  collected from the RFID system, a probabilistic model is developed for workstation takt time based on Equation (8). The distribution type and parameter for exterior and interior wall takt time at different workstations are presented in Table 4.4. Similar probabilistic models can be developed for panel waiting time based on Equation (10); Figure 4.21 shows the probability density function (PDF) and distribution parameter for exterior panel waiting time at the framing station. The noise/waiting time frequency of the exterior panel at the framing station is also calculated ( $F_n^{noise} = 31\%$ ) from instances of noise observed  $n_s = 462$  and total number of observations  $N = 1464$ , satisfying Equation (11).

**Table 4.4: Probabilistic model of workstation takt time**

Workstation	Wall Type	Sample Size	Distribution Type and Parameter
Framing	Exterior	848	Beta (0.73, 2.24, 45.00, 6.10)

Sheathing	Interior	1,260	Beta (0.72, 6.33, 67.00, 3.79)
	Exterior	930	Beta (1.26, 4.79, 54.7, 5.96)
Multi-function bridge	Interior	1,273	Beta (0.83, 6.00, 67.43, 2.83)
	Exterior	909	Lognormal (2.33, 0.62)
Spray-booth	Exterior	240	Triangular (63.14, 0.76, 46.37)
Window/Door installation	Exterior	815	Triangular (317.00, 11.00, 141.00)
Window bypass	Both	1,058	Gamma (46.84, 1.79)

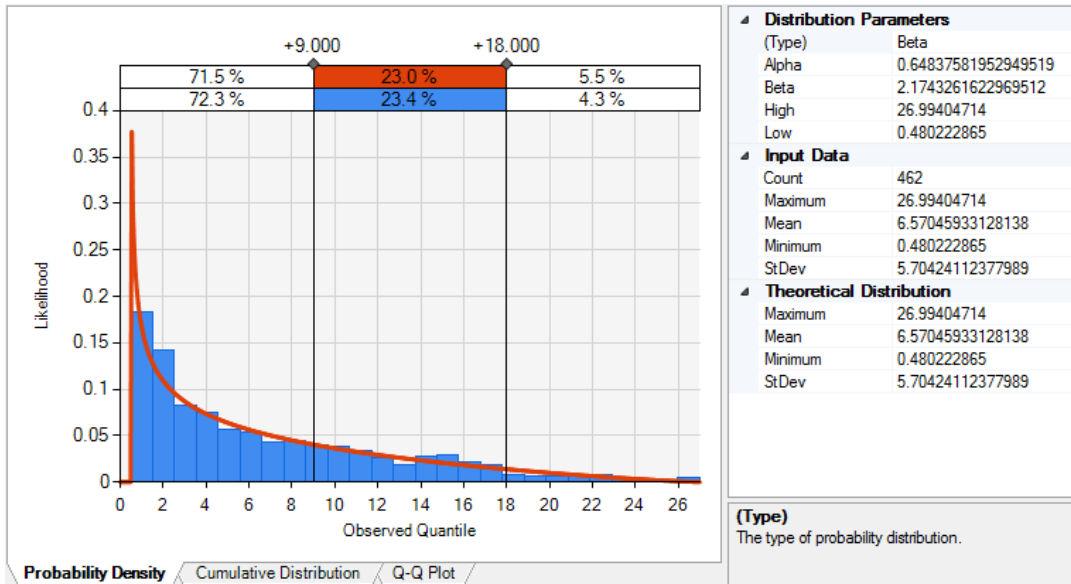


Figure 4.21: Probability distribution function of exterior wall waiting time at framing station

#### 4.4 Simulation Model Development

A simulation model is developed for ACQBUILT’s wall prefabrication process.

The information flow within the simulation module is shown in Figure 4.22. Wall

panel information  $\{SP_{i,j}\}_{i=1,2,\dots,N_j}, \{MP_{i,j}\}_{i=1,2,\dots,M_j}$  is fed into the simulation model

from the scheduling module through the central database. Also, the historical

panel processing time,  $PT_{n,p}^{real}$ , from the RFID system and time study are used for

simulation input modelling. Symphony.NET is used as the simulation modelling

environment and actual RFID data is used for model validation. The final model is integrated with the multipanel schedule optimization model, and also provides a performance benchmark for standard production performance. Simulation input modelling is divided into two parts—task time formula and panel information, which are described in detail in the following sections.

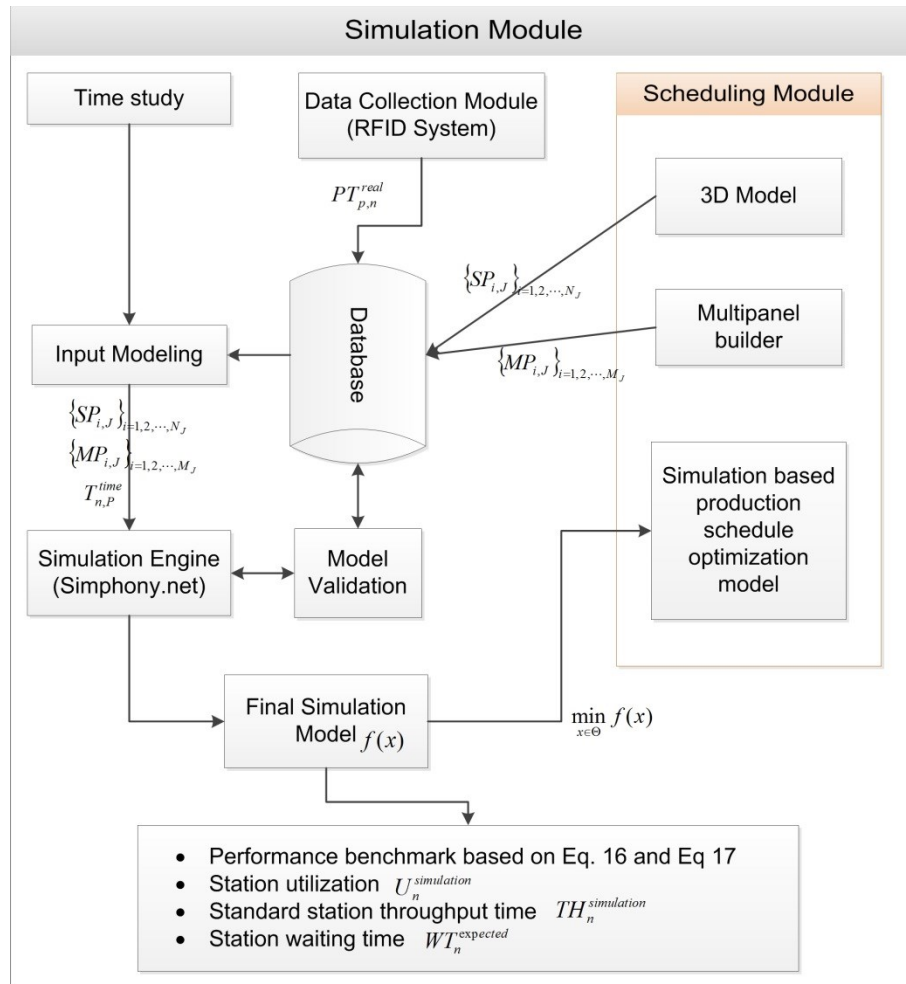


**Figure 4.22: Simulation module information flow**

#### 4.4.1 Input modelling - Task time formula

In order to estimate the panel processing time, a time study is conducted at the framing station, sheathing station, and multi-function bridge. Every task that takes

place in these workstations is observed and timed. The task duration depends on different panel attributes such as length, number of studs, window, blocking, sheets of sheathing, nailing line, and so on. Some examples of the task time formula are shown in Table 4.5. As the CNC machine carries out most of the task at the framing station and the multi-function bridge, there is little variability in the task time. Although, the sheathing station is driven by manual workers, thus the process time for each task can be considered deterministic by splitting the entire task into sub-task groups. By following this approach, the probabilistic variable can be ignored and may be considered almost deterministic (Halpin and Riggs, 1992). During the time study, the duration of individual delay is observed, and the distribution for delay time and the probability of delay occurrence are calculated. This delay information is added to each workstation as a stochastic element.

**Table 4.5: Example of task time formula for different tasks of wall prefabrication process**

Task Name	Task Time Formula (minutes)	Workstation
Nail single stud	$0.15 * \text{Number of single studs}$	Framing station
Nail double stud	$0.34 * \text{Number of double studs}$	Framing station
Nail window frame	$1.28 * \text{Number of windows}$	Framing station
Install hooks	$0.50 * \text{Number of drill holes}$	Sheathing station
Place and nail sheathings	$1.60 * \text{Number of sheets}$	Sheathing station
Nail sheathings (CNC machine)	$1.16855 + \text{Nailcount} * .002102538 + \text{Nailline} * 0.026392405$	Multi-function bridge
Move wall from one station to another	$0.50 * \text{Number of panels}$	n/a

From the actual time data collected from the RFID system, it is noted that the time a wall panel remain at the spray-booth and the window/door installation area is

not dependent on the panel attributes such as spray area and number of window and door openings. As mentioned in an earlier section, multiple wall panels can be processed simultaneously in these workstations, and the time a wall panel remain in that station is also dependent on the panel at the front of the line. The task durations at these workstations are estimated based on historical data.

Figure 4.23 shows the probabilistic density charts of the panel processing time at the spray-booth and the window/door installation area. The task time estimation for each workstation is validated by comparing the simulated time with the actual time.

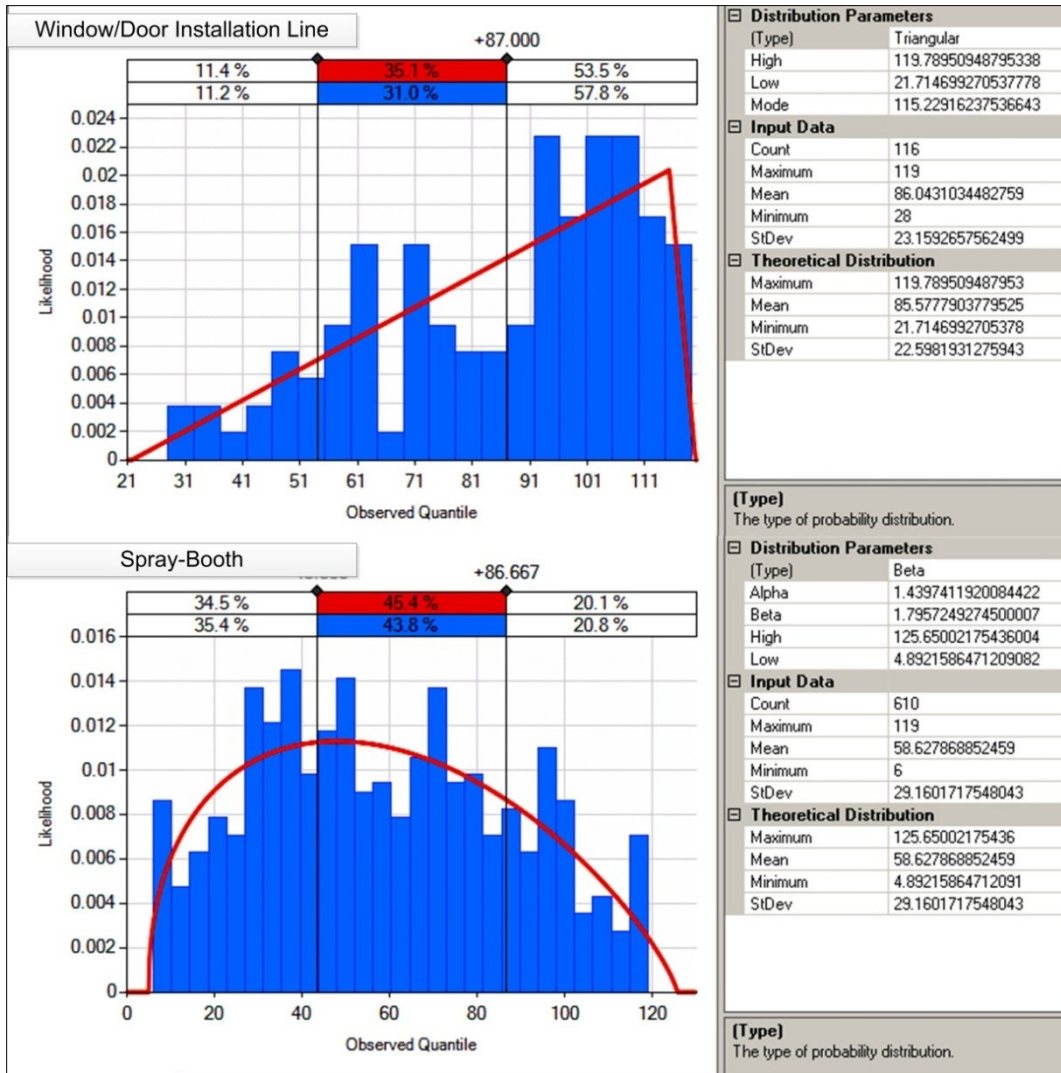


Figure 4.23: Probabilistic density chart for window and spray-booth area processing time

#### 4.4.2 Input modelling - Panel information

Each wall panel has different attributes such as type, length, width, height, number of windows/doors, and so on. This information is required to estimate the panel processing time and to determine the entity route in the model. For this purpose, panel information is read from the 3D BIM model and stored in a database. The simulation model uses structured query language (SQL) to extract necessary panel information from the database and assigns the necessary

attributes to the model entity. Figure 4.24 and Figure 4.25 show the multipanel and single-panel information tables, respectively. These two tables are connected to each other by a primary and foreign key relationship, which is the *MultiPanelID*.

MultiPanelID	Job	Type	Length	Width	Height	Window	Door	OSB	Cutzone	Drillhole	Stud	MStud	Wall
EW-1_0400-15-0047_00	0400-15-0047	EXT	12218	2467	140	0	0	11	1	5	24	0	1
EW-10_0400-15-0047_00	0400-15-0047	EXT	11608	2467	140	0	0	10	1	5	25	0	1
EW-11_0400-15-0047_00	0400-15-0047	EXT	11145	2467	140	2	0	12	1	7	13	0	1
EW-16_0400-15-0047_00	0400-15-0047	EXT	2124	2467	140	1	0	4	0	3	4	0	1
EW-2_0400-15-0047_00	0400-15-0047	EXT	11913	2467	140	0	0	10	1	5	26	3	1
EW-3_0400-15-0047_00	0400-15-0047	EXT	12130	2467	140	0	1	16	3	8	13	0	2
EW-7_0400-15-0047_00	0400-15-0047	EXT	1699	2467	140	0	0	2	1	2	5	0	1
EW-9_0400-15-0047_00	0400-15-0047	EXT	11424	2467	140	0	0	10	0	4	23	1	1
IW-12_0400-15-0047_00	0400-15-0047	INT	12181	2467	89	0	3	0	3	6	22	1	2
IW-13_0400-15-0047_00	0400-15-0047	INT	12167	2467	89	0	3	0	3	6	21	2	2
IW-14_0400-15-0047_00	0400-15-0047	INT	9079	2467	89	0	3	0	3	0	15	0	2
IW-15_0400-15-0047_00	0400-15-0047	INT	2508	2467	140	0	0	0	0	0	5	2	1
IW-4_0400-15-0047_00	0400-15-0047	INT	11850	2467	89	0	5	0	7	3	21	0	4
IW-8_0400-15-0047_00	0400-15-0047	INT	3200	2467	89	0	0	0	3	0	9	0	2
M_00-125_0400-15-0047	0400-15-0047	INT	1145	1515	89	0	0	0	0	0	2	2	1
M_00-126_0400-15-0047	0400-15-0047	INT	94	1515	89	0	0	0	0	0	2	0	1
M_00-220_0400-15-0047	0400-15-0047	INT	2908	940	89	0	0	0	0	0	5	1	1
MW-5_0400-15-0047_00	0400-15-0047	MEC	2299	2467	184	0	0	0	0	0	6	0	1
MW-6_0400-15-0047_00	0400-15-0047	MEC	1210	2467	235	0	0	0	0	0	2	0	1

Figure 4.24: Screenshot of multipanel data table

MultiPanelID	SinglePanelID	Job	Type	Floor	Length	Width	Height	Window	Door
EW-2_0400-15-0047_00	0400-15-0047-00-101	0400-15-0047	EXT	1st	10674	2467	140	0	0
EW-3_0400-15-0047_00	0400-15-0047-00-102	0400-15-0047	EXT	1st	6687	2467	140	1	1
EW-1_0400-15-0047_00	0400-15-0047-00-103	0400-15-0047	EXT	1st	11284	2467	140	0	0
EW-2_0400-15-0047_00	0400-15-0047-00-104	0400-15-0047	EXT	1st	1054	2467	140	0	0
EW-3_0400-15-0047_00	0400-15-0047-00-105	0400-15-0047	EXT	1st	460	2467	140	0	0
EW-3_0400-15-0047_00	0400-15-0047-00-106	0400-15-0047	EXT	1st	2724	2467	140	1	0
EW-7_0400-15-0047_00	0400-15-0047-00-107	0400-15-0047	EXT	1st	460	2467	140	0	0
EW-7_0400-15-0047_00	0400-15-0047-00-108	0400-15-0047	EXT	1st	1054	2467	140	0	0
EW-1_0400-15-0047_00	0400-15-0047-00-109	0400-15-0047	EXT	1st	610	2467	140	0	0
EW-3_0400-15-0047_00	0400-15-0047-00-110	0400-15-0047	EXT	1st	2124	2467	140	0	1
IW-8_0400-15-0047_00	0400-15-0047-00-111	0400-15-0047	INT	1st	610	2467	89	0	0
IW-4_0400-15-0047_00	0400-15-0047-00-112	0400-15-0047	INT	1st	1188	2467	89	0	0
IW-4_0400-15-0047_00	0400-15-0047-00-113	0400-15-0047	INT	1st	1756	2467	89	0	0
IW-4_0400-15-0047_00	0400-15-0047-00-114	0400-15-0047	INT	1st	3578	2467	89	0	0
IW-8_0400-15-0047_00	0400-15-0047-00-115	0400-15-0047	INT	1st	765	2467	89	0	0
IW-4_0400-15-0047_00	0400-15-0047-00-116	0400-15-0047	INT	1st	813	2467	89	0	0
IW-8_0400-15-0047_00	0400-15-0047-00-117	0400-15-0047	INT	1st	670	2467	89	0	0
MW-5_0400-15-0047_00	0400-15-0047-00-118	0400-15-0047	MEC	1st	2299	2467	184	0	0
MW-6_0400-15-0047_00	0400-15-0047-00-119	0400-15-0047	MEC	1st	1210	2467	235	0	0
IW-8_0400-15-0047_00	0400-15-0047-00-120	0400-15-0047	INT	1st	711	2467	89	0	0
IW-4_0400-15-0047_00	0400-15-0047-00-121	0400-15-0047	INT	1st	918	2467	89	0	0
IW-4_0400-15-0047_00	0400-15-0047-00-122	0400-15-0047	INT	1st	810	2467	89	0	0
IW-4_0400-15-0047_00	0400-15-0047-00-123	0400-15-0047	INT	1st	1410	2467	89	0	0
IW-4_0400-15-0047_00	0400-15-0047-00-124	0400-15-0047	INT	1st	810	2467	89	0	0

Figure 4.25: Screenshot of single-wall panel data table

### 4.4.3 Symphony.NET

The simulation model of the wall prefabrication process is developed in Symphony.NET using a general purpose modelling template as shown in Figure 4.26. In Symphony.NET, different modelling elements are used to resemble the actual production process. These modelling elements are *create*, *task*, *resource*, *capture*, *release*, *valve*, *set attribute*, *counter*, *execute*, *branch*, *composite*, *destroy*, and *statistics*. The entity, representing the multipanel, undergoes different tasks to complete the simulation. The *create* element is used to generate the model entity, and the *set attribute* is used to read the database and assign panel attributes to the entity. The *resource* element represents workers and CNC machines, and each entity is required to capture the associated resource in order to complete a task. *Capture*, *release*, and *file* elements are used to model the capturing and releasing of a resource. When no resource is available, the entity waits in the *file* element and the waiting time is recorded. The *task* element represents a work package that takes place in a workstation. The task time formula or the distribution parameters are written in the *task* element to simulate the processing time. After completing the task, the entity releases the resource and moves forward.

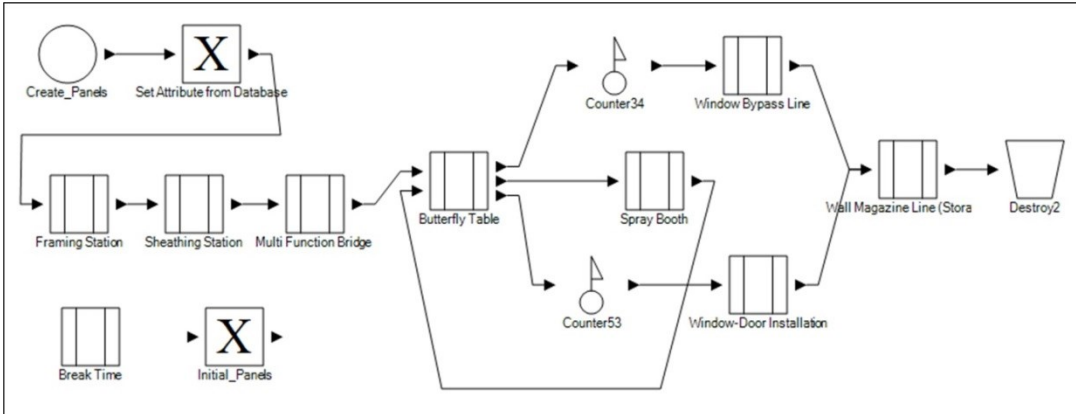


**Figure 4.26: Simulation model developed in Simphony.NET using general purpose template**

Each *composite* element represents a workstation and can hold multiple modelling elements. For example, the framing station composite element has *capture*, *resource*, *task*, *release*, and *branch* elements. After entering the framing composite element, the entity captures the framing resource and completes the task. The framing station can process one panel at a time; hence, the maximum availability of framing resources is set to one. In order to add a stochastic element to the framing station, a delay task with triangular distribution is added after the main processing task. A probabilistic *branch* is used ahead of the delay task to route a certain percentage of the entity toward the delay task, and the rest of the entity will skip the delay task. Conditional *branch* elements are used to route the element based on the panel type. The simulation logic of the *branch* element at the butterfly table is shown below:

```
public static partial class Formulas
{
    public static System.Boolean Formula(Simphony.General.Branch context)
    {
        //check the panel type
        if (paneltype == "EXT") return true;//goes to spray booth
        else return false;//goes to interior package
    }
}
```

In order to define the capacity of a workstation, a combination of *valve* and *branch* elements is used. The capacity of the workstation is in length, e.g., the capacity of the window installation line, spray-booth, and sheathing table-2 are 150 ft, 160 ft, and 40 ft, respectively. A global variable is assigned to each workstation to track the current occupied length. A valve is placed in front of a *branch* element, and the current occupied length is checked in the *branch* element. The detail logic of the *branch* element is shown in the pseudo code below:

```
public static partial class Formulas
{
    public static System.Boolean Formula(Simphony.General.Branch context)
    {
        int current_occupied_length = Scenario.Ints[2]; //global variable
        int panellength = CurrentEntity.Ints[1]; //current entity's length

        //total capacity of the workstation = 150 feet
        //check if the current panel have enough space in the workstation
        if (panellength + currentlength < 150)
        {
            //increase the current occupied length of the workstation
            Scenario.Ints[2] = Scenario.Ints[2] + panellength;

            return true; // go to the workstation
        }
        else
        {
            return false; //Wait at the valve element
        }
    }
}
```

Once an entity enters and exits the workstation element, the occupied current length is increased or decreased accordingly and the valve is opened. If there is an entity waiting at the valve, it will go to the *branch* element to check if the workstation has the required capacity for that entity. The valve is closed

automatically every time an entity passes through. In this way, only one entity can check the capacity at a given time.

At the butterfly station, each entity goes through the cut-panel *composite* element, where multiple entities are generated out of one entity based on the wall number attribute. This process simulates the cutting process of a multipanel into single-wall panels at the butterfly table. Figure 4.27 shows the detail arrangement of the cut-panel *composite* element. At first, the wall number count of the entity is checked at the *branch* element. If the count is equal to one, the entity goes directly to *set single panel* element. Otherwise, it goes to *generate* element, where the original entity follows the upper path and the generated entity follows the lower path and waits at the valve (as shown in Figure 4.27). After the single-wall panel attributes are assigned to the original entity, the valve is opened. The single-wall panel attributes are assigned using SQL from the *Single-wall\_Panel* database table.

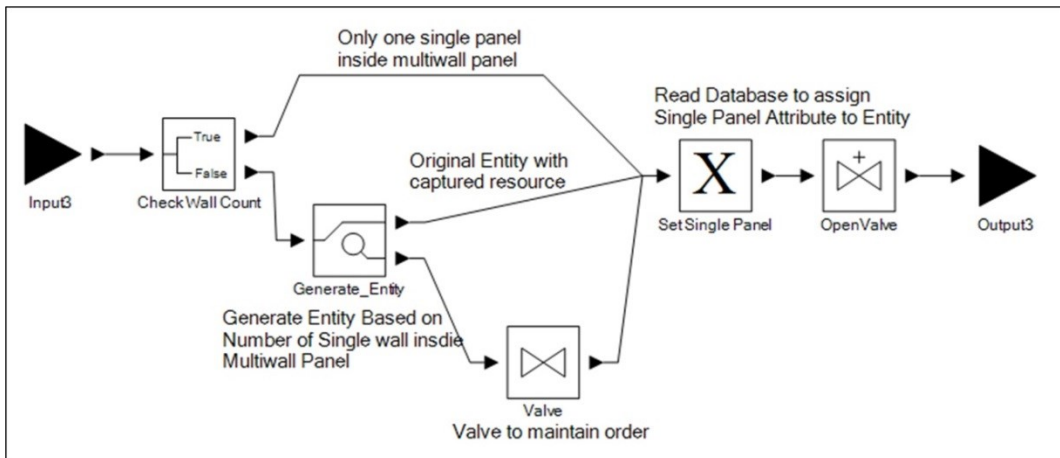


Figure 4.27: Cut-panel composite element detail

Break time is simulated by using the *preamp* element. When a break is due, an entity is created and it uses the *preamp* to capture all the resources, which stops all the tasks. The *preamp* element can capture a resource even if it is in use by another entity. When the break period is over, the resources are released and regular tasks start again from the point where they were interrupted. Once an entity passes through all the workstations, all statistics, such as workstation cycle time and delay time, are collected and the entity is destroyed by the *destroy* element. The simulation model can be run until all the entities are completed or maximum simulation time is reached. The maximum simulation time can be set as the total working time for a day in order to simulate one day's worth of production. The *counter* element is used to count and track the number of entity passes through a specific path. This is used for the verification process of the model.

The RFID system updates the panel database in real time, and the simulation model can identify the current workstation capacity and panel location from the database. Using an *execute* element, the model reads the database at the beginning to obtain the detail of the panels that are currently located at different workstations such as window/door installation line, spray-booth, and so on. The model then creates an entity based on the number of in-process wall panels and assigns the panel attributes to the entity. This connects the simulation model to the actual production line and enables the model to provide accurate analysis of the system.

#### 4.4.4 Model Validation

The simulation model is verified by performing parameter variability-sensitivity analysis and tracking (Sargent 2010). Certain input parameters are adjusted if the model results change based on the expected outcome. For example, if the cycle time of a downstream workstation increases, the previous workstation should have a longer waiting time. Furthermore, the total number of entities created should match the total number of entities destroyed. Also, the model entities are traced along the simulation time to determine if the model logic is correct.

Each workstation time is validated by comparison with actual workstation data. The simulation model is run for different working days and the mean throughput time for each station for each day is then compared with the actual production data collected for the same day of production from the RFID system. Table 4.6 summarizes the comparison of workstation throughput time between simulation and actual production. The result shows that the accuracy of the simulation model for five individual workstations ranges from approximately 70% to 99%. After validating the individual workstation time, the total simulated production time for a set of multipanels is compared with actual data. Table 4.7 summarizes seven observations of actual and simulated production time, and the accuracy of the simulation model ranges from 89% to 100%.

**Table 4.6: Comparison of actual and simulated workstation throughput time**

Workstation	Observation	Actual throughput (minutes)	Simulated throughput, mean value	Accuracy
Framing Station	1	10.04	11.87	82%
	2	13.77	11.85	86%

	3	15.69	13.57	86%
	4	11.41	12.48	90%
	5	11.40	13.39	82%
Sheathing	1	18.24	20.66	87%
Station	2	26.91	19.32	72%
	3	27.22	26.97	99%
	4	26.37	22.59	86%
	5	21.07	25.98	77%
Multi-function	1	7.87	9.06	85%
Bridge	2	13.14	8.64	66%
	3	12.67	9.16	72%
	4	11.79	11.46	97%
	5	10.17	12.53	77%
Spray-booth	1	64.00	62.35	97%
	2	85.13	64.70	76%
	3	61.53	67.28	91%
	4	85.60	61.19	71%
	5	71.35	61.89	87%
Window/Door	1	113.18	109.37	97%
Installation Line	2	150.40	110.35	73%
	3	78.00	103.73	67%
	4	117.62	98.45	84%
	5	174.75	120.21	69%

**Table 4.7: Comparison of simulated and actual total production time**

Observation	Number of Multipanels	Actual Production Time (hr)	Mean Simulated Production Time (hr)	Accuracy
1	23	12.50	12.30	98%
2	29	9.50	10.45	90%
3	18	8.50	8.33	98%
4	15	6.50	6.80	95%
5	28	11.50	10.20	89%
6	19	8.00	7.36	92%
7	40	12.41	12.40	100%

#### 4.4.5 Results

The simulation model provides detailed information of the production process such as waiting time of the workstation, expected time to complete a job,

utilization of the workstation, and panel processing time comparison with actual processing time. Figure 4.28 shows the cumulative density function (CDF) for producing 49 multipanels, and the total production time should range between 764 and 993 minutes with an 80<sup>th</sup> percentile value of 930 minutes.

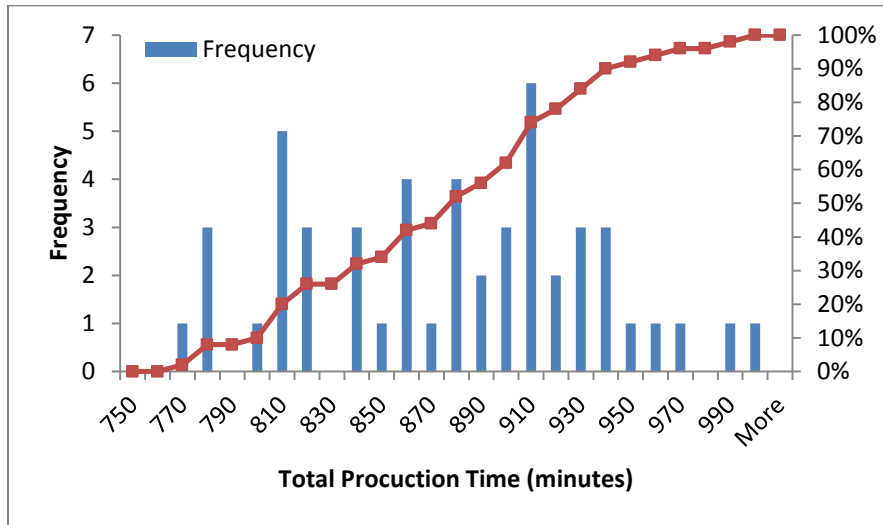


Figure 4.28: Cumulative density function of total production time

Figure 4.29, Figure 4.30, and Figure 4.31 show comparisons between simulation and actual (RFID) multipanel throughput time and cumulative throughput time at the framing station, sheathing station, and multi-function bridge, respectively. The simulation time consists of task processing time, delay, and waiting time. Table 4.8 shows the waiting time percentage,  $\tilde{W}T_A$ , and mean utilization,  $\tilde{U}T_A$ , of workstation,  $A$ . The waiting time percentage and mean utilization are calculated based on Equation (29) and (30), respectively.

$$\tilde{W}T_A = \frac{\sum_{i=1}^{i_{\max}} WT_A^i}{\sum_{i=1}^{i_{\max}} (PT_A^i + WT_A^i)} \quad (29)$$

$$\tilde{U}T_A = \frac{\sum_{i=1}^{i_{\max}} PT_A^i}{\sum_{i=1}^{i_{\max}} (PT_A^i + IT_A^i)} \quad (30)$$

Panel waiting time,  $WT_A^i$ , panel processing time,  $PT_A^i$ , and idle time,  $IT_A^i$ , are collected from the simulation model. The results show that there is a significant amount of waiting time at the multi-function bridge (more than half the time), which leads to low utilization of the CNC machine at that workstation. The long processing time at the window/door installation line and spray-booth is the reason for this waiting time. Also, the utilization of four workers at the sheathing station is 32.85%, whereas if three workers are used, the utilization increased to 54%. However, this also increases the sheathing station throughput time by approximately 1 minute (23.75 to 24.78 minutes).

**Table 4.8: Waiting time and utilization of workstation**

Workstation	Waiting Time (%)
Framing Station	15.85%
Sheathing Station	32.85%
Multi-function Bridge	54.07%
Resource	Mean Utilization
CNC machine at Framing Station	73.14%
Sheathing Station with 4 workers	44.23%
Sheathing Station with 3 workers	53.59%
CNC machine at Multi-function Bridge	37.72%

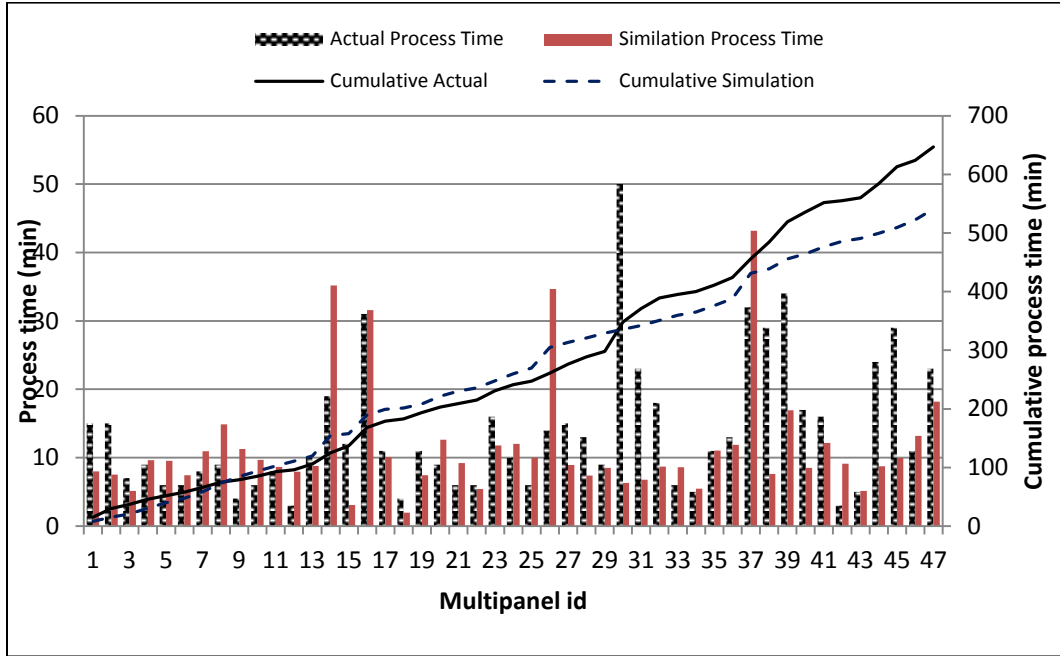


Figure 4.29: Framing station throughput time comparison

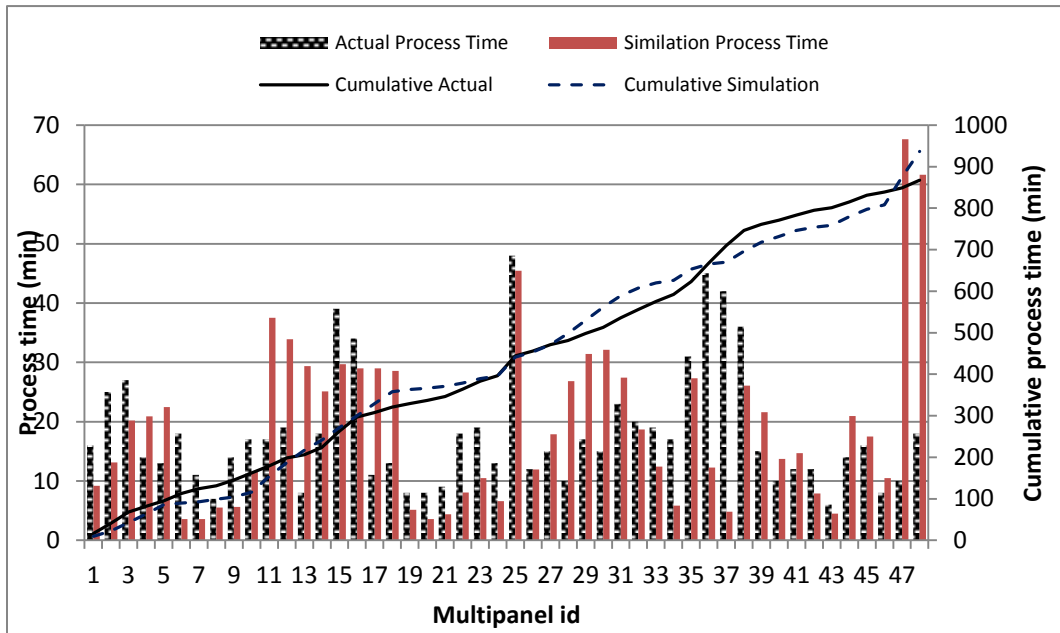
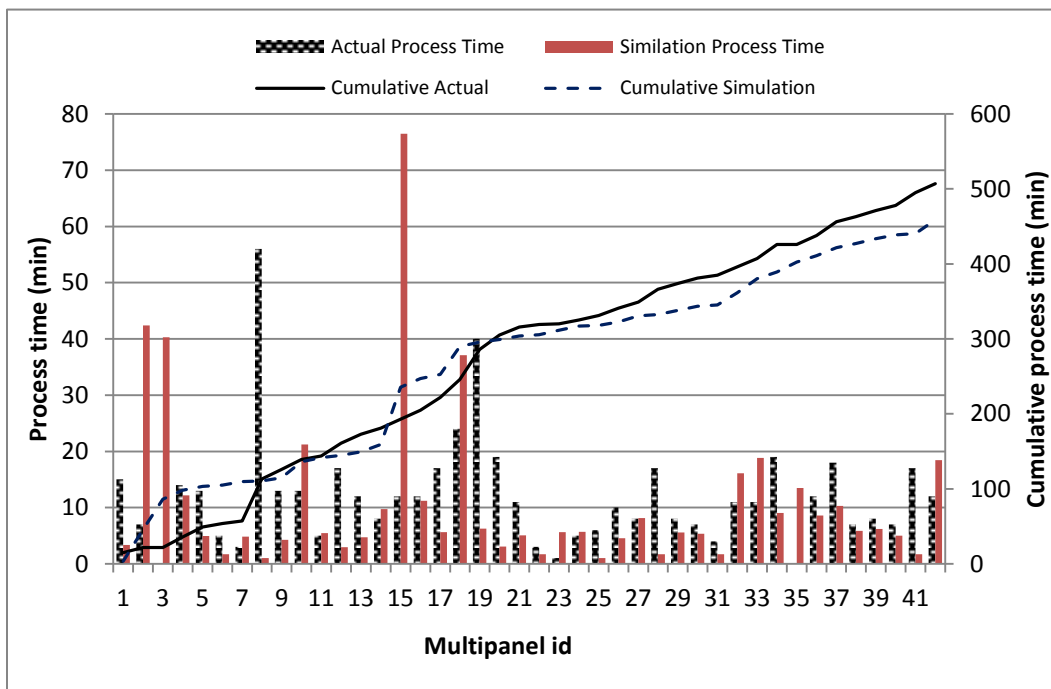


Figure 4.30: Sheathing station throughput time comparison

The simulation result can be used as a performance benchmark by comparing the simulation result with actual results based on Equations (16) and (17). As shown

in Figure 4.29, Figure 4.30, and Figure 4.31, the actual throughput time matches with the simulation time, meaning that the performance is standard. However, if the actual time is higher than the simulation time, the delay time can be identified from the simulation result (as shown in Figure 4.32). Similarly, if the actual time is lower than the simulation time, the performance of that day is better than regular production.



**Figure 4.31: Multi-function bridge station throughput time comparison**

Currently, panelized construction production performance is not standardized. The regular performance indicators are  $\text{ft}^2/\text{day}$  and linear  $\text{ft}/\text{day}$ . However, given that production time largely depends on the type of wall panel and other attributes such as the number of studs, sheets of sheathings, length, and so on, these indicators do not reflect the actual performance. For example, a wall panel with three windows takes more time than a wall panel with no windows, even if the

total square footage is similar. As a result, a simulation model that would take into account the appropriate factors that have an impact on productivity and/or cost can be a useful tool for managers, since they will be able to accurately predict the performance of production lines in consideration of the complexity of the manufactured elements.

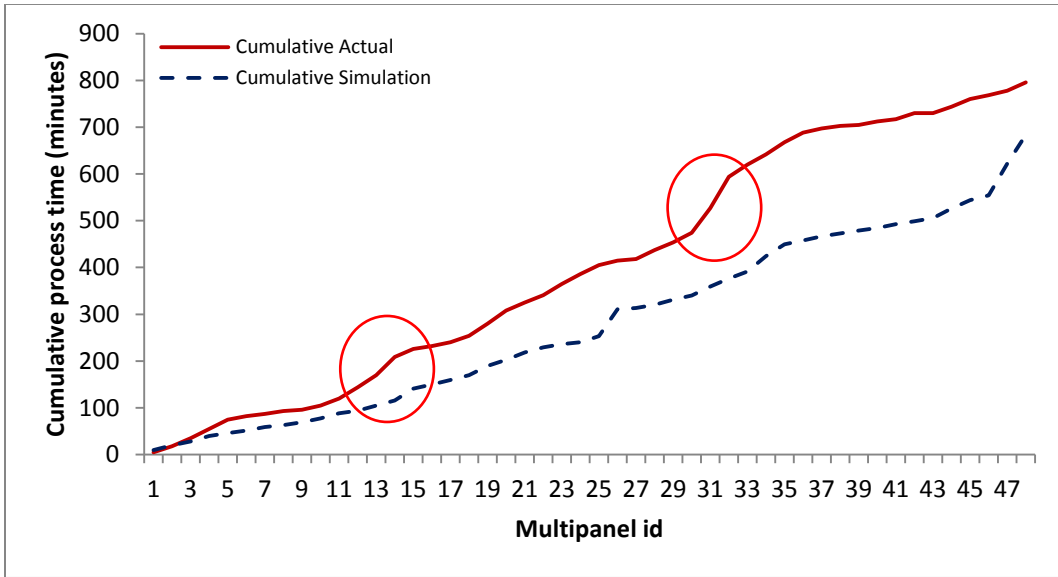


Figure 4.32: Delay identification

#### 4.5 Simulation-based Production Schedule Optimization

The simulation-based multipanel scheduling optimization problem is formulated based on Equation (31), where the objective function is to minimize the total production time and can be written as,

$$\min_{x \in \Theta} \{Ef(x, \xi)\} \quad (31)$$

Variability in panel processing time at different workstations creates the randomness,  $\xi$ , in the model; a set of multipanel production sequence,  $x$ , is the

decision variable; and, the total production time,  $f(x, \xi)$ , for one replication is the output of the simulation model subject to model constraint,  $\Theta$ . The expected value of the objective function,  $Ef(x, \xi)$ , is estimated by creating multiple replications of the total production time,  $f(x, \xi)$ , for one multipanel production sequence,  $\mathcal{X}$ . As mentioned in the methodology section, two meta-heuristic algorithms, i.e., particle swarm optimization (PSO) and simulated annealing (SA), have been used as a searching strategy,  $L_n$ , in the solution space, where a new set of multipanel sequence,  $\mathcal{X}$ , is created in each iteration. In the following two sections, basic principles of PSO and SA algorithms, and how they have been integrated into the multipanel scheduling optimization model, are presented. Then, the results of these two meta-heuristic search algorithms are compared, followed by a discussion on the challenges associated with optimization in the presence of noise.

#### 4.5.1 Particle swarm optimization

Particle swarm optimization (PSO) is a population-based evolutionary algorithm proposed by Kennedy and Eberhart (1995). In the PSO algorithm, search is performed by a set of particles,  $i$ , and the information is shared between all the particles in order to find the optimal solution. Each particle has a velocity and position value in a d-dimensional space. The position and velocity values of the  $i^{th}$  particle are denoted as  $x_i = (x_{i1}, x_{i2}, \dots, x_{id})$  and  $v_i = (v_{i1}, v_{i2}, \dots, v_{id})$ , respectively. Each particle moves toward the best solution of the entire swarm (i.e., the “global best”) by updating its position and velocity after every iteration.

Initially, the position and velocity are assigned randomly to each particle. Then the values are updated based on the results of all previous iterations based on Equations (32) and (33).

$$v_{id}^{k+1} = w \times v_{id}^k + c_1 r_1 \times (p_{id}^k - x_{id}^k) + c_2 r_2 \times (p_{gd}^k - x_{id}^k) \quad (32)$$

$$x_{id}^{k+1} = x_{id}^k + v_{id}^{k+1} \quad (33)$$

Each particle's best position and the global best position are represented by  $P_{id}$  and  $P_{gd}$ , respectively. The global best is the position of a particle that has the best fitness value among all the particles.  $c_1$  and  $c_2$  are the cognitive parameter and social parameter, respectively. In this model, both values are set to 2.  $r_1$  and  $r_2$  are random numbers uniformly distributed from 0 to 1.  $k$  is the iteration number, and  $w$  is the weight inertia required to control the impact of the previous velocity value on the current velocity. A good range of  $w$  is between 0.9-1.2 (Shi and Eberhart 1998). In this model, the value of  $w$  is initially set to 0.9 and, after every iteration,  $w$  is decremented by a factor of 0.975 (i.e.,  $w^{k+1} = w^k \times 0.975$ ). The search process is terminated once the maximum number of iterations is reached.

Particle swarm optimization algorithm can provide faster solutions at the early stage of the search process (Guo et al. 2009). As simulation-based optimization algorithm is already a time consuming process, a quick-converging algorithm has been selected to improve the computational time. If the scheduling module

requires longer run time to provide optimal multipanel sequence, it will be impractical to use such a system in the industry. PSO algorithms have already been used by several researchers to solve the flow shop scheduling problem (Guo et al. 2009; Tasgetiren et al. 2007) and project scheduling problem (Koulinas et al. 2014). Furthermore, in some comparison studies, researchers found that PSO outperforms genetic algorithm in computational efficiency (Hassan et al. 2004; Guo et al. 2009). Although, the performance of an algorithm can vary largely depending on the nature of the problem, the positive reviews of the PSO algorithm over GA and other search algorithms leads to the selection of PSO as the search algorithm for the multipanel sequencing problem.

Figure 4.33 shows the PSO-based multipanel sequencing using DES model. At first, the PSO model assigns initial position and velocity values to each particle. The position values are generated randomly between 0.0 and 4.0. Initial velocities are created randomly between -4.0 and 4.0. Based on initial position value, the simulation model is run for each particle and the total production time is stored as particle best fitness and the associated sequence is stored as particle best sequence. After completing the initial simulation run for all particles, the global best fitness is set as the minimum particle best fitness, and the associated sequence is set as the global best sequence. Then the velocity and position values for each particle are updated based on Equations (32) and (33) and the simulation model is run for each particle; if the simulation result is less than the particle best fitness value, the particle best sequence is updated to the current sequence as well as the particle best fitness. After completing this process for all particles, the best

global fitness value and sequence are updated. After each run, if the termination criterion is met, the optimization process terminates and stores the global best sequence into the database.

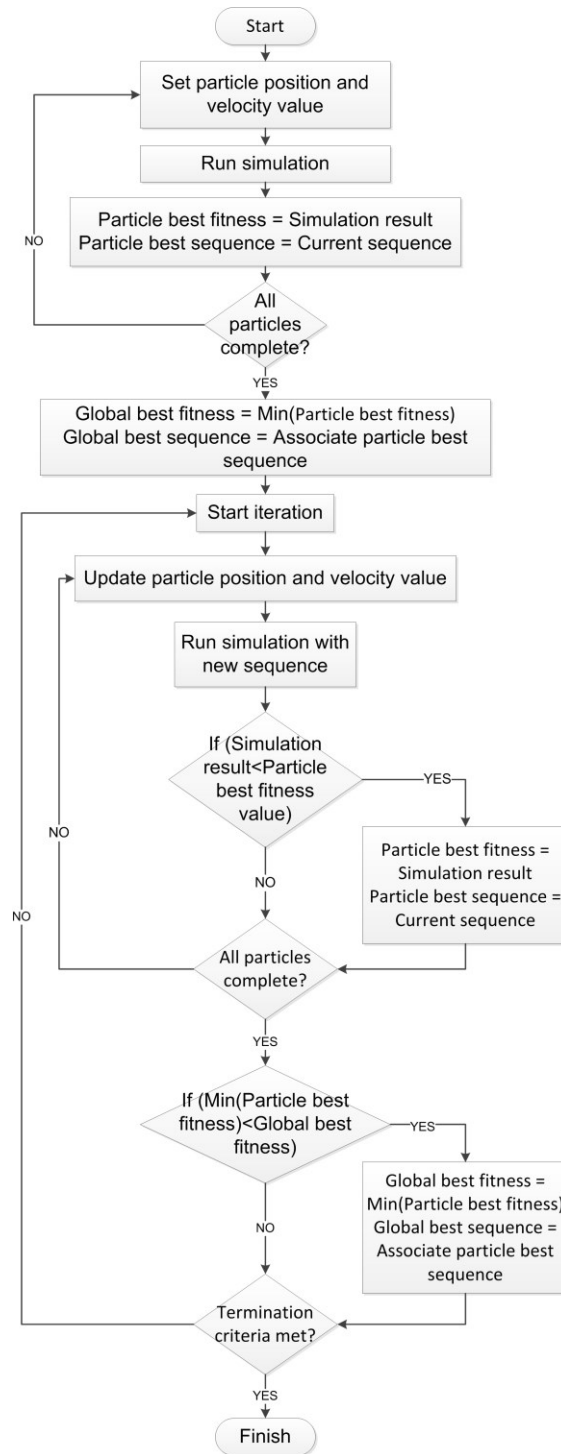


**Figure 4.33: PSO algorithm for multipanel sequencing**

#### **4.5.2 Simulated annealing**

Simulated annealing (SA), which is inspired by the method of heating and cooling metals, is a suitable technique for large-scale optimization problems, especially for those where the global maximum is hidden among many local maxima (Press et al. 1992). The SA algorithm is one of the heuristic algorithms that can provide good, though not necessarily optimal, solutions within reasonable computational time (Eglese 1990). It is a local search algorithm (a decent algorithm) that begins with an initial solution, which can be chosen randomly. One of the disadvantages of a decent algorithm is that it can become trapped in local minima/maxima. To encounter this problem, SA sometimes accepts a neighbouring solution which has higher value in the fitness function, but the acceptance or rejection is determined by a factor named acceptance probability. The advantages of SA are that it is easy to implement, it can be applied to a wide range of problems, and it can provide high quality solutions (Eglese 1990). Ji et al. (2009) have used SA to solve flow shop scheduling problems for five jobs in four machines and 10 jobs in five machines. The results show that SA can effectively converge to global optimal; however, the authors concluded that further research is necessary to assess the performance of SA in large-scale flow shop scheduling problems. SA is applied in multipanel sequencing problems to measure the performance of this algorithm in a large-scale problem compared to population-based PSO algorithm.

The implementation of the algorithm is relatively simple. At first, a random solution is created and the fitness value is calculated as the current best solution. Then a neighbouring solution is created and the fitness value is calculated. If the

fitness value of the neighbouring solution is better than the current best solution, it replaces the current best solution. However, if the fitness value of neighbouring solution  $f_n$  is not better than the best fitness function  $f_b$  (i.e.,  $f_n - f_b \leq 0$ ), rather than discarding the solution, an acceptance probability value is calculated based on Equation (34).

$$a = e^{-\frac{f_n - f_b}{T}} \quad (34)$$

where  $a$  is acceptance probability and  $T$  is temperature. The initial value of  $T$  is set as 1 and, after every iteration,  $T$  is decremented by a factor of 0.9 (i.e.,  $T^{k+1} = T^k \times 0.9$ ). After calculating the acceptance probability, it is compared to a randomly generated number between 0 and 1. If the acceptance probability,  $a$ , is greater than the random value, the best fitness,  $f_b$ , is updated by the neighbouring solution,  $f_n$ .

$$\text{if } \{a > \text{Rand}(0,1)\} \rightarrow f_b = f_n \quad (35)$$

Figure 4.34 shows the SA algorithm for the multipanel sequencing problem. The simulation model is run with a random sequence and the result is stored as the best fitness. Then a neighbouring solution is created by swapping two randomly selected multipanel positions. The simulation model is run again and if the result is greater than best fitness, the acceptance probability is calculated and compared with a random number to decide whether to discard or keep the neighbouring solution. The process continues until the termination criterion is met, and the best

multipanel sequence is stored into the database as the optimum production sequence.

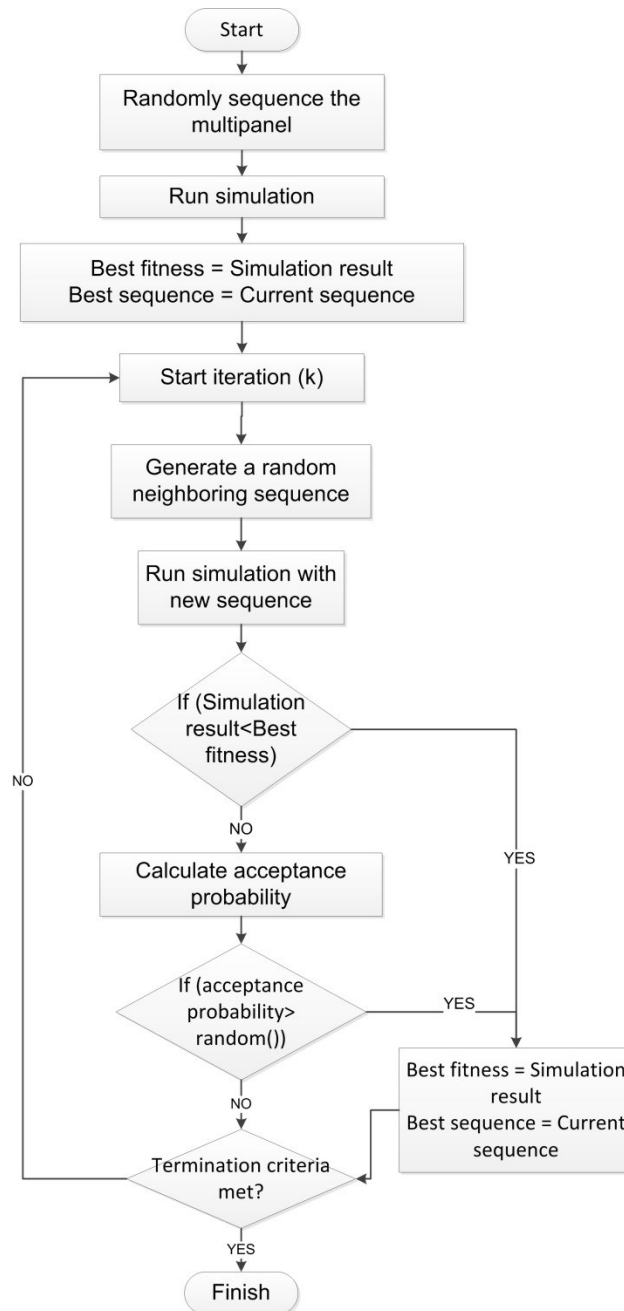


Figure 4.34: SA algorithm for multipanel sequencing

### 4.5.3 Comparison between PSO and SA optimization result

The multipanel sequence is optimized using both PSO and SA methods and the result is presented in Table 4.9. The simulation model provides a range of total production time with a mean value and standard deviation for the optimal multipanel sequence. Both optimization models are run for four different multipanel sets. Then the simulation model is run with the actual production sequence (original sequence), and the productivity improvement is calculated with respect to the original sequence. Currently, interior wall panels are interspersed among exterior panels to generate the production schedule. The number of interior panels produced between exterior panels is determined based on the ratio between interior and exterior wall counts. In other words, two ratios, the remaining ratio,  $\varphi_{rem}$ , and scheduled ratio,  $\varphi_{sch}$ , are calculated after placing each multipanel into the schedule; these ratios are calculated based on Equations (36) and (37), respectively.

$$\varphi_{sch} = \frac{E_{sch}}{I_{sch}} \quad (36)$$

$$\varphi_{rem} = \frac{E_{rem}}{I_{rem}} \quad (37)$$

where  $E_{sch}$  and  $I_{sch}$  are the scheduled exterior and interior multipanels;  $E_{rem}$  and  $I_{rem}$  are the remaining exterior and interior multipanels. Provided that the remaining ratio is higher than the scheduled ratio, the next available exterior wall will be scheduled. Otherwise, the next available interior wall is scheduled. In the event that no exterior wall is left for scheduling, the remaining interior walls are

scheduled, or vice versa. The optimization result shows that the original sequence can be improved by implementing simulation-based optimization using both PSO and SA algorithms.

The computational time (CPU time) for both algorithms is similar; however, PSO can provide better results with a productivity improvement of 6-10%, while SA can improve the productivity by 4-7%. In all observations in Table 4.9, the PSO method has been run with 10 particles for 10 iterations, and the SA method has been run with 100 iterations. In all three cases, 30 replications (simulation run-count) are used in the simulation model.

**Table 4.9: Optimization result for PSO and SA algorithm**

Obs.	No. of Multi-panel for optimization	Algorithm	Total Production Time (minutes)			Improvement	CPU Time (h:mm)
			Range (Min-Max)	Mean Value	Std. dev.		
1	28	PSO	426-587	510	34.23	8.7%	0:59
		SA	458-613	521	34.33	6.8%	0:53
		Original Seq.	503-658	559	42.92	-	-
2	19	PSO	332-477	407	39.10	6.4%	0:30
		SA	349-475	410	33.34	5.7%	0:28
		Original Seq.	360-532	435	38.11	-	-
3	27	PSO	463-614	522	34.09	10%	1:18
		SA	439-643	536	52.27	7%	1:14
		Original Seq.	489-677	577	40.48	-	-
4	14	PSO	256-426	341	37.01	6%	0:21
		SA	301-421	346	25.28	4%	0:21

Original Seq.	306-442	363	-	-
------------------	---------	-----	---	---

In order to gain more insight from the simulation result of all three types (original sequence, PSO, and SA), the histogram of the total production time (makespan) is compared. As shown in Figure 4.35, the histogram of the total production time (makespan) follows a normal distribution for PSO, SA, and the original sequence.

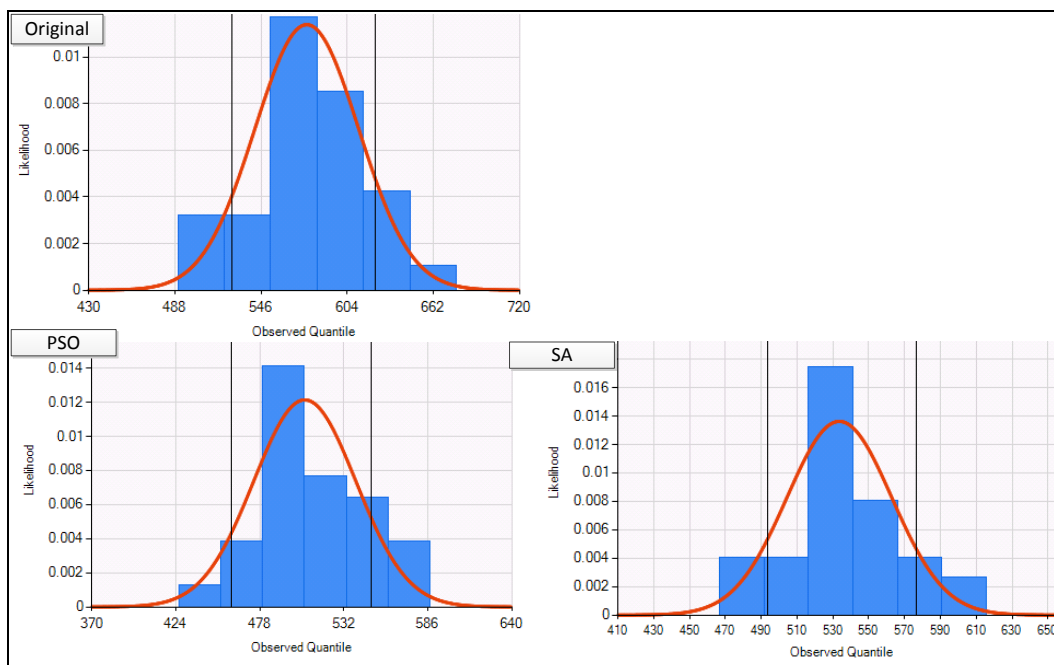


**Figure 4.35: Distribution of makespan for original sequence, PSO and SA**

Figure 4.36 shows the convergence chart of the PSO and SA optimization process for four observations. In all four cases, both optimization models reach the optimum solution before the 90<sup>th</sup> iteration. PSO method improved the productivity in the 4 observations compared to SA method by a small margin (2-3%). Similar performance has been observed by Guo et al. (2009), Ethni et al. (2009), and Bank et al. (2012). Guo et al. (2009) have used PSO to optimize operation

scheduling, and PSO algorithm performed better than GA and SA. Ethni et al. (2009) have used PSO and SA to identify machine stator and motor winding faults, and the results showed that PSO algorithm performs better in this type of application over SA. Bank et al. (2012) have studied flow shop scheduling problems to determine the job sequence. PSO algorithm, with the proposed local search, outperformed SA algorithm. The optimization result of the multipanel sequencing problem establishes that the simulation model can be effectively used as a fitness function in the optimization model for the purpose of solving the stochastic flow shop scheduling problem within reasonable computational time (approximately 30 minutes).

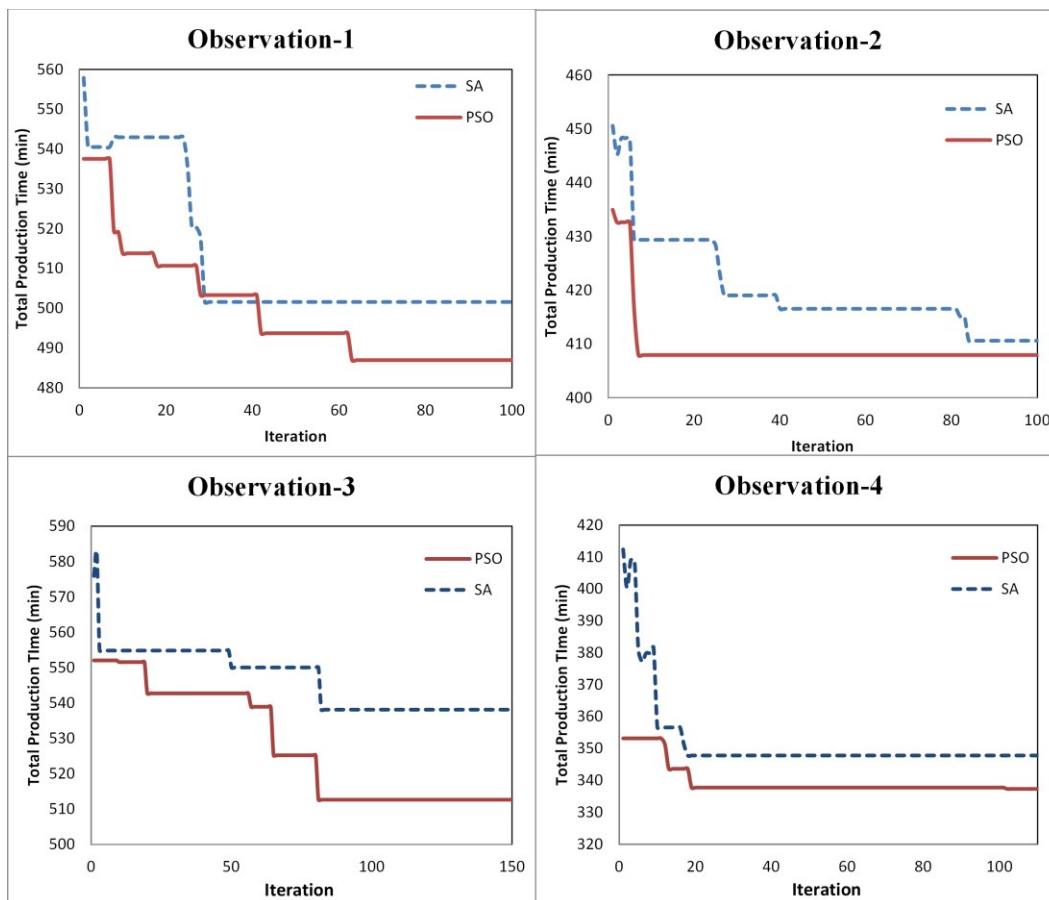
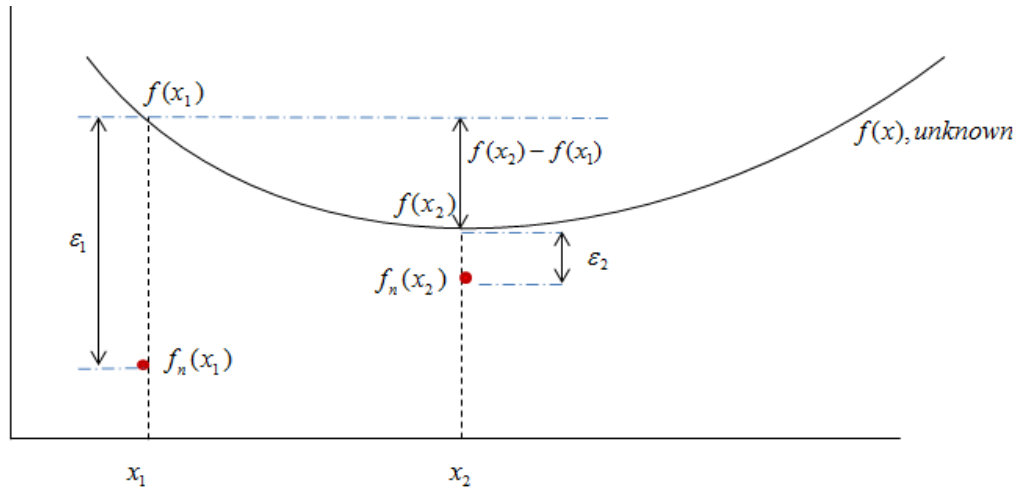


Figure 4.36: Convergence charts of PSO and SA optimization

#### 4.5.4 Optimizing in the presence of noise

One of the challenges associated with the simulation-based optimization is the presence of noise in the fitness function. The difference between the exact solution  $f(x)$  and the estimated solution  $f_n(x)$  for replication  $n$  is the simulation error or noise, which is unavoidable in the stochastic environment. For example, there are two estimated solutions,  $f_n(x_1)$  and  $f_n(x_2)$ , of the exact solution  $f(x_1)$  and  $f(x_2)$  (unknown) for  $n$  replications (as shown in Figure 4.37). The noise (unknown) of these two estimated solutions are  $\varepsilon_1 = f_n(x_1) - f(x_1)$  and  $\varepsilon_2 = f_n(x_2) - f(x_2)$ . In a minimization model, if  $f_n(x_1) < f_n(x_2)$ ,  $f_n(x_1)$  is taken as the optimal solution and vice versa. However, if  $(\varepsilon_1 - \varepsilon_2) > f(x_2) - f(x_1)$ , the estimated solution can mislead where  $f_n(x_2)$  is a better solution over  $f_n(x_1)$ . This problem is more prominent if the number of replications  $n$  is small in the simulation model. By increasing the simulation run-length, the noise  $\varepsilon$  within the estimated solution can be reduced; however, it increases the model runtime.



**Figure 4.37: Effect of noise in the estimated solution**

The optimization model is run for 27 multipanels using PSO search algorithm for 5, 10, 20, 30, 40, and 50 replications and the mean value, 90<sup>th</sup> percentile, and model runtime for each solution,  $x_5, x_{10}, x_{20}, x_{30}, x_{40}$  &  $x_{50}$ , are plotted as shown in Figure 4.38. The result shows that the optimization result with 5 replications  $f_5(x)$  becomes an attractive solution, as there is no significant improvement in the result and the computational time is smaller. However, if the model run-length (number of replications) is increased to 50 for each of these solutions, the optimization result varies largely between 5 replications and 50 replications. The 90<sup>th</sup> percentile for each run-length is compared to the solution's 50 run-length's 90<sup>th</sup> percentile, as shown in Figure 4.39. It shows that the higher number of replications increases the reliability of the optimal solution and can reduce the error generated from outliers.

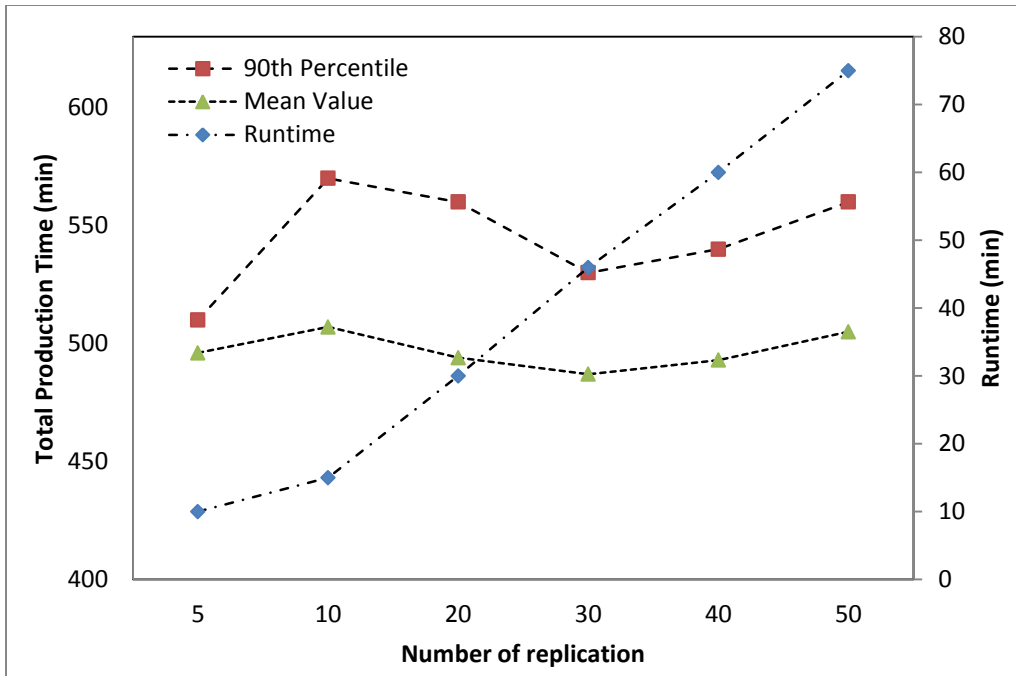


Figure 4.38: Mean, 90<sup>th</sup> percentile, and runtime for different number of replications

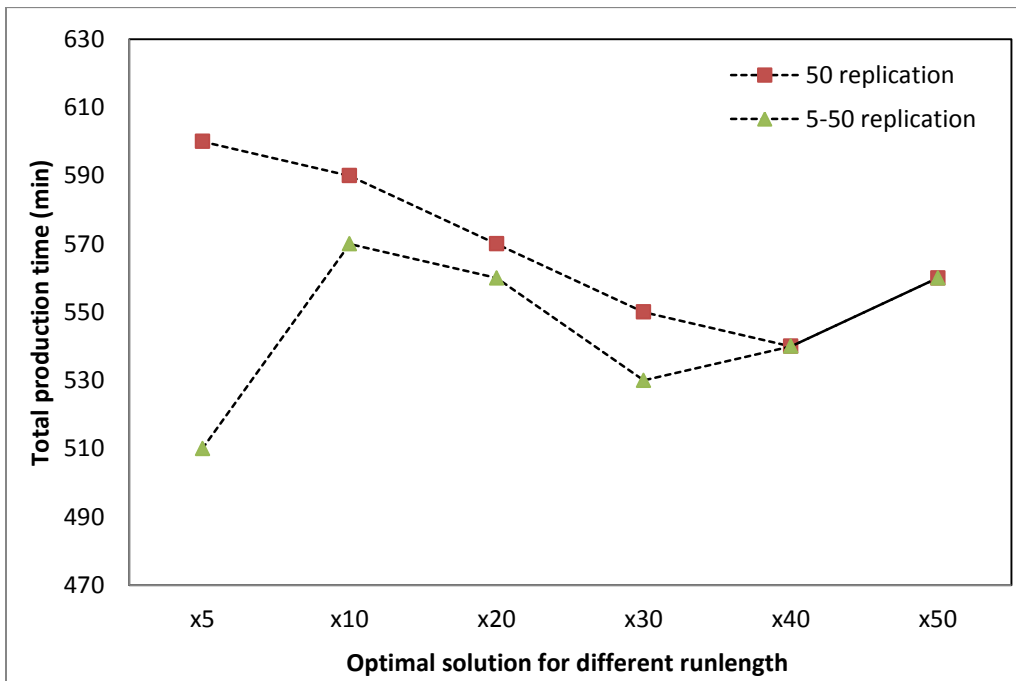


Figure 4.39: Optimal solution for different run-lengths

Based on this analysis, the following rules can be set in simulation-based optimization problems:

1. Start the optimization with a small simulation run-length (e.g.,  $n = 5$ ). Run the simulation model with the optimal sequence  $x_n$  for 50 replications ( $n_{high}$ ) and store the 90<sup>th</sup> percentile  $f_{n_{high}}^{90\%}(x_n)$ .
2. Run the optimization model with a new run-length  $n_{new} > n$  and run the simulation model with the optimal sequence  $x_{n_{new}}$  for 50 replications ( $n_{high}$ ), and store the 90<sup>th</sup> percentile  $f_{n_{high}}^{90\%}(x_{n_{new}})$ .
3. If  $f_{n_{high}}^{90\%}(x_{n_{new}}) < f_{n_{high}}^{90\%}(x_n)$ , continue the iteration with a new simulation run-length value until it satisfies the termination criteria  $f_{n_{high}}^{90\%}(x_{n_{new}}) \geq f_{n_{high}}^{90\%}(x_n)$ .

Note that, the selection of  $n_{high}$  is important as it determines the validity of the current solution  $x_n$ . In the above rule, it is set as 50, which is selected based on observations made by running the simulation model for 30, 40, 50, and 60 replications. From the simulation results, it is observed that after 50 replications, the simulation result (mean, standard deviation, and 90<sup>th</sup> percentile) remains constant. For this reason, the  $n_{high}$  value is selected as 50. During the iteration process, if the  $n_{new} > n_{high}$  condition is reached before reaching the termination criteria,  $n_{high}$  is needed to be reset with a higher value.

## 4.6 Financial Module

In traditional stick-built home construction, the labour hours required from capping, framing, and finishing operations for a project can be easily tracked as the actual work takes place at the job site. In a manufacturing environment, the workers work on multiple jobs simultaneously in different workstations. The labour hours and cost associated to each individual job is a difficult task to assess. To confront this issue, ACQBUILT, Inc. purposed to develop and implement a cost control module specifically for the prefabricated home building facility. As mentioned in the methodology section, daily production volume and automated labour hour collection from each work area enables the financial module to provide unit cost for each work area every two weeks. This establishes a base line for the management to set a financial target for each work area for cost control purposes. Also, in each work area, the labour hours associated to each job are tracked separately by calculating a percentage value from the total square footage of production and the square footage of individual jobs.

The financial module has been implemented at ACQBUILT's prefabricated home building facility based on Equation (20). The information from the financial module is shown in Figure 4.40. Material quantity takeoff,  $Q_J$ , and daily production volume,  $PV_{A,d}^J$ , are extracted from the 3D model and RFID system, respectively. The payroll department provides the labour cost for each work area per pay-period,  $C_{A,p}^e$ . Unit cost,  $UC_{A,p}$ , and job cost,  $TC_J$ , are calculated based on Equation (21) and Equation (24). Table 4.10 summarizes the labour unit cost per ft<sup>2</sup> for each work area over a one-week period. The labour unit cost is

compared with the target cost of each area. The values have been scaled up in the interest of confidentiality.

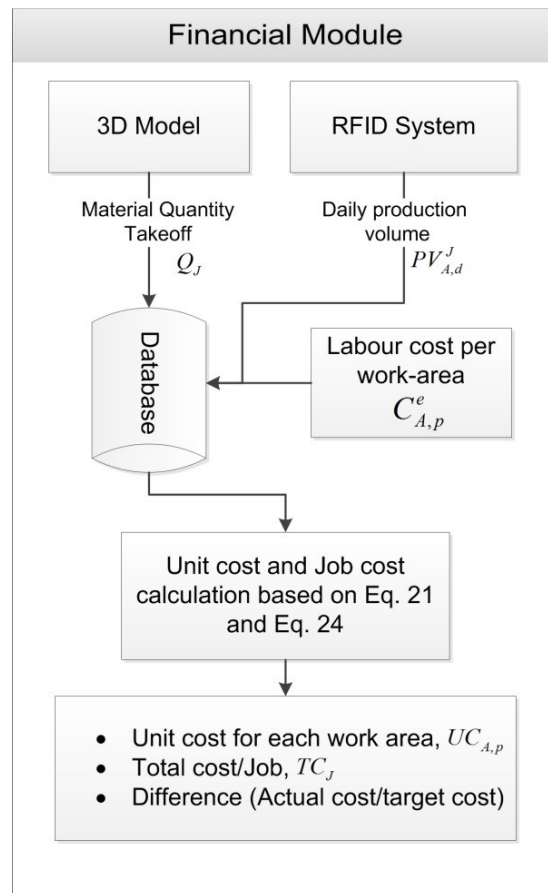


Figure 4.40: Financial module information flow

Table 4.10: Target cost and actual cost of each work area over one-week period

Work Area	Target Cost	Actual Unit Cost
Floor	\$4.30	\$4.02
Wall framing	\$8.60	\$9.75
Exterior insulation	\$1.43	\$1.91
Roof framing	\$11.95	\$13.00
Exterior finishing	\$4.30	\$5.16
Roof shingling	\$1.43	\$1.24
Material handling	\$3.35	\$3.44

Logistics	\$5.26	\$6.31
-----------	--------	--------

Table 4.11 depicts the daily total cost for job A, which is calculated from the daily percentage volume and payroll information. The values have been scaled up in the interest of confidentiality. As shown in Table 4.11, a typical house requires different elements to be built such as stairs, floors, wall framing, roof framing and shingling, exterior insulation, and exterior finishing work. Some of these activities can take multiple days to complete (e.g., roof framing and shingling, wall framing). The financial module captures the square footage of each activity each day and divides that by the total square footage of production to calculate the percentage volume. For example, the main floor panels of job A are built on August 8, 2015, and the total floor production volume is 5,370 ft<sup>2</sup>. The main floor of job A is 1,343 ft<sup>2</sup> in areas. From this daily output, the percentage volume of floor work area for job A is calculated as 25% (i.e., (1,343/5,370)×100). The total labour cost in that area for that day is then multiplied by the calculated ratio in order to estimate the labour cost for job A.

**Table 4.11: Daily labour cost for some work areas of house model A**

Date	Percentage Volume	Work Area	Total Cost
8/20/2015	0.35	Basement stairs	\$1,449.68
8/19/2015	0.25	Main floors	\$3,893.31
9/1/2015	0.43	Walls framing	\$8,541.48
9/1/2015	0.25	Exterior insulation	\$2,161.90
9/2/2015	0.05	Walls framing	\$1,240.31
9/2/2015	0.30	Windows/Doors	\$2,892.66
9/2/2015	0.35	Roofs	\$19,870.36

9/2/2015	0.25	Exterior insulation	\$2,292.39
9/3/2015	0.50	Main floor stairs	\$2,086.37
9/3/2015	0.10	2 <sup>nd</sup> floors	\$1,172.15
9/3/2015	0.16	Roofs	\$8,505.25
9/3/2015	0.15	Exterior finishing	\$3,492.55

This enables tracking of the labour cost for each individual job. The material cost is calculated from the automated material takeoff from the BIM model and is added to the labour cost. The financial module provides a framework for panelized homebuilders to monitor and control the labour cost of individual activities involved in building a house. The unit cost measure of each work area allows ACQBUILT, Inc. to increase/decrease work force in order to increase the productivity in a particular area if the unit cost is higher than the target.

# 5 Conclusion

---

## 5.1 Summary

This thesis presents an integrated planning and control system for the prefabrication of panelized construction for residential buildings. The proposed system has four modules interconnected through a central database: scheduling, data collection, simulation, and financial. The scheduling module reads wall panel information of the specified house model to generate quantity takeoff information and to optimize the cutting of single-panel walls from multipanels in order to reduce material waste and increase production efficiency. Using simulated annealing (SA) optimization, single-wall panels are merged into multipanels, and then the sequencing of the multipanel is optimized to reduce total production time based on a simulation-based optimization method. Both single-wall panel and multipanel information and production schedules are then stored in the central database. The data collection module utilizes the RFID system to automatically capture the panel location and the processing time at each workstation without any human involvement. This module provides a real-time location system (RTLS) to identify wall panel location as well as daily productivity; it also provides utilization and productive panel processing times at each workstation by utilizing the Kalman filtering process. The simulation module uses historical time data, time study, and the Symphony.NET simulation engine to mimic the wall production line and provide a simulation-based performance evaluation system. Finally, the financial module utilizes payroll information and daily production

volume at every workstation from the RFID system in order to provide unit cost per ft<sup>2</sup> for each workstation, as well as the total labour and material cost of the entire house. The proposed system has been successfully implemented in ACQBUILT's wall production line. The RFID system has been installed and a DES model has been developed for the wall production line using Symphony.NET.

The implementation results of the proposed method demonstrate that the integrated production planning and control system is able to efficiently optimize single-wall panels into multipanels, and to generate optimum production schedule, daily production status, performance evaluation, and cost information. The RFID system can effectively provide real-time panel locations in the wall panel production line. The simulation model is able to identify delay by comparing actual time with simulated time, and it also estimates production lead time in advance. The communication between the production controller and team leader of each workstation is improved through the availability in real time of required information from the RFID system. The single-panel-to-multipanel merging optimization reduces machine set-up time and material waste, and eliminates manual work. With the RFID system, progress of work is monitored automatically, and the cost control system provides an accurate job costing and area-specific unit cost report, thereby enabling the production manager to effectively schedule the necessary labour force into different work areas. Moreover, the actual panel processing data collected from the RFID system helps

to validate the simulation model in order to provide reliable statistics of the production process.

The simulation-based optimization model has been implemented using PSO and SA algorithms for multipanel sequencing. The proposed method can improve the current multipanel sequence and can reduce the total panel production time by up to 10%. The study also shows that PSO algorithm can provide better results than can SA. As for the challenges associated with the simulation-based optimization model, where the presence of noise can shift the result from a good solution, this issue can be neutralized by increasing the number of replications within the simulation model for a given solution. However, this increases the computational time of the optimization model. From experimental results, a rule has been proposed to select the optimum number of replications to be used in the simulation-based optimization model.

## **5.2 Research Contributions**

### **5.2.1 Academic contributions**

There have been several studies carried out on the optimization problem of job sequence for different manufacturing industries as well as a simulation-based control system. However, no study has focused specifically on developing an integrated production planning and control system for prefabricated home building, which requires specific attention due to its unique manufacturing process. Unlike in traditional manufacturing, in panel prefabrication each job is unique due to customization, and the volume of the product is also large (an

average wall panel is 35 ft in length). Also, early in the production line the products are produced in batches (multipanel) and are later unbatched. The work load for exterior and interior wall panels varies significantly, which can cause imbalance in the line by creating long waiting times or starvation for panels. Finally, in the panelized production system, factory production is only half of the building process; the wall, floor, and roof panels must also be shipped to site and installed in order to complete a job. For this reason, the factory schedule is largely dependent on the site installation schedule.

The academic contributions of this thesis are summarized as follows:

- (i)* This thesis has developed a methodology for an integrated production planning and control system for the prefabrication of panelized homes.
- (ii)* A discrete-event simulation (DES)-based optimization model has been developed to solve the probabilistic flow shop scheduling problem for the prefabrication process for panelized homes. Hence, it contributes to solving the panel sequencing optimization problem of the prefabrication assembly line for home building in a stochastic environment.
- (iii)* A RFID system has been designed for the purpose of real time location system (RTLS) and automated production data collection system. The RFID system generates production data such as workstation utilization, waiting time, productive panel processing time, and idle time of workstation.

### **5.2.2 Industrial contributions**

The industrial contributions are summarized as follows:

- (iv) The multipanel optimization reduces material waste and increases productivity by reducing machine set-up time.
- (v) The scheduling module automates the production scheduling process, which reduces operator time as well as overall production time.
- (vi) The production control system provides a real-time location system, daily production output, workstation utilization, throughput time, and cost control.
- (vii) The simulation-based performance monitoring system provides better guidelines for performance evaluation as well as production lead time for future jobs.

### 5.3 Limitations and Future Research

Based on this research, the following future research is proposed:

- (i) **Hybrid optimization:** The simulation-based optimization model can be further improved by investigating different approaches, such as hybrid optimization. PSO algorithm with local search (knowledge-based heuristic rule, simulated annealing) can be implemented to improve the result and computational time.
- (ii) **Resource optimization:** This thesis has proposed to improve the prefabrication process by optimizing the multipanel sequence while keeping the resources/workforce constant. However, the process can be further improved by optimizing the resources within the production line. In future research, resources can be added as an additional decision

variable into the optimization model in order to improve the production process.

- (iii) **RFID based simulation modelling:** In this thesis, the simulation model is developed based on a time study, which is time-consuming manual work. In future research, a probabilistic model can be developed based on each type of panel from the RFID system, and can be used in the simulation model as the input parameter in each workstation. This will eliminate the time study required for simulation input modelling, such that the model can be updated dynamically based on actual production data collected from the RFID system.
- (iv) **Automation of roof panel production:** While for many panelized construction companies in North America a significant portion of wall and floor panels are built by the machine and completely drawn in BIM software, the roof panels are still built manually. The development of an automated roof production system with BIM modelling will significantly improve the panelized production efficiency and reduce waste.
- (v) **Special-purpose simulation modelling environment for panelized home production facility:** A simulation modelling platform with 3D visualization and RFID integration for a real-time location system will further benefit the panelized home production process. A custom template for a panelized production line will be easy to implement for industrial use, and 3D visualization will provide better understanding of the simulation output.

- (vi) **Mid-rise panelized building construction:** Mid- to high-rise buildings must have additional structural elements (tie rods, mid-height blocking, etc.) according to building code, and in-depth research is needed to identify the challenges associated with the prefabrication of mid- to high-rise buildings.
- (vii) **Closed wall system:** In current practice in North America, open walls are prefabricated in the plant and electrical, plumbing, and drywall are installed on site after installing floor, wall, and roof panels. In order to reduce drywall waste and job cycle time, closed wall panels (which include drywall, electrical, and plumbing) can be produced in the prefabrication plant, and collaborative research will help with the progress of the closed wall prefabrication system.

This thesis has several limitations as mentioned below:

- (i) The computational time of the multipanel sequencing model can become very high if the problem size increases. In current practice, the optimization model is used to schedule one job at a time. If the model is used to schedule multiple jobs, the problem size can increase, as can the computational time.
- (ii) Simulation-based performance benchmarking requires constant modification to make sure the simulation model represents the most updated production process. Simulation model validation is required after each modification made to the production process.

(iii) The RFID design cannot capture the waiting time as it calculates the actual processing time based on the entry and exit timestamps of the panel. Although Kalman filtering is applied to separate the waiting time/noise from the RFID data, if there is a high percentage of waiting time or delay, the RFID data will not capture the productive processing time accurately from the proposed RFID setup.

## References

- AbouRizk, S. (2010). "Role of simulation in construction engineering and management." *Journal of Construction Engineering and Management*, 136(10), 1140–1153.
- AbouRizk, S. M., Hague, S. A., and Ekyalimpa, R. (2015). *Construction Simulation: An Introduction using Symphony*. Hole School of Construction Engineering, University of Alberta.
- AbouRizk, S. M. and Hajjar, D. (1998). "A framework for applying simulation in construction." *Canadian Journal of Civil Engineering*, 25(3), 604–617.
- AbouRizk, S. M. and Mohamed, Y. (2000). "Symphony: An integrated environment for construction simulation." *Proceedings of the 2000 Winter Simulation Conference*, Orlando, FL, USA, Dec. 10-13.
- Al-Bataineh, M., AbouRizk, S., and Parkis, H. (2013). "Using simulation to plan tunnel construction." *Journal of Construction Engineering and Management*, 139(5), 564–571.
- AlDurgham, M. M. and Barghash, M. A. (2008). "A generalised framework for simulation-based decision support for manufacturing." *Production Planning & Control*, 19(5), 518–534.

- Altinkilinc, M. (2004). "Simulation-based layout planning of a production plant." *Proceedings of the 2004 Winter Simulation Conference*, Washington, DC, USA, Dec. 5-8, 1079–1084.
- Alvanchi, A., Azimi, R., Lee, S., AbouRizk, S. M., and Zubick, P. (2012). "Off-site construction planning using discrete event simulation." *Journal of Architectural Engineering*, 18(2), 114–122.
- Arkan, I. and van Landeghem, H. (2013). "Robotics and computer-integrated manufacturing evaluating the performance of a discrete manufacturing process using RFID: A case study." *Robotics and Computer-Integrated Manufacturing*, 29(6), 502–512.
- Azimi, R., Lee, S., AbouRizk, S. M., and Alvanchi, A. (2011). "A framework for an automated and integrated project monitoring and control system for steel fabrication projects." *Automation in Construction*, 20(1), 88–97.
- Baker, K. R. and Trietsch, D. (2009). *Principles of Sequencing and Scheduling*. John Wiley & Sons: Hoboken, NJ, USA.
- Bank, M., Fatemi Ghomi, S. M. T., Jolai, F., and Behnamian, J. (2012). "Application of particle swarm optimization and simulated annealing algorithms in flow shop scheduling problem under linear deterioration." *Advances in Engineering Software*, 47(1), 1–6.

- Beck, J. C. and Wilson, N. (2007). "Proactive algorithms for job shop scheduling with probabilistic durations." *Journal of Artificial Intelligence Research*, 28, 183–232.
- Burns, L. D., and Daganzo, C. F. (1987). "Assembly line job sequencing principles." *International Journal of Production Research*, 25(1), 71–99.
- Cagnina, L. and Esquivel, S. (2004). "Particle swarm optimization for sequencing problems: A case study." *Proceedings of the Congress on Evolutionary Computation*, Portland, OR, USA, Jun. 19-23, 536–541.
- Canadian Manufactured Housing Institute. (2011). *CMHI Manufactured Building Survey Report*.
- Carson, J. S. (2002). "Model verification and validation." *Proceedings of the 2002 Winter Simulation Conference*, San Diego, CA, USA, Dec. 8-11, 52–58.
- Dengiz, B. and Alabas, C. (2000). "Simulation optimization using tabu search." *Proceedings of the 2000 Winter Simulation Conference*, Orlando, FL, USA, Dec. 10-13, 805–810.
- Domdouzis, K., Kumar, B., and Anumba, C. (2007). "Radio-frequency identification (RFID) applications: A brief introduction." *Advanced Engineering Informatics*, 21(4), 350–355.
- Eglese, R. W. (1990). "Simulated annealing: A tool for operational research." *European Journal of Operational Research*, 46(3), 271–281.

- Emory, E. (1983). "A heuristic algorithm for the m-machine, n-job flow-shop sequencing problem." *International Journal of Management Science*, 11(1), 91–95.
- Ethni, S. A., Zahawi, B., Giaouris, D., and Acarnley, P. P. (2009). "Comparison of particle swarm and simulated annealing algorithms for induction motor fault identification." *Proceedings of the 7th IEEE International Conference on Industrial Informatics*, Cardiff, UK, Jun. 23-26, 7–11.
- Ferrer, G., Heath, S. K., and Dew, N. (2011). "An RFID application in large job shop remanufacturing operations." *International Journal of Production Economics*, 133(2), 612–621.
- Garza-Reyes, J. A., Oraifige, I., Soriano-Meier, H., Forrester, P. L., and Harmanto, D. (2012). "The development of a lean park homes production process using process flow and simulation methods." *Journal of Manufacturing Technology Management*, 23(2), 178–197.
- Ghanem, A. G. and AbdelRazig, Y. A. (2006). "A framework for real-time construction project progress tracking." *Earth & Space (Proceedings of the International Conference on Engineering, Construction, and Operations in Challenging Environments)*, Houston, TX, USA, Mar. 5-8.
- Goodrum, P. M., McLaren, M. a., and Durfee, A. (2006). "The application of active radio frequency identification technology for tool tracking on construction job sites." *Automation in Construction*, 15(3), 292–302.

- Guo, Y. W., Li, W. D., Mileham, A. R., and Owen, G. W. (2009). "Applications of particle swarm optimisation in integrated process planning and scheduling." *Robotics and Computer-Integrated Manufacturing*, 25(2), 280–288.
- Guo, Z. X., Ngai, E. W. T., Yang, C., and Liang, X. (2015). "An RFID-based intelligent decision support system architecture for production monitoring and scheduling in a distributed manufacturing environment." *International Journal of Production Economics*, 159, 16–28.
- Halpin, D. W. (1977). "CYCLONE: Method for modeling of job site processes." *Journal of the Construction Division*, 103(3), 489–499.
- Halpin, D. W. and Riggs, L. S. (1992). *Planning and Analysis of Construction Operations*. John Wiley & Sons, Hoboken, NJ, USA.
- Hammad, A., Senghore, O., Hastak, M., and Syal, M. (2002). "Simulation model for manufactured housing processes." *Computing in Civil Engineering (Proceedings of the Information Technology in Civil Engineering International Workshop)*, Washington, DC, USA, Nov. 2-3, 286–297.
- Hassan, R., Cohanin, B., de Weck, O., and Venter, G. (2004). "A comparison of particle swarm optimization and the genetic algorithm." *Proceedings of the 46th AIAA/ASME/ASCE/AHS/ASC Structures, Structural Dynamics and Materials Conference*, Austin, TX, USA, Apr. 18-21.

- Huo, L., Liu, B., and Tian, Z. (2010). "The application of RFID technology in JIT production control." *Proceedings of the International Conference of Logistics Engineering and Management*, Chengdu, China, Oct. 8-10, 2547–2553.
- Jaselskis, E. J., Anderson, M. R., Jahren, C. T., Rodriguez, Y., and Njos, S. (1995). "Radio-frequency identification applications in construction industry." *Journal of Construction Engineering and Management*, 121(2), 189–196.
- Jeong, J. G., Hastak, M., Syal, M., and Hong, T. (2011). "Internal relationship modeling and production planning optimization for the manufactured housing." *Automation in Construction*, 20(7), 864–873.
- Ji, M., He, M., and Wang, Q. (2009). "Application of a novel simulated annealing in flow shop scheduling problem." *Proceedings of the Fifth International Conference on Computing, Networking and Communications*, 339–342, Aug. 14-16.
- Jian, N., and Henderson, S. G. (2015). "An introduction to simulation optimization." *Proceedings of the 2015 Winter Simulation Conference*, Los Angeles, CA, USA, Dec. 7-9.
- Johnson, S. M. (1954). "Optimal two- and three-stage production schedules with set-up time included." *Naval Research Logistics Quarterly*, 1(1), 61–68.

- Kennedy, J., and Eberhart, R. C. (1995). "Particle swarm optimization." *Proceeding of IEEE International Conference on Neural Networks*, Piscataway, NJ, USA, Nov. 27-Dec. 1.
- Koulinas, G., Kotsikas, L., and Anagnostopoulos, K. (2014). "A particle swarm optimization based hyper-heuristic algorithm for the classic resource constrained project scheduling problem." *Information Sciences*, 277, 680–693.
- Leu, S.-S. and Hwang, S.-T. (2002). "GA-based resource-constrained flow-shop scheduling model for mixed precast production." *Automation in Construction*, 11(4), 439–452.
- Li, W. D., Ong, S. K., and Nee, A. Y. C. (2004). "Optimization of process plans using a constraint-based tabu search approach." *International Journal of Production Research*, 42(10), 1955–1985.
- Liker, J. K. (2004). *The Toyota Way: 14 Management Principles from the World's Greatest Manufacturer*. McGraw-Hill Education: New York, NY, USA.
- Liu, Z., Wang, C., Sun, T., and Engineering, E. (2010). "Production sequencing of mixed-model assembly lines based on simulated annealing algorithm." *Proceedings of the International Conference of Logistics Engineering and Management*, Chengdu, China, Oct. 8-10, 1803–1808.

- Lu, M., Lam, H.-C., and Dai, F. (2008). "Resource-constrained critical path analysis based on discrete event simulation and particle swarm optimization." *Automation in Construction*, 17(6), 670–681.
- Lui, H., Altaf, M. S., Lei, Z., Lu, M., and Al-Hussein, M. (2015). "Automated production planning in panelized construction enabled by integrating discrete-event simulation and BIM." *Proceedings of the International Construction Specialty Conference*, Vancouver, BC, Canada, Jun. 8-10.
- Mahdavi, I., Shirazi, B., and Sahebjamnia, N. (2011). "Development of a simulation-based optimisation for controlling operation allocation and material handling equipment selection in FMS." *International Journal of Production Research*, 49(23), 6981–7005.
- Meyer, G. G., Wortmann, J. C., and Szirbik, N. B. (2011). "Production monitoring and control with intelligent products." *International Journal of Production Research*, 49(5), 1303–1317.
- Mirdamadi, S., Fontanili, F., and Dupont, L. (2007). "Discrete event simulation-based real-time shop floor control." *Proceedings of the European Conference on Modelling and Simulation*, Riga, Latvia, Jun. 1-4.
- Mönch, L. (2007). "Simulation-based benchmarking of production control schemes for complex manufacturing systems." *Control Engineering Practice*, 15(11), 1381–1393.

- Montasir, A. and Moselhi, O. (2012). "RFID+ for tracking earthmoving operations." *Proceedings of the Construction Research Congress*, West Lafayette, IN, USA, May 21-23, 1011–1020.
- National Association of Home Builders. (2009). "Fast facts for panelized homes."
- Ngai, E. W. T., Chau, D. C. K., Poon, J. K. L., Chan, A. Y. M., Chan, B. C. M., and Wu, W. W. S. (2012). "Implementing an RFID-based manufacturing process management system: Lessons learned and success factors." *Journal of Engineering and Technology Management*, 29(1), 112–130.
- Ngai, E. W. T., Moon, K. K. L., Riggins, F. J., and Yi, C. Y. (2008). "RFID research: An academic literature review (1995–2005) and future research directions." *International Journal of Production Economics*, 112(2), 510–520.
- Peters, B. A., and Smith, J. S. (1998). "Real-time, simulation-based shop floor control." *Proceedings of ArenaSphere '98*, Pittsburgh, PA, USA, 188-194.
- Press, W. H., Teukolsky, S., Vetterling, W., and Flannery, B. (1992). *Numerical Recipes in C: The Art of Scientific Computing*. Cambridge University Press.
- Ranjbar, M., Davari, M., and Leus, R. (2012). "Two branch-and-bound algorithms for the robust parallel machine scheduling problem." *Computers & Operations Research*, 39(7), 1652–1660.

- Rezg, N., Xie, X., and Mati, Y. (2004). "Joint optimization of preventive maintenance and inventory control in a production line using simulation." *International Journal of Production Research*, 42(10), 2029–2046.
- Roberts, C. M. (2006). "Radio frequency identification (RFID)." *Computers & Security*, 25(1), 18–26.
- Sargent, R. G. (2010). "Verification and validation of simulation models." *Proceedings of the 2010 Winter Simulation Conference*, IEEE, Baltimore, MD, USA, Dec. 5-8, 166–183.
- Senghore, O., Hastak, M., Abdelhamid, T. S., Abuhammad, A., and Syal, M. G. (2004). "Production process for manufactured housing." *Journal of Construction Engineering and Management*, 130(5), 708–718.
- Serrano, I., Ochoa, C., and Castro, R. De. (2008). "Evaluation of value stream mapping in manufacturing system redesign." *International Journal of Production Research*, 46(16), 4409–4430.
- Shafai, L. (2012). "Simulation based process flow improvement for wood framing home building production lines." MSc thesis, University of Alberta, Edmonton, AB, Canada.
- Shewchuk, J. P., and Guo, C. (2012). "Panel stacking, panel sequencing, and stack locating in residential construction: Lean approach." *Journal of Construction Engineering and Management*, 138(9), 1006–1017.

- Shi, Y., and Eberhart, R. (1998). "A modified particle swarm optimizer." *Proceedings of the International Conference on Evolutionary Computation*, Anchorage, AK, USA, May 4-9, 69–73.
- Son, Y. J., Wysk, R. A., and Jones, A. T. (2003). "Simulation-based shop floor control: Formal model, model generation and control interface." *Transactions*, 35(1), 29–48.
- Taha, Z., Tahrir, F., and Zuhdi, A. (2011). "Job sequencing and layout optimization in virtual production line." *Journal of Quality*, 18(4), 351–374.
- Tasgetiren, M. F., Liang, Y.-C., Sevkli, M., and Gencyilmaz, G. (2007). "A particle swarm optimization algorithm for makespan and total flowtime minimization in the permutation flowshop sequencing problem." *European Journal of Operational Research*, 177(3), 1930–1947.
- Tasgetiren, M. F., Sevkli, M., and Gencyilmaz, G. (2004). "Particle swarm optimization algorithm for single machine total weighted tardiness problem." *Proceedings of the Congress on Evolutionary Computation*, Portland, OR, USA, Jun. 19-23, 1412–1419.
- Völker, S., and Gmilkowsky, P. (2003). "Reduced discrete-event simulation models for medium-term production scheduling." *Systems Analysis Modelling Simulation*, 43(7), 867–883.

- Whitner, R. B., and Balci, O. (1989). "Guidelines for selecting and using simulation model verification techniques." *Proceedings of the 1989 Winter Simulation Conference*, Washington, DC, Dec. 4-6, 559–568.
- Wu, C. W., Brown, K. N., and Beck, J. C. (2009). "Scheduling with uncertain durations: Modeling-robust scheduling with constraints." *Computers & Operations Research*, 36(8), 2348–2356.
- Xie, H., Shen, X., Hao, Q., Yu, H., and Tang, Y. (2011). "Production simulation for prefab housing facilities." *Proceedings of the 3<sup>rd</sup> International Construction Specialty Conference*, Ottawa, ON, Canada, Jun. 14-17.
- Yu, H. (2010). "An integrated approach toward lean for production homebuilders." PhD thesis, University of Alberta, Edmonton, AB, Canada.
- Zhong, R. Y., Dai, Q. Y., Qu, T., Hu, G. J., and Huang, G. Q. (2013). "RFID-enabled real-time manufacturing execution system for mass-customization production." *Robotics and Computer-Integrated Manufacturing*, 29, 283–292.
- Zhong, R. Y., Huang, G. Q., Lan, S., Dai, Q. Y., Zhang, T., and Xu, C. (2015). "A two-level advanced production planning and scheduling model for RFID-enabled ubiquitous manufacturing." *Advanced Engineering Informatics*, 29, 799–812.